NASA Technical Memorandum 89039

Aerodynamic Measurements and Thermal Tests of a Strain-Gage Balance in a Cryogenic Wind Tunnel

Richmond P. Boyden, Alice T. Ferris,
William G. Johnson, Jr., David A. Dress,
and Acquilla S. Hill

Langley Research Center
Hampton, Virginia

National Aeronautics
and Space Administration

Scientific and Technical
Information Branch

1987

Summary

An internal strain-gage balance designed and constructed in Europe especially for use in cryogenic wind tunnels has been tested in the Langley 0.3-Meter Transonic Cryogenic Tunnel. The purpose of the tests was to evaluate the performance of the balance in an actual cryogenic wind-tunnel test environment. The evaluation was made at equilibrium balance temperatures and it consisted of comparing the data taken at a tunnel stagnation temperature of 300 K with the data taken at 200 K and 110 K while maintaining either the Reynolds number or the stagnation pressure. The tests were made both with and without a convection shield on the balance. A sharp-leading-edge delta-wing model was used to provide the aerodynamic loading for these tests. The data at constant temperature were obtained over a range of angle of attack from about $-6°$ to about $17°$ and at Mach numbers of 0.3 and 0.5.

An additional part of this investigation involved measuring the transient temperature response of the balance during both normal and rapid changes in the tunnel stagnation temperature. The variation of the temperature with time was measured at three locations on the balance near the physical locations of the strain gages. These measurements were made at angles of attack of $0°$ and about $15°$ and at Mach numbers of 0.3, 0.5, and 0.65.

Results obtained with the balance during the force tests were found to be accurate and repeatable both with and without a convection shield on the balance. The use of a convection shield significantly increased the time required for the balance to stabilize at a new temperature during the temperature response tests.

Introduction

The development of the cryogenic wind-tunnel concept in 1971 to increase the Reynolds number capability in ground-based aerodynamic test facilities (ref. 1) has stimulated research both in the United States and in other countries into the modification of existing wind-tunnel instrumentation to enable it to operate satisfactorily at very low temperatures. For the past several years research has been underway at the Langley Research Center into the problems involved in accurately measuring the aerodynamic forces and moments on three-dimensional aircraft models with internal strain-gage balances in transonic cryogenic wind tunnels. (See refs. 1 to 9.) The goal of this work has been the development of internal strain-gage balances suitable for aerodynamic research in the U.S. National Transonic Facility (NTF), a large cryogenic wind tunnel that is now in operation at Langley. A description and a status report on the NTF are contained in reference 10.

Internal strain-gage balances have been in wide use in wind tunnels for many years both at ambient temperatures and at elevated temperatures. The NTF, however, requires the use of internal strain-gage balances capable of accurately measuring forces and moments at temperatures from a low near 77.4 K (the temperature of liquid nitrogen at ambient pressure) up to about 340 K. Stagnation pressures in the NTF can be varied from ambient up to 890 kPa (8.8 atm). In particular, the low temperatures used in cryogenic wind tunnels compound the problems of design, calibration, and use of strain-gage balances. In recent years, personnel of the Langley Instrument Research Division have been involved in a comprehensive balance development and evaluation effort with research done on balance construction, strain gages, adhesives, solder, wires, moistureproofing, and convection shields. This entire development program is aimed at minimizing the effects of cryogenic temperatures on strain-gage balance output. Details of this effort have been reported in references 2 to 9. Results of the Langley aerodynamic evaluation tests of strain-gage balances in cryogenic wind tunnels have been summarized in reference 8.

Development work on the use of strain-gage balances at cryogenic temperatures has also taken place at other research centers. The use of existing strain-gage balances with the addition of heaters for a blowdown cryogenic wind tunnel with relatively short run times is covered in references 11 and 12. Research in several European countries on both heated and unheated strain-gage balances was summarized in 1985 in reference 13.

This paper presents the results from aerodynamic tests using a European strain-gage balance in the Langley 0.3-Meter Transonic Cryogenic Tunnel (0.3-m TCT). The wind tunnel tests were made during April 1984 and a few preliminary results were presented in reference 14. The balance was designed and constructed specifically for testing at temperatures ranging from ambient to cryogenic by the staff of the National Aerospace Laboratories (NLR) in the Netherlands at the request of the European Transonic Wind Tunnel (ETW) Technical Group. The ETW is a large transonic cryogenic wind tunnel planned for construction in Europe (ref. 15), and the work on this balance is part of the overall research effort on instrumentation for the ETW. The development of this balance is discussed in detail in reference 16. The wind-tunnel tests were performed under a collaborative agreement on cryogenic transonic wind-tunnel testing between NASA and the ETW

countries under the auspices of the AGARD Fluid Dynamics Panel.

The primary purpose of these tests was to determine the performance of the European strain-gage balance under actual cryogenic wind-tunnel test conditions. The test objectives were (1) to obtain force and moment data at cryogenic temperatures of 110 K and 200 K to compare with data taken at an ambient temperature of 300 K in order to determine the performance and accuracy of the balance and (2) to measure the temperature response of the model, balance, and sting during normal and rapid changes in tunnel stream temperature.

Temperature response data are needed for determination of the time required for the balance to reach a new temperature equilibrium after the wind-tunnel stagnation temperature has been changed. The stabilization time for the balance can be as long as half an hour. Data are also required in order to make comparisons with finite-element computer programs used to predict balance temperature response. The thermal response of the balance can be affected by such things as the model configuration, convection shield, sting, angle of attack, Mach number, and tunnel pressure.

A sharp-leading-edge delta-wing model was used to load the balance aerodynamically, since such a configuration should be relatively insensitive to any changes in test Reynolds number resulting from changes in operating pressure or temperature (ref. 8). These tests were made primarily at Mach numbers of 0.3 and 0.5 and at angles of attack from approximately $-6°$ to $17°$. Two transient temperature runs were made at a Mach number of 0.65. Tunnel stagnation pressure was varied from 122 kPa (1.2 atm) to 491 kPa (4.8 atm) in order to compare results for constant Reynolds number obtained at different values of tunnel stagnation temperature. The pressure was also varied at a constant tunnel temperature to determine balance sensitivity and accuracy with different levels of aerodynamic load.

Symbols

Aerodynamic coefficient data presented in this report are referred to the body system of axes. The origin for these axes is the moment reference center located on the model axis of symmetry at 25 percent of the model mean geometric chord. Model dimensions given below are those with the model at 294 K.

$\bar{c}$ mean geometric chord, $\frac{2}{3}c_{root}$, 0.1580 m

c_{root} model root chord, 0.2370 m

C_A axial-force coefficient, $\frac{\text{Axial force}}{qS}$

C_m pitching-moment coefficient, $\frac{\text{Pitching moment}}{qS\bar{c}}$

C_N normal-force coefficient, $\frac{\text{Normal force}}{qS}$

M free-stream Mach number

p_t stagnation pressure, kPa or atm

q free-stream dynamic pressure, Pa

R Reynolds number based on $\bar{c}$

S wing planform area, 0.01504 m^2

T_t stagnation temperature, K

$\bar{x}$ moment transfer distance between balance moment center and model moment center, positive forward, 0.06248 m

α angle of attack, deg

Apparatus and Procedure

Wind Tunnel

The Langley 0.3-Meter Transonic Cryogenic Tunnel (0.3-m TCT) is a single return, fan-driven wind tunnel which uses nitrogen as the test gas. The two-dimensional test section (fig. 1) used for this investigation is 20.3 cm in width and 61.0 cm in height. The test section has a slotted floor and ceiling and solid sidewalls. The traversing wake-survey probe, shown in figure 1(b), was removed for these tests. A motor-driven turntable, 22.8 cm in diameter, was centrally located in each sidewall for the mounting of two-dimensional airfoil models. The Mach number of the 0.3-m TCT with the two-dimensional test section could be varied from 0.05 to 0.95. Stagnation pressure can be varied from 122 kPa (1.2 atm) to 608 kPa (6.0 atm) and the stagnation temperature range is from about 77 K to 327 K. Additional information on the operation of the 0.3-m TCT is contained in references 14, 17, and 18.

Model

The model used to provide the aerodynamic loading for this test is a sharp-leading-edge $75°$ delta wing as shown in figure 2. It is the same model used for the evaluation tests of the Langley strain-gage balance in reference 8. As previously mentioned, one advantage of using a sharp-leading-edge delta-wing model is that the aerodynamic characteristics of this configuration are relatively insensitive to changes in Reynolds number. Also, the thick diamond-shaped cross section in the spanwise direction prevents any aeroelastic distortion of the model from affecting the aerodynamic results. The balance was located with respect to the model center of pressure so that full-scale normal force on the balance resulted in nearly

full-scale pitching moment being applied on the balance. The moment transfer distance from the balance moment center to the model moment reference center is shown in figure 2. No artificial roughness was applied to the model to trip the boundary layer during these tests.

The model was machined from a single piece of A-286 steel. A balance adapter made of Teledyne Vasco VascoMax C-200 maraging steel was used between the balance and the model. A single expansion-type steel dowel pin was used to properly locate the balance, adapter, and model with respect to one another.

Three type T (copper-constantan) thermocouples were used to record the model surface temperature. The thermocouples were located on the model as shown in figure 2. A shallow groove to contain the thermocouples was machined into the surface of the model. The groove connected the three thermocouple locations and extended to the rear of the model to provide a path for routing the thermocouple lead wires. After the thermocouples had been installed, an epoxy potting compound was used to fill the groove, and the surface of the model was restored to a smooth condition.

Model Support System

A strut with a circular arc airfoil section was attached to the turntable on each side of the tunnel test section. The strut supported a short sting on which the balance and model were mounted. This arrangement is shown in figure 3, and a photograph of the model, sting, and support strut is shown in figure 4. The turntables, which are driven through a yoke arrangement by an electric stepper motor, provide the angular rotation in pitch for the model. The sting was made from VascoMax C-200 maraging steel and the airfoil strut was made of A-286 steel. The sidewall turntables were made from 7075-T6 aluminum alloy. A photograph of the arrangement of the model, sting, and support strut in the test section of the 0.3-m TCT is shown in figure 5.

Two type T thermocouples were installed along the top surface of the sting to record the temperature of the sting surface during the runs in which the stagnation temperature was varied with time. These two thermocouples were spot-welded to the sting. One thermocouple was located in the plane of the base of the model and the other was placed 3.30 cm further aft on the sting.

Balance

The European balance, designated NLR 771, used for these tests is a one-piece, internal strain-gage balance fabricated and gaged specifically for cryogenic use. It is a three-component balance (normal force, axial force, and pitching moment) that is 2.54 cm in maximum diameter and 21.21 cm long. It is made of Vakumelt Ultrafort 301 steel and has Micro-Measurements K-alloy strain gages. As indicated in the photograph in figure 6(a), the balance has a forward and an aft bending-moment bridge. These two bridges incorporate additional strain gages mounted in a transverse direction to that of the actual strain-sensing gages in order to minimize temperature effects in a manner similar to that used on the Langley balance HRC-2 described in reference 8. The axial-force bridge does not require these additional transverse gages to minimize temperature effects on axial-force output. Outputs of the two bending-moment bridges are added and subtracted to produce voltages which are proportional, respectively, to normal force and pitching moment. The balance has 10 type T thermocouples located as shown in figure 6(b). The thermocouples are used to monitor balance temperature and are also used in the data reduction procedure.

The European balance relies on the concept of mathematical correction of temperature effects on the balance voltage outputs instead of using temperature compensation wire in one arm of the bridge for electrical correction of the balance outputs as has been done in the Langley series of balances intended for cryogenic use. (See refs. 6 and 9.) The basic philosophy used in the design of the European balance is to correct for the effects of temperature on the balance zeroes and sensitivities and for the effects of temperature gradients on the balance outputs, by measuring the various effects during calibration. The balance outputs are then corrected in the data reduction procedure for these effects by use of the temperature measurements made on the balance.

The balance was tested with and without a convection shield. The convection shield is a tubular shield cantilevered forward over the gage section of the balance. It has been found to improve the stability of the outputs on the Langley balances in previous aerodynamic tests in the 0.3-m TCT as noted in references 2 and 8.

The three-component NLR 771 strain-gage balance has the following full-scale design loads:

Normal force	890 N
Axial force	112 N
Pitching moment	28 N-m

The typical accuracy of a strain-gage balance of ± 0.5 percent of full-scale design load may be expressed in terms of each of the aerodynamic coefficients and is then dependent on the particular

model reference dimensions and on the dynamic pressure used in the particular test. For these tests, the ±0.5 percent accuracy, with the dynamic pressure in pascals, may be given as

$$\Delta C_N = \pm 296/q$$
$$\Delta C_A = \pm 37.2/q$$
$$\Delta C_m = \pm 58.9/q$$

Additional details on this balance may be found in references 13 and 16.

Test Procedures and Data Corrections

Two types of data acquisition runs were made during these tests. The force data runs were made at constant stagnation temperature where the force and moment data were acquired over a range of angle of attack. The other type of runs was a series of transient temperature runs in which the stagnation temperature was varied and thermocouples on the balance, model, and sting measured the temperature response with time of the various components. Details for each of the two types of runs are described below.

Force data runs. The European method of computing forces and moments from the balance outputs was not used for the data presented in this report. Prior to the actual wind-tunnel tests, the European strain-gage balance was recalibrated at room temperature using the standard Langley calibration procedure for force balances. In addition, the variations of the balance strain-gage output sensitivities with temperature were measured by applying loads to the balance while it was in a cryogenic chamber at various fixed temperatures. The balance data from the cryogenic chamber runs were correlated by use of the least-squares method to obtain second-order equations to correct the balance sensitivities for temperature effects. These equations were then incorporated into the standard Langley force-balance data reduction procedure, which is based on the work in reference 19. The sensitivity shift for each of the strain-gage bridges is shown in figure 7.

The force and moment data presented in this report are equilibrium temperature results in that the balance temperatures were allowed to stabilize before data were taken. All the force and moment data presented herein for stagnation temperatures lower than 300 K were reduced with "cold" wind-off balance zeroes. These cold zeroes were obtained by lowering the tunnel stagnation temperature to the desired value with the tunnel running, waiting for the balance temperatures to stabilize, and then quickly stopping the tunnel fan to record the wind-off balance zeroes from the three balance components. With this procedure, the balance temperatures for the cold zeroes could be held within ±3 K of the desired temperature.

Model angle of attack was determined from the output of a digital shaft encoder geared to one of the turntables. The shaft encoder has a resolution of 0.01°. This arrangement required that a correction for sting and balance deflection under load be made in the data reduction process in order to compute the model angle of attack.

The model geometric dimensions used to nondimensionalize the aerodynamic coefficients were corrected for thermal contraction effects resulting from the temperature changes. As pointed out in reference 2, these corrections are about 0.4 percent in C_N and C_A and 0.6 percent in C_m for a steel model at 110 K. A polynomial equation fitted to the thermal contraction data in reference 20 for A-286 steel was used to correct the model dimensions.

The axial-force data have been corrected for model cavity pressure in that the test section static pressure has been considered to act over the projected area of the balance cavity in the vertical plane normal to the model axis of symmetry.

Typical test points for the force data runs are illustrated in figure 8 at a Mach number of 0.5 for the different combinations of tunnel stagnation pressure, stagnation temperature, and Reynolds number.

Transient temperature runs. For these runs, the tunnel stagnation temperature was changed from one stabilized value to another while the Mach number, stagnation pressure, and angle of attack were held approximately constant. Both a slow rate and a fast rate of changing the stagnation temperature were used in order to simulate possible requirements for use of a strain-gage balance in a large cryogenic tunnel such as the U.S. National Transonic Facility or the proposed European Transonic Wind Tunnel. The slow rate had to be used for large temperature changes and involved varying the temperature a maximum of 10 K/min in order to stay within requirements imposed because of cooldown and warmup limitations on the structure of the 0.3-m TCT. The fast rate allowed as rapid a temperature change as possible within the limits of the tunnel temperature control system, but only over a maximum temperature excursion of 50 K. A fast rate of temperature change between test points has been suggested as a method of conserving nitrogen in large cryogenic wind tunnels.

The stagnation temperature for the transient temperature runs was measured with a type T thermocouple located near the tunnel centerline on an existing temperature survey rig (see ref. 17) at the beginning of the screen section just upstream of the contraction section. A thermocouple was used instead of a platinum resistance thermometer, which is normally used to measure stagnation temperature during steady state tests, in order to obtain a faster response time for the transient temperature runs. The estimated accuracy of the type T thermocouples as installed in the tunnel is about ±3 K over the range of temperature used in the test. Thermocouple number 2 located on the model in the position indicated in figure 2 was used to provide the model temperature. The thermocouple spot-welded to the upper surface of the sting in line with the base of the model was used to measure sting temperature. The balance temperatures shown in the figures for the transient temperature runs were obtained by averaging the two thermocouple readings at each of the three bridge locations. With the thermocouple designations as indicated in figure 6(b), these average temperatures are

$$\text{Balance rear temperature} = \frac{1}{2}(\text{TH7} + \text{TH8})$$

$$\text{Balance middle temperature} = \frac{1}{2}(\text{TH5} + \text{TH6})$$

$$\text{Balance front temperature} = \frac{1}{2}(\text{TH3} + \text{TH4})$$

During a constant pressure, constant Mach number cooldown or warmup run, the tunnel fan speed, liquid nitrogen injection rate, and gaseous nitrogen exhaust rate must be closely controlled. Closed-loop feedback control systems in the 0.3-m TCT can drive the tunnel flow parameters to set-point conditions of Mach number, pressure, and temperature and then stabilize the tunnel at those conditions (see refs. 14, 21, and 22). However, these systems were designed primarily for operation under steady state conditions and normal tunnel cooldown or warmup. For the fast temperature changes needed for these tests, the temperature had to be manually controlled at least until the temperature was within about 10 K of the final temperature. Normally, automatic control of Mach number and pressure was used for all the runs.

As the tunnel was warmed up or cooled down for a transient temperature run, thermal expansion or contraction of the rods which connect the angle-of-attack drive to the turntables in the sidewalls of the test section caused a small variation in model attitude with time. The resultant small changes in angle of attack had to be manually corrected during the course of each run by small adjustments of the angle-of-attack drive.

Discussion of Results

Force and Moment Tests at Equilibrium Temperature

Convection shield on. The results of the wind tunnel tests of the European strain-gage balance with the convection shield on are contained in figures 9 through 13. Figure 9 is a comparison of the results obtained at a stagnation temperature of 300 K, which would be a typical operating temperature for a noncryogenic subsonic or transonic tunnel, with the results obtained at stagnation temperatures of 200 K and 110 K for Mach numbers of 0.3 and about 0.5. The stagnation pressure was chosen to provide approximately the same Reynolds number for each Mach number over the range of test temperatures. For the run made at 200 K and 287 kPa in figure 9(b), the Mach number had to be changed to 0.52, which resulted in a slightly higher Reynolds number. This was caused by a limitation inherent in the actual hardware used in the speed control for the tunnel fan in the Langley 0.3-m TCT. The agreement of the results obtained at the cryogenic temperatures of 200 K and 110 K with the results obtained at the ambient temperature of 300 K in figure 9 is considered very good. Bands for the balance accuracy discussed earlier of ±0.5 percent of the full-scale design loads have been expressed in terms of the nondimensionalized coefficients and are shown along the right-hand edge of figure 9. The accuracy bands would generally apply to other data at similar values of Mach number and stagnation pressure. In all cases the data fall within the ±0.5 percent accuracy bands. Note that the balance is subjected to nearly full-scale design loads on both normal force and pitching moment when operating at a Mach number of 0.5, a total pressure of 491 kPa, and an angle of attack of about 16°. In contrast, the balance is subjected to only about 40 percent of design axial load under the same test conditions.

Figure 10 shows the results for a repeat run made later in the test program at a temperature of 300 K, a Mach number of 0.5, and a pressure of 491 kPa. Excellent agreement was obtained over the angle-of-attack range for these two runs.

The results of runs made at constant pressure for stagnation temperatures of 300 K and 110 K are compared in figure 11. Both the pitching-moment and normal-force data are in excellent agreement considering the large differences in the Reynolds number. This confirms, as expected from the results of reference 8, that the delta-wing model is relatively

insensitive to changes in Reynolds number. However, the axial-force data are in only good agreement.

Figures 12 and 13 are comparisons of results for various stagnation pressures with the temperature held constant at 300 K and 110 K, respectively. The axial-force data at the lower pressure of 122 kPa and a Mach number of 0.3 are less smooth with changes in angle of attack than are the data at the higher pressure. This is believed to be a resolution problem that results from the low aerodynamic loads at the lower pressure. However, the data are still within the accuracy bands which were mentioned earlier.

Convection shield off. Figures 14 through 17 contain the results of the tests made with the convection shield removed from the balance. Figure 14 is a comparison of the results at stagnation temperatures of 300 K, 200 K, and 110 K for Mach numbers of 0.3 and about 0.5 at approximately constant Reynolds number. The data for the run made at a Mach number of 0.3 and 110 K with the convection shield off were not included because of an unresolved problem with data scatter. Agreement of the data in figure 14 is considered very good.

Figure 15 shows a comparison of repeat runs made at a temperature of 200 K, a Mach number of 0.52, and a pressure of 287 kPa. Excellent agreement was obtained for these two runs.

The results obtained at constant pressure for 300 K and 110 K are shown in figure 16. Very good agreement of the data is evident except for the axial-force results. These are in only good agreement, especially at a Mach number of 0.3.

Figure 17 shows the results at 110 K for two pressures and a Mach number of 0.5. The agreement is very good except for the minor differences which are evident at angles of attack above 12°.

Convection shield on and off. Some of the above data were replotted to compare the results with the balance convection shield on and off in figures 18, 19, and 20 for stagnation temperatures of 300 K, 200 K, and 110 K, respectively. In this set of figures, each plot is for the same Mach number, pressure, and temperature, so that the only variable is whether the balance was tested with or without the convection shield. All these data are considered to be in very good agreement. One may conclude therefore that the use of the convection shield did not significantly affect the accuracy of the results of the aerodynamic tests made at equilibrium temperatures.

Overall, the unheated European strain-gage balance behaved very well over the range of temperatures during the force tests, and the balance gave accurate, repeatable results with and without the convection shield.

Transient Temperature Tests

The results of the transient temperature tests with the balance convection shield on and off are shown in figures 21 to 26. Table I lists the individual figures showing convection shield usage, Mach number, initial stagnation temperature, final stagnation temperature, stagnation pressure, and angle of attack. Each separate plot shows the variation with time of the tunnel stagnation temperature, model temperature, sting temperature, and average balance temperature at the three strain-gage bridge locations. The sting temperature has been omitted from some of the transient temperature plots in figures 21 to 23 because of erratic readings caused by a mechanical junction problem with that particular thermocouple. The sting thermocouple was repaired before the tests with the convection shield removed from the balance. Therefore, the sting temperature is included in all the plots for figures 24 to 26.

A typical figure of one of the transient temperature runs consists of several hundred data points plotted against time with a straight-line fairing between data points. The symbols shown in the figures for the transient temperature runs have been used only at discrete intervals in order to identify each of the six temperature traces normally shown in each figure. The time interval between individual data points during each run was 1 or 2 sec when conditions were changing rapidly during the first 2 or 3 min of cooldown or warmup, 5 sec during the next several minutes, 10 sec during the next several minutes, 20 sec for the next several minutes, and 30 sec for the final portion of a run where the temperatures were changing slowly and were asymptotically approaching the tunnel stagnation temperature. A desktop microcomputer was used to time the data interval and to command the facility data acquisition computer to record a data point. The data interval was changed during a run by keyboard entry to the microcomputer at the discretion of the test engineer, who was continuously monitoring the thermocouple outputs.

The discussion of the transient temperature results is limited to some of the more important points along with some of the limitations that had to be imposed on individual runs.

Convection shield on. Figure 21(a) shows a normal tunnel cooldown run at a Mach number of 0.3 where the tunnel is cooled down from 300 K to 110 K in about 30 min. The small spikes which are evident in

the tunnel stagnation temperature data and the inadvertent 20-K rise at about 44 min on the time scale are a result of minor control problems experienced by the tunnel operator. The model and sting temperatures closely follow the tunnel stagnation temperature as the lag time is only about half a minute. The balance temperatures have a lag time of about 8 to 10 min with the temperature in the middle of the balance near the axial force beams having, as would be expected, the longest lag time. Conduction from the model to the front of the balance and from the sting to the rear of the balance apparently accounts for the lag time of the front and the rear of the balance being less than the lag time of the middle section.

Figure 21(b) is an example of a rapid cooldown from 300 K to 260 K. The tunnel stagnation temperature reaches 260 K in less than 10 sec. The temperature overshoot down to about 247 K is a result of the initial manual control of the temperature and the rapid response of the tunnel flow properties to wide-open valves on the liquid nitrogen injection. However, the balance temperatures take almost 28 min to approach the tunnel stagnation temperature. The small offsets or differences in temperature of up to about two degrees which are evident at the beginning and at the end of the run in figure 21(b), and in some of the other figures, are the result of small inaccuracies in the thermocouple data. The temperature differences, especially at the beginning of a run, are not the result of allowing insufficient time for the temperatures of the balance, model, and sting to stabilize since time was allowed before starting a run for the various components to reach an equilibrium temperature.

The effect of pressure on the time required for the balance temperatures to cool down from 150 K to 110 K can be seen by comparing figures 21(c) and 21(d). The higher pressure run (488 kPa) required only about 20 min for the balance temperatures to reach the new stream temperature, while the lower pressure run (122 kPa) required about 28 min.

The warmup runs at a Mach number of 0.3 begin with figure 21(f). The data show that about 3 min were required to raise the stream temperature from 110 K to 120 K at 488 kPa. The process of increasing the tunnel temperature, especially at low Mach number, is inherently slower than that of decreasing the temperature because of the low amount of power input to the flow through the fan drive relative to the cooling capacity of the liquid nitrogen injection system. Almost 12 min was required for the balance to warm up from 110 K to 120 K.

The large downward spike in the tunnel temperature evident in figure 21(h) at an elapsed time of about 32 min was caused by a restart of the pump in the liquid nitrogen supply line. It was necessary to turn off the pump during some of the warmup runs because with the pump running there was sufficient leakage past the digital valve that modulates the flow of liquid nitrogen into the tunnel to prevent the tunnel from warming up at an adequate rate.

The runs at a Mach number of 0.5 with the convection shield on are shown in figure 22. The results for the cooldown runs at Mach numbers of 0.5 and 0.3 are similar. Figure 22(c) depicts a repeat run, done much later in the test program, of the run shown in figure 22(b); it shows good repeatability.

Increasing the angle of attack from 0° (fig. 22(f)) to 15° (fig. 22(g)) did not noticeably change the time required for the balance to reach the new temperature of 110 K from 150 K. However, it did result in the front of the balance changing temperature in a manner similar to the middle of the balance, with the rear of the balance having the shortest temperature response time.

Figure 22(i), which shows a warmup run from 110 K to 120 K, can be compared with figure 21(f). The comparison shows a large difference in the time required to change the tunnel temperature; the Mach 0.5 run took about half a minute while the Mach 0.3 run took about 3 min. In figure 22(i) the obvious increase in the number of symbols (and data points) starting at 9 min into the run and lasting for about a minute and a half was caused by an incorrect change of the data interval. The data quality was not affected by the shortened data time interval.

Mach number does strongly influence the warmup runs. This can be seen by comparing figure 22(j), where the balance had reached the final temperature in about 30 min, with figure 21(g), where just the tunnel temperature took about 1 hr to increase from 110 K to 150 K.

Convection shield off. A cooldown run from 150 K to 110 K (fig. 24(b)) required about 19 min for the unshielded balance to reach 110 K at 122 kPa. The corresponding run with the convection shield on (fig. 21(c)) took 28 min. At the higher pressure of 488 kPa (fig. 24(c)) with the convection shield removed, the balance required around 9 min to reach the final temperature as opposed to 20 min with the shield on (fig. 21(d)). Even with the convection shield removed, the middle section of the balance, which contains the axial-force bridge, was still the slowest of the three balance sections to change temperature.

Only about 6 min were needed for the unshielded balance to cool down from 120 K to 110 K at 488 kPa (fig. 24(d)). This is in contrast with the 14 to 16 min that were required for the corresponding run (fig. 21(e)) for the shielded balance.

Various operational problems with the wind-tunnel systems did not allow the runs shown in figures 24(f), 24(g), and 24(h) to be continued until the balance temperatures were fully stabilized. In addition, as indicated in figure 24(h), almost 14 min of data during that particular run could not be recorded because of a malfunction in the data acquisition computer.

The results of the transient temperature tests show that the use of the convection shield resulted in a significantly longer time for the balance to stabilize at a new temperature. If stabilization of balance temperature is an operational requirement, this longer stabilization time for a balance will increase the costs of running a cryogenic tunnel, a nontrivial consideration for large cryogenic tunnels such as the NTF or the ETW. The problem of data accuracy from strain-gage balances when balance temperatures have not reached final equilibrium needs further examination. Therefore, an area of conflict between data accuracy requirements and economics of operation for cryogenic wind tunnels can exist for strain-gage balances that require temperature stabilization to achieve high accuracy.

Summary of Results

A European internal strain-gage balance especially designed for use in cryogenic wind tunnels has been tested in the Langley 0.3-Meter Transonic Cryogenic Tunnel. The model used to provide the aerodynamic loading for these tests was a highly swept sharp-leading-edge delta wing. Two types of runs were made to evaluate the balance. For the first type, force and moment data were acquired with the balance at equilibrium temperature for a range of angle of attack. Data were obtained at cryogenic temperatures of 110 K and 200 K to compare with data obtained at an ambient temperature of 300 K to determine balance performance and accuracy. For the second type, the temperature response with time of the balance was measured at fixed angles of attack during both normal and rapid changes in tunnel stagnation temperature. Both types of runs were made with and without a convection shield on the balance.

The results obtained with the European cryogenic balance during the force tests were found to be accurate and repeatable both with and without the use of the convection shield. For the temperature response runs the use of the convection shield did result in a significantly longer amount of time for the balance to stabilize at a new temperature.

NASA Langley Research Center
Hampton, VA 23665-5225
February 11, 1987

References

1. Goodyer, Michael J.; and Kilgore, Robert A.: High-Reynolds-Number Cryogenic Wind Tunnel. *AIAA J.*, vol. 11, no. 5, May 1973, pp. 613–619.
2. Kilgore, Robert A.; and Davenport, Edwin E.: *Static Force Tests of a Sharp Leading Edge Delta-Wing Model at Ambient and Cryogenic Temperatures With a Description of the Apparatus Employed.* NASA TM X-73901, 1976.
3. Ferris, Judy: Cryogenic Wind Tunnel Force Instrumentation. *First International Symposium on Cryogenic Wind Tunnels*, Univ. of Southampton, Apr. 1979, pp. 32.1–32.8.
4. Kilgore, Robert A.: Model Design and Instrumentation Experiences With Continuous-Flow Cryogenic Tunnels. *Cryogenic Wind Tunnels*, AGARD-LS-111, May 1980, pp. 9-1–9-22.
5. Ferris, Alice T.: *Force Instrumentation for Cryogenic Wind Tunnels Using One-Piece Strain-Gage Balances.* NASA TM-81845, 1980.
6. Ferris, Alice T.; and Moore, Thomas C.: Force Instrumentation for Cryogenic Wind Tunnels Using One-Piece Strain-Gage Balances. *Instrumentation in the Aerospace Industry Volume 27, Advances in Test Measurement—Volume 18, Part One*, Instrument Soc. of America, 1981, pp. 149–153.
7. Polhamus, E. C.; and Boyden, R. P.: The Development of Cryogenic Wind Tunnels and Their Application to Maneuvering Aircraft Technology. *Combat Aircraft Manoeuvrability*, AGARD-CP-319, Dec. 1981, pp. 15-1–15-12.
8. Boyden, Richmond P.; Johnson, William G., Jr.; and Ferris, Alice T.: *Aerodynamic Force Measurements With a Strain-Gage Balance in a Cryogenic Wind Tunnel.* NASA TP-2251, 1983.
9. Ferris, Alice T.: *Cryogenic Strain Gage Techniques Used in Force Balance Design for the National Transonic Facility.* NASA TM-87712, 1986.
10. Bruce, Walter E., Jr.: The U.S. National Transonic Facility—I and II. *Special Course on Cryogenic Technology for Wind Tunnel Testing*, AGARD-R-722, July 1985, pp. 14-1–14-10 and pp. 15-1–15-10.
11. Cadwell, J. D.: Design, Fabrication, and Instrumentation Preparation of a Verification Model for the Douglas Aircraft Four Foot Cryogenic Wind Tunnel (4CWT). *First International Symposium on Cryogenic Wind Tunnels*, Univ. of Southampton, Apr. 1979, pp. 34.1–34.9.
12. Cadwell, J. D.: Model Design and Instrumentation for Intermittent Cryogenic Wind Tunnels. *Cryogenic Wind Tunnels*, AGARD-LS-111, May 1980, pp. 10-1–10-8.
13. Bazin, M.: Cryogenic Wind Tunnel Instrumentation. *Special Course on Cryogenic Technology for Wind Tunnel Testing*, AGARD-R-722, July 1985, pp. 6-1–6-28.
14. Kilgore, Robert A.: The NASA Langley 0.3-m Transonic Cryogenic Tunnel. *Special Course on Cryogenic Technology for Wind Tunnel Testing*, AGARD-R-722, July 1985, pp. 13-1–13-15.

15. Tizard, J. A.; and Hartzuiker, J. P.: The European Transonic Windtunnel Project ETW. *Special Course on Cryogenic Technology for Wind Tunnel Testing*, AGARD-R-722, July 1985, pp. 12-1–12-23.

16. Schoenmakers, T. J.: *Development of a Non-Insulated Cryogenic Strain-Gauge Balance.* Memo. TP-82-006, U, Nationaal Lucht- en Ruimtevaartlaboratorium (Netherlands), Sept. 1982.

17. Kilgore, Robert A.: *Design Features and Operational Characteristics of the Langley 0.3-Meter Transonic Cryogenic Tunnel.* NASA TN D-8304, 1976.

18. Kilgore, Robert A.: Development of the Cryogenic Tunnel Concept and Application to the U.S. National Transonic Facility. *Towards New Transonic Windtunnels*, AGARD-AG-240, Nov. 1979, pp. 2-1–2-27.

19. Smith, David L.: *An Efficient Algorithm Using Matrix Methods To Solve Wind-Tunnel Force-Balance Equations.* NASA TN D-6860, 1972.

20. Schwartzberg, Fred R.; Osgood, Samuel H.; Herzog, Richard G.; and Knight, Marvin (compiler, AFML): *Cryogenic Materials Data Handbook (Revised) 1970, Volume I.* AFML-TDR-64-280, Vol. I. (Revised 1970), U.S. Air Force, July 1970. (Available from DTIC as AD 713 619.)

21. Thibodeaux, Jerry J.; and Balakrishna, S.: *Development and Validation of a Hybrid-Computer Simulator for a Transonic Cryogenic Wind Tunnel.* NASA TP-1695, 1980.

22. Balakrishna, S.: *Modeling and Control of Transonic Cryogenic Wind Tunnels: A Summary Report.* NASA CR-159376, 1980.

Table I. List of Figures for Transient Temperature Runs

Figure	Shield	Mach	From T_t, K	To T_t, K	p_t, kPa	α, deg
21(a)	On	0.30	300	110	122	0
21(b)	↓	↓	300	260	122	↓
21(c)			150	110	122	
21(d)			150	110	488	
21(e)			120	110	488	
21(f)			110	120	488	
21(g)			↓	150	122	
21(h)				150	122	15.0
21(i)				150	488	0
21(j)			260	300	122	0
22(a)	On	0.50	300	260	122	0
22(b)	↓	↓	300	260	491	↓
22(c)			300	260	491	
22(d)			200	150	287	
22(e)			150	110	122	
22(f)			150	↓	491	
22(g)			150		↓	15.0
22(h)			120			0
22(i)			110	120		↓
22(j)			110	150	122	
22(k)			110	300	491	
22(l)	↓	↓	260	300	491	↓
23	On	0.65	110	300	122	0
24(a)	Off	0.30	300	110	122	0
24(b)	↓	↓	150	↓	122	↓
24(c)			150		488	
24(d)			120		488	
24(e)			110	120	488	
24(f)			↓	150	122	
24(g)				↓	122	15.0
24(h)					122	15.0
24(i)	↓	↓	↓	↓	488	0
25(a)	Off	0.50	250	200	287	0
25(b)	↓	↓	200	150	287	↓
25(c)			150	110	122	
25(d)			150	110	491	
25(e)			150	110	491	14.8
25(f)			110	150	122	0
25(g)	↓	↓	110	300	491	0
26	Off	0.65	110	300	122	0

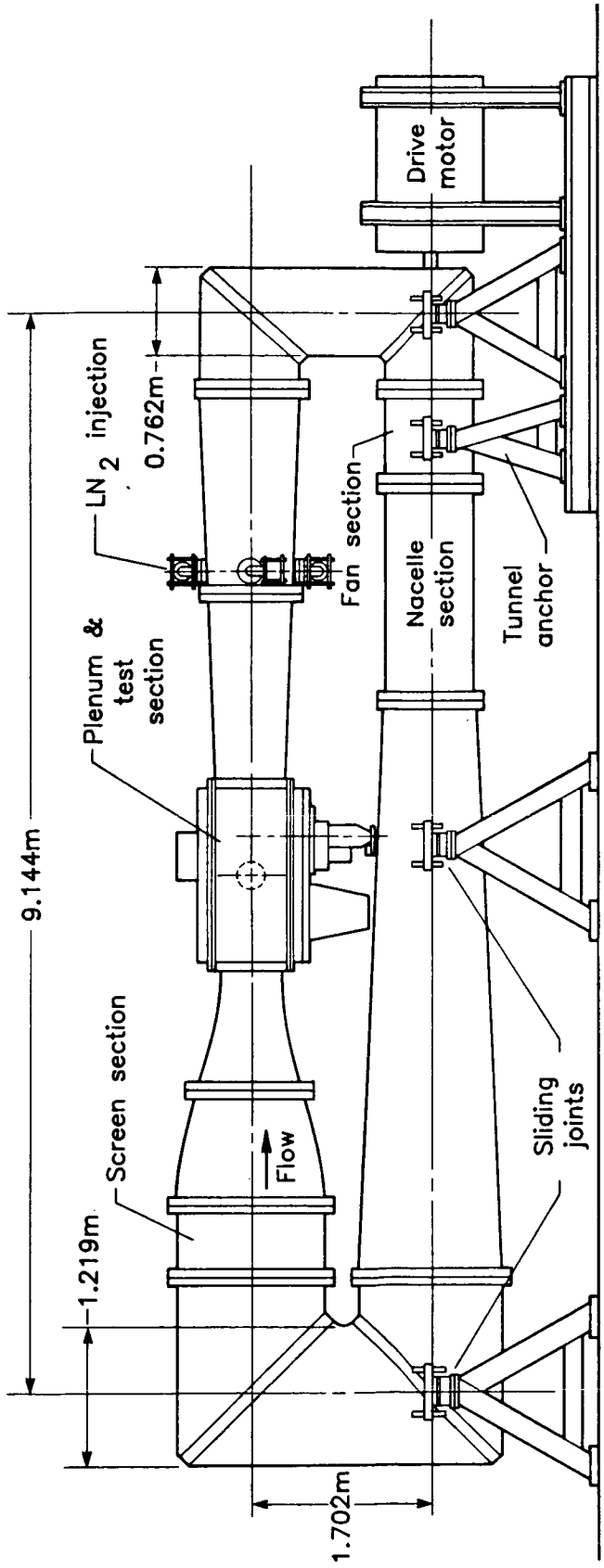

(a) Side view of tunnel with two-dimensional test section.

Figure 1. Langley 0.3-m TCT.

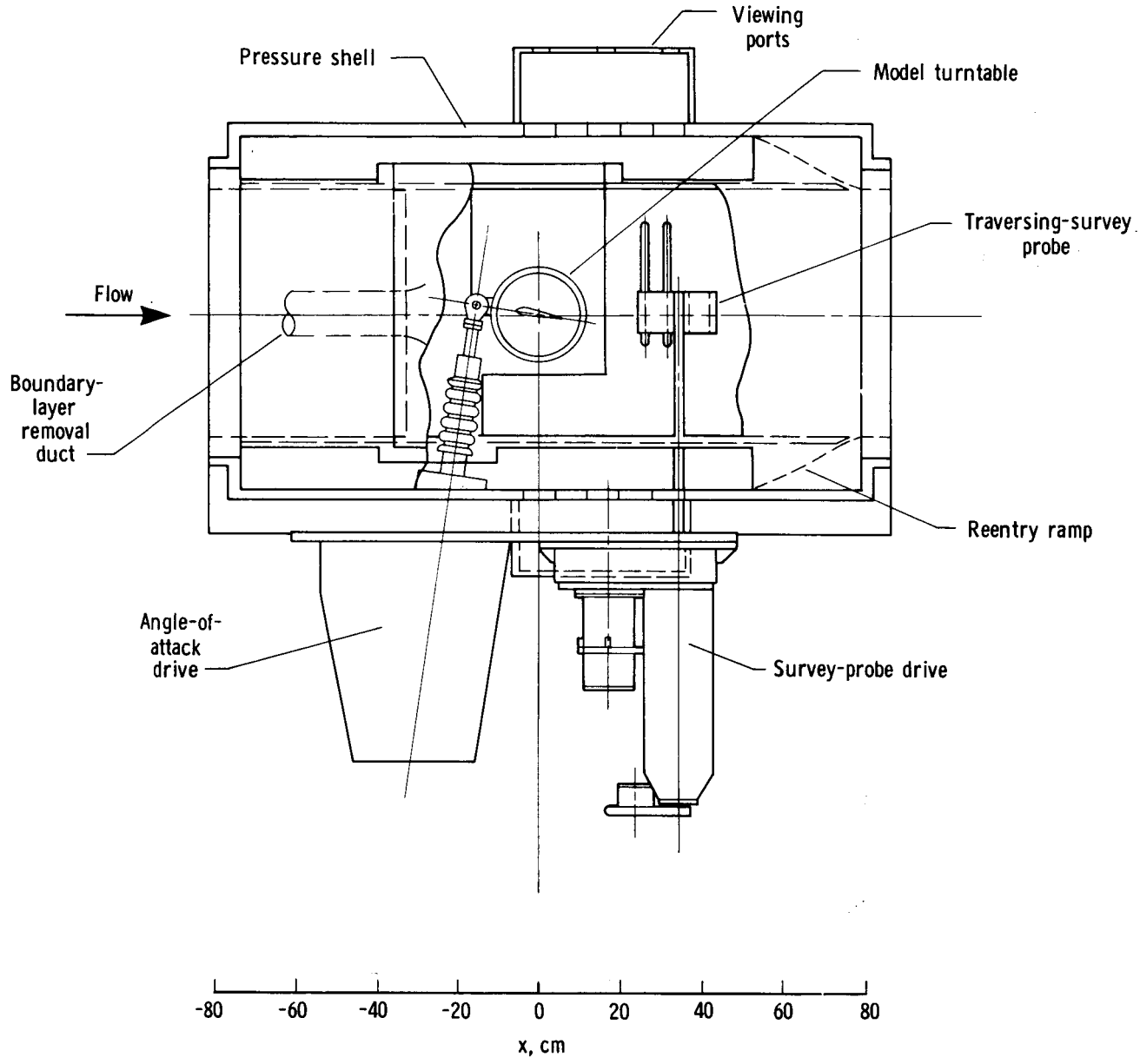

(b) Side view with details of two-dimensional test section.

Figure 1. Concluded.

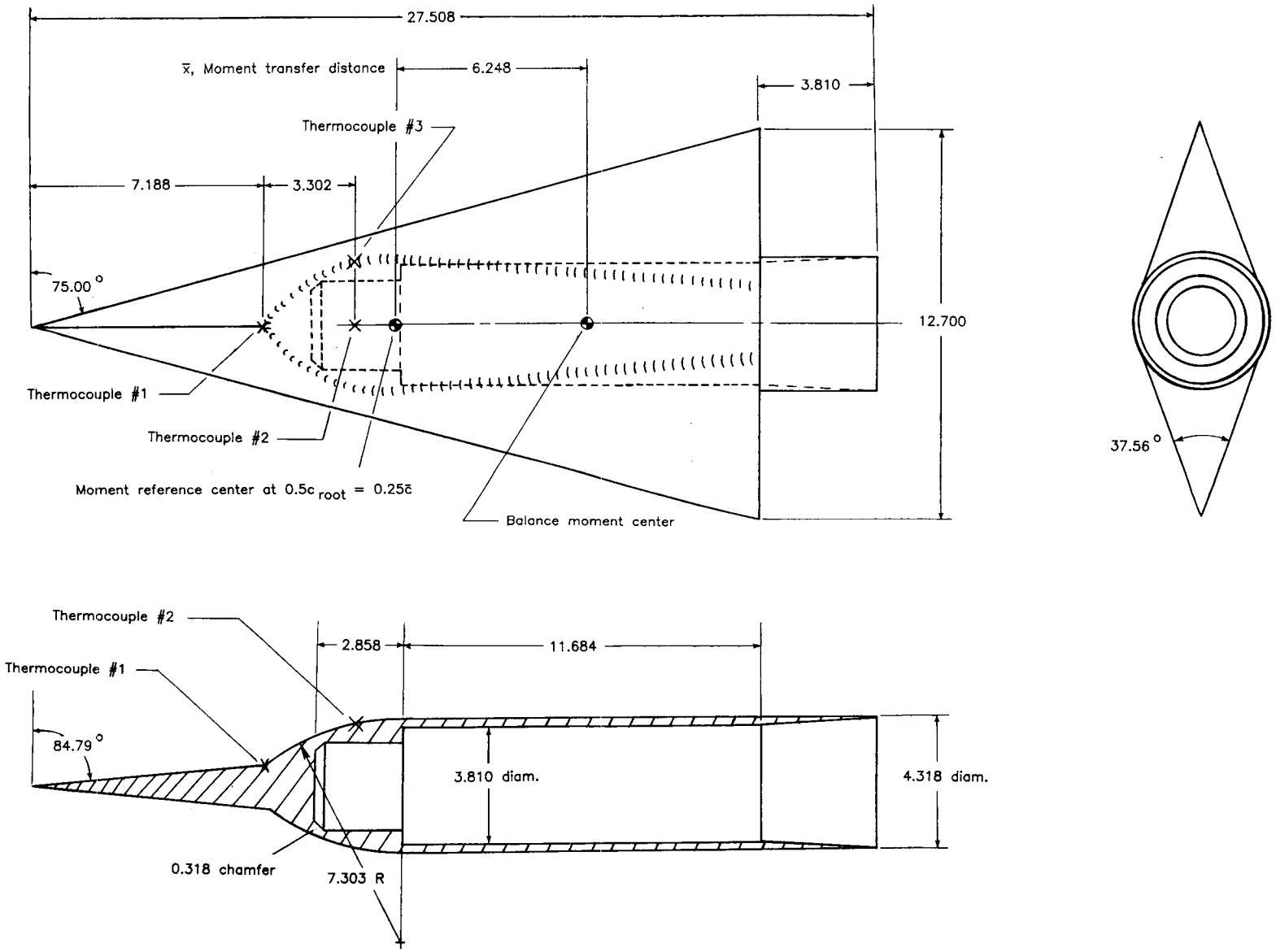

Figure 2. Three-view drawing of model. (Dimensions are in centimeters.)

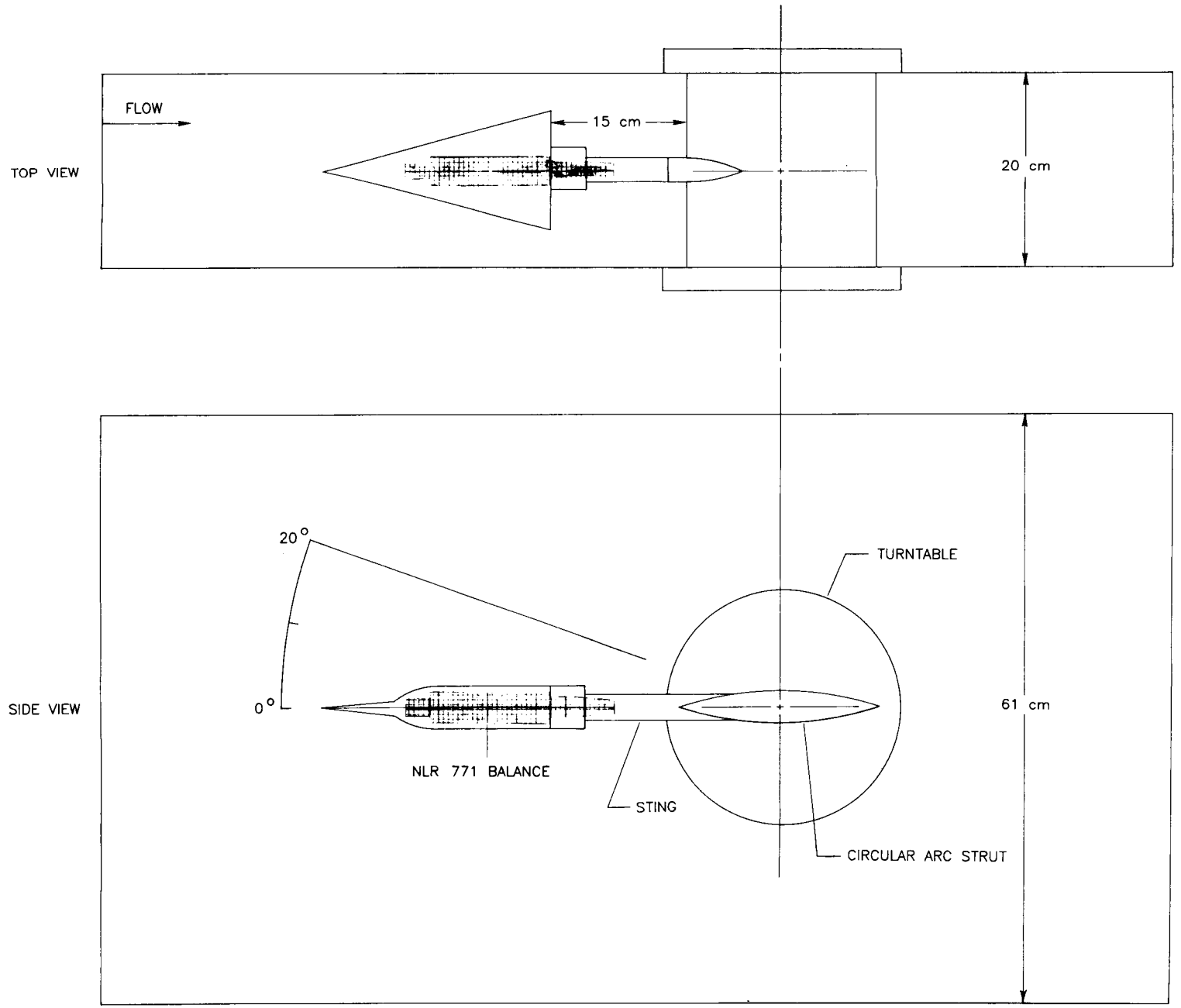

Figure 3. Arrangement of model, sting, and strut support in the Langley 0.3-m TCT.

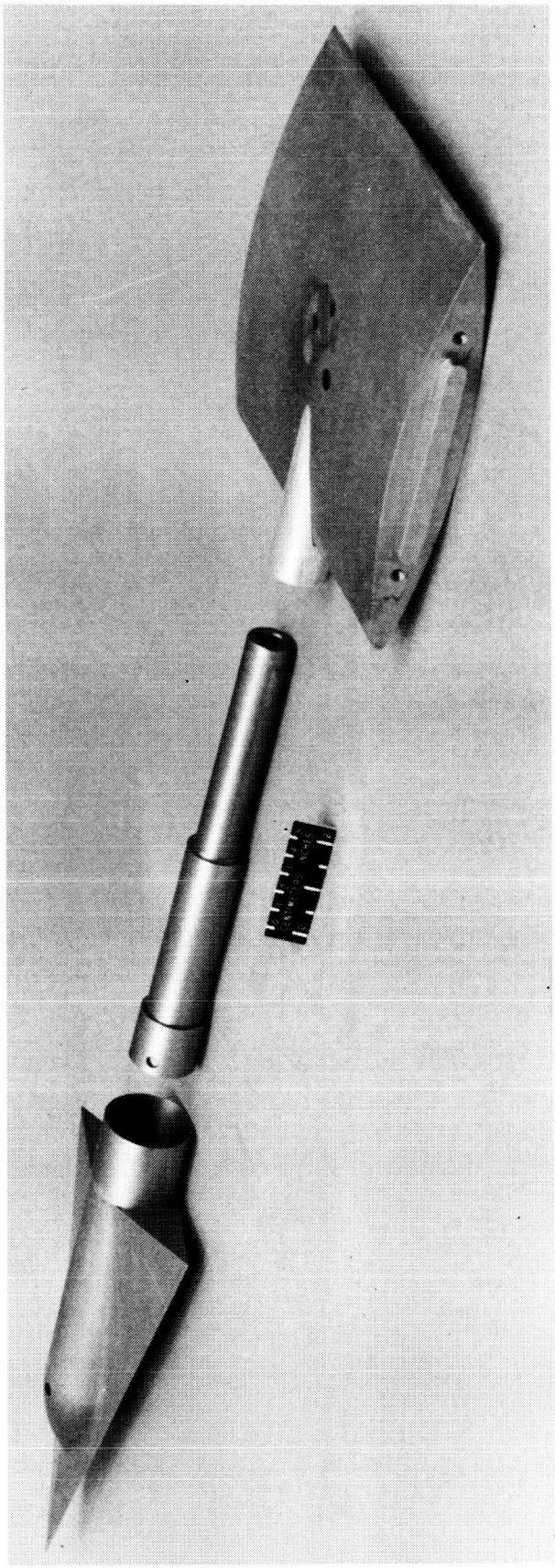

L-79-1689

Figure 4. Model, sting, and support strut.

L-84-4283

Figure 5. Top view of model, sting, and support strut in the Langley 0.3-m TCT.

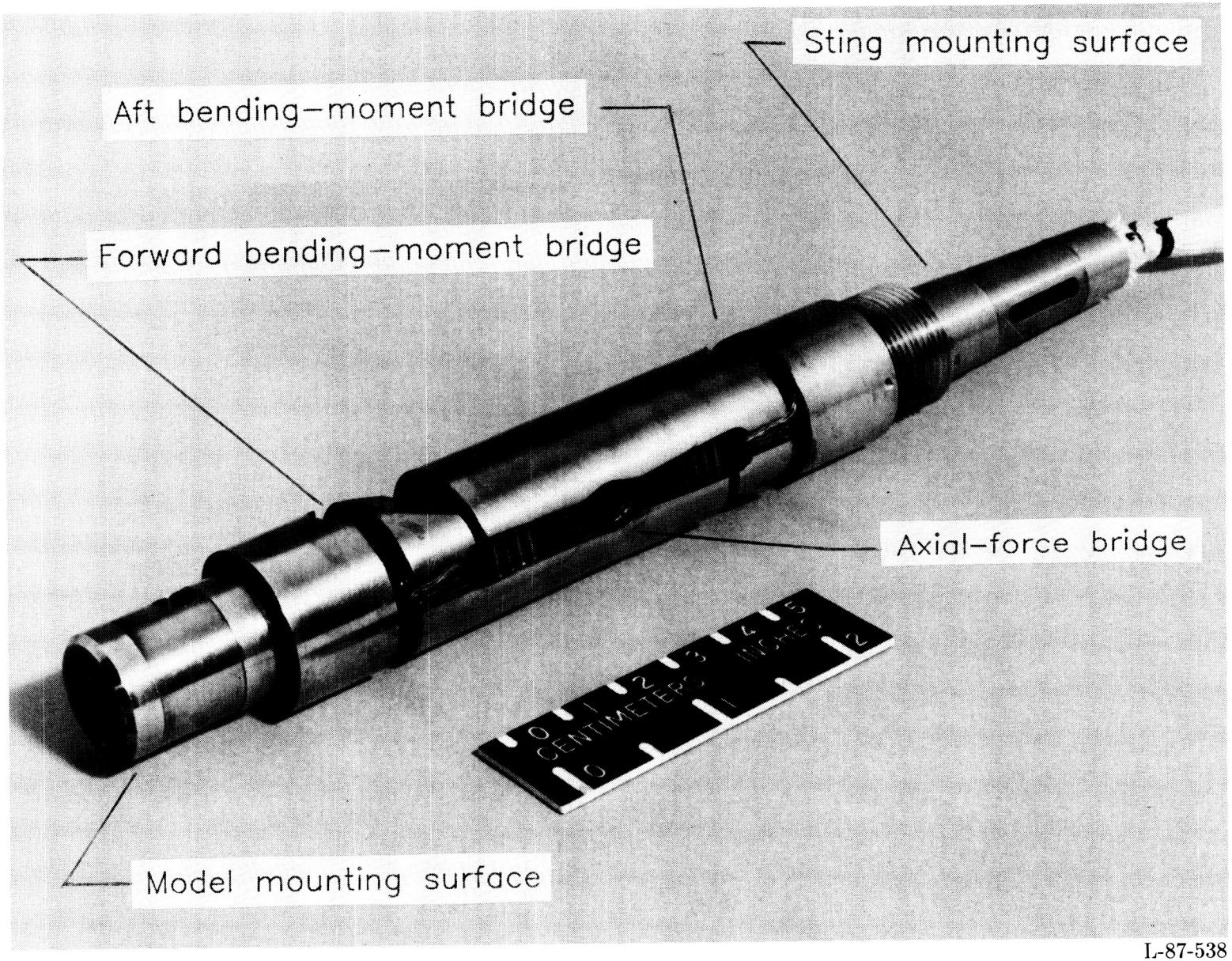

L-87-538

(a) Locations of bridges and mounting surfaces.

Figure 6. NLR 771 cryogenic strain-gage balance.

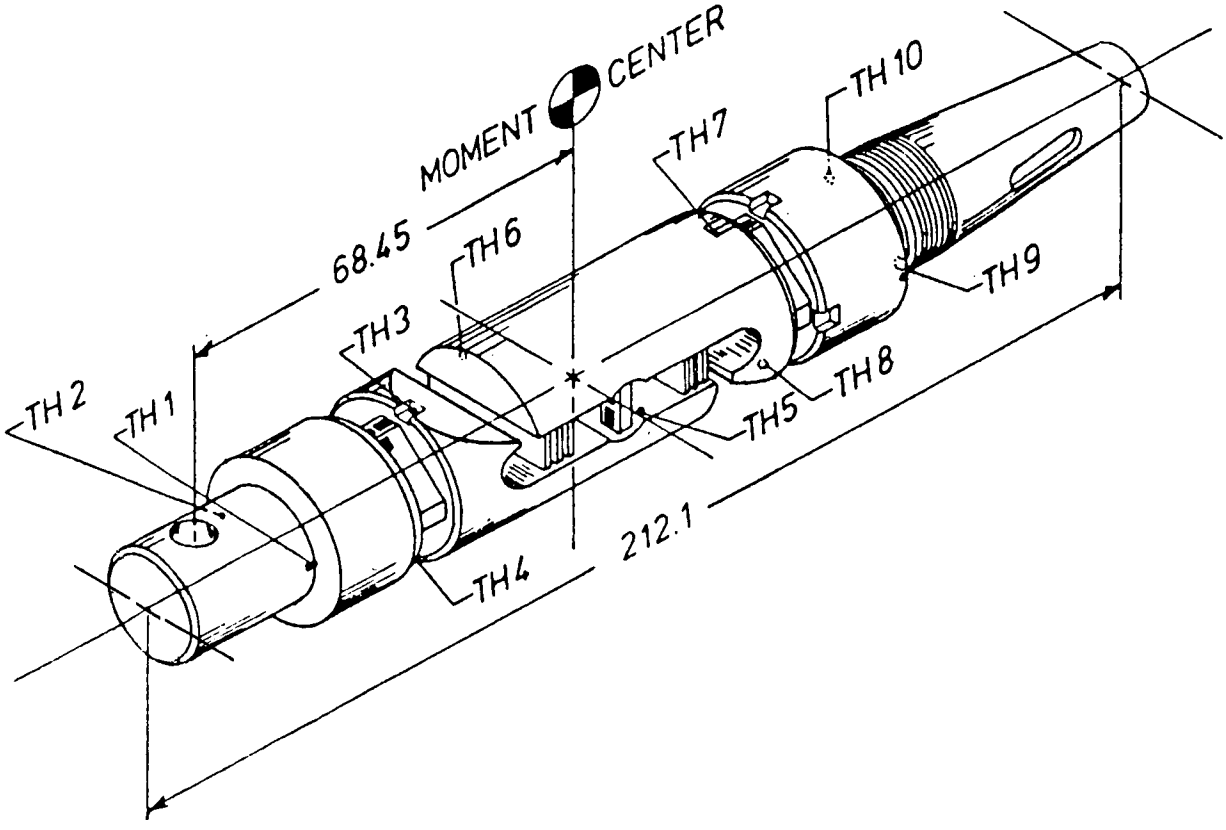

(b) Thermocouple locations. (Dimensions are in millimeters.)

Figure 6. Concluded.

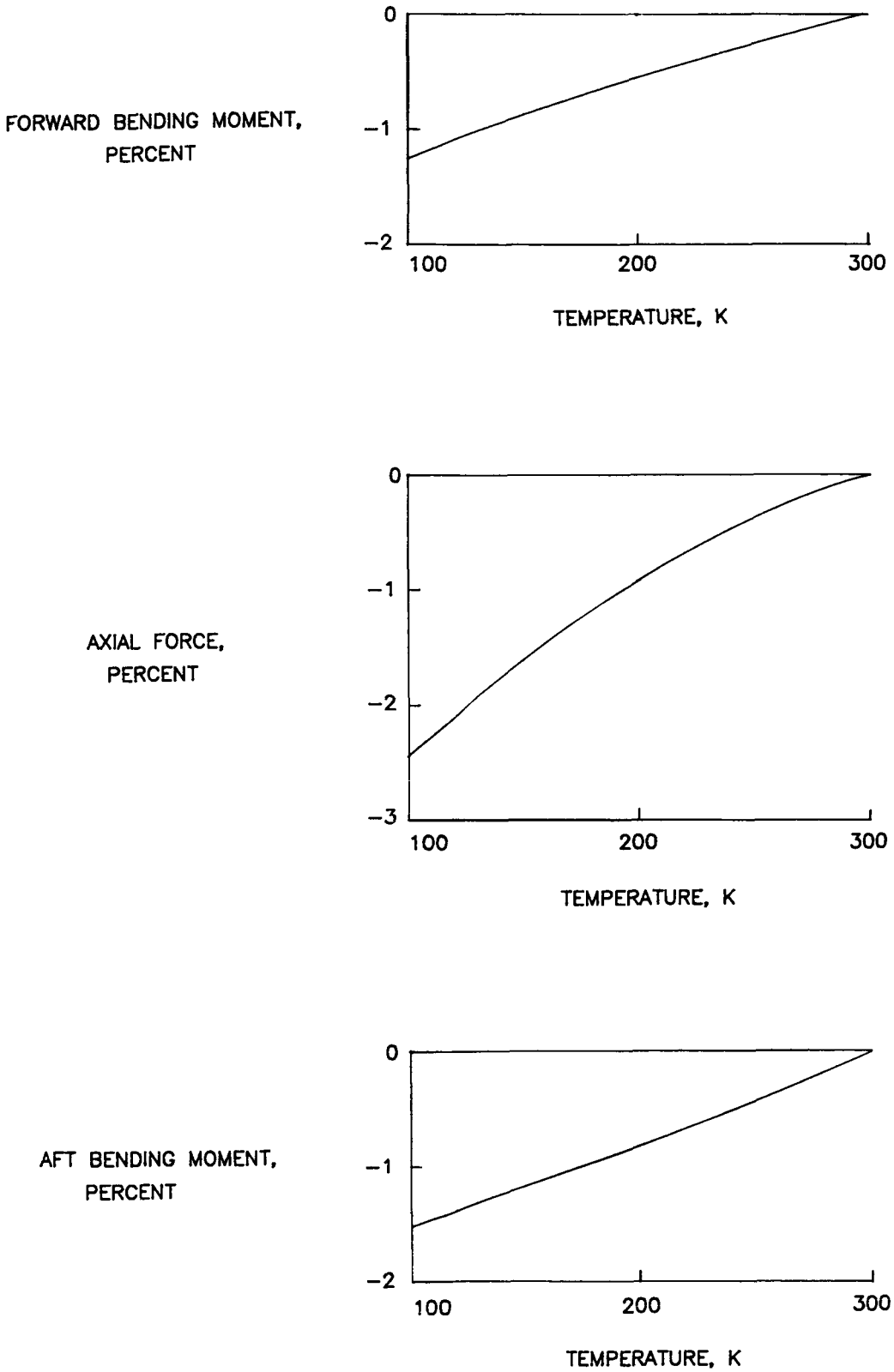

Figure 7. Sensitivity shift of strain-gage bridges on NLR 771 balance.

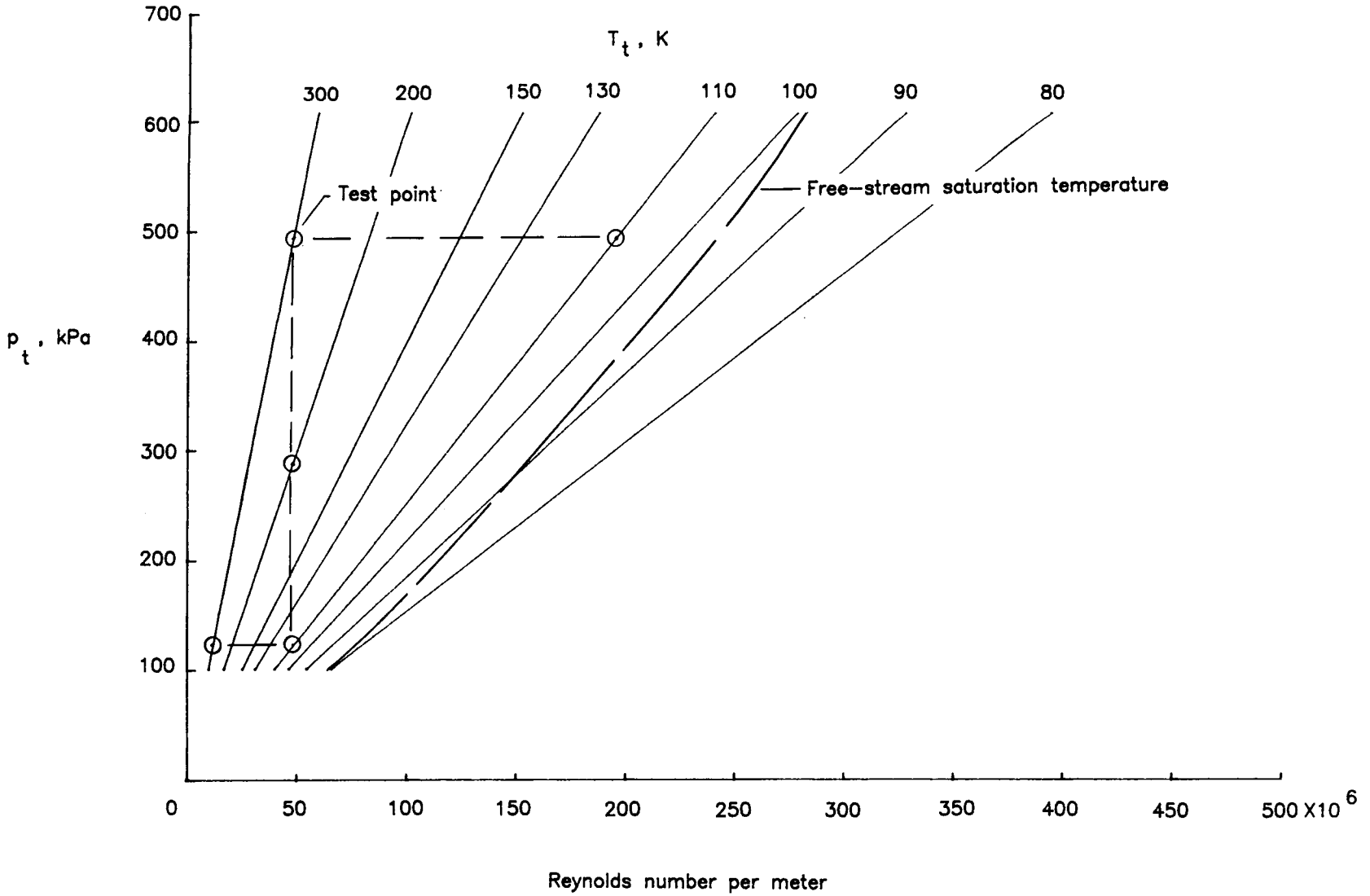

Figure 8. Envelope of typical test conditions in the Langley 0.3-m TCT for $M = 0.5$.

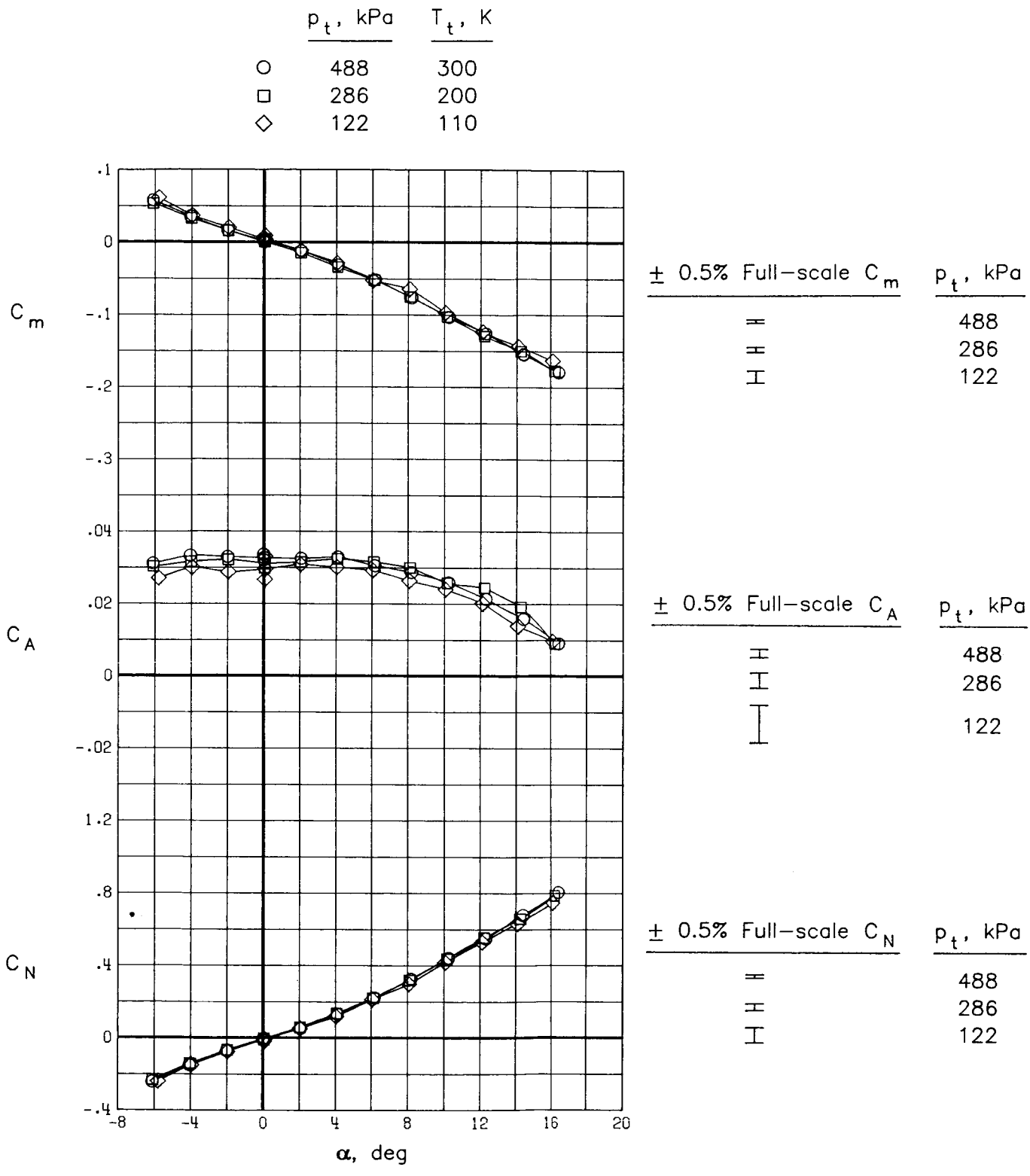

(a) $M = 0.3$; $R = 4.85 \times 10^6$.

Figure 9. Comparison of results with convection shield on at approximately constant Reynolds number.

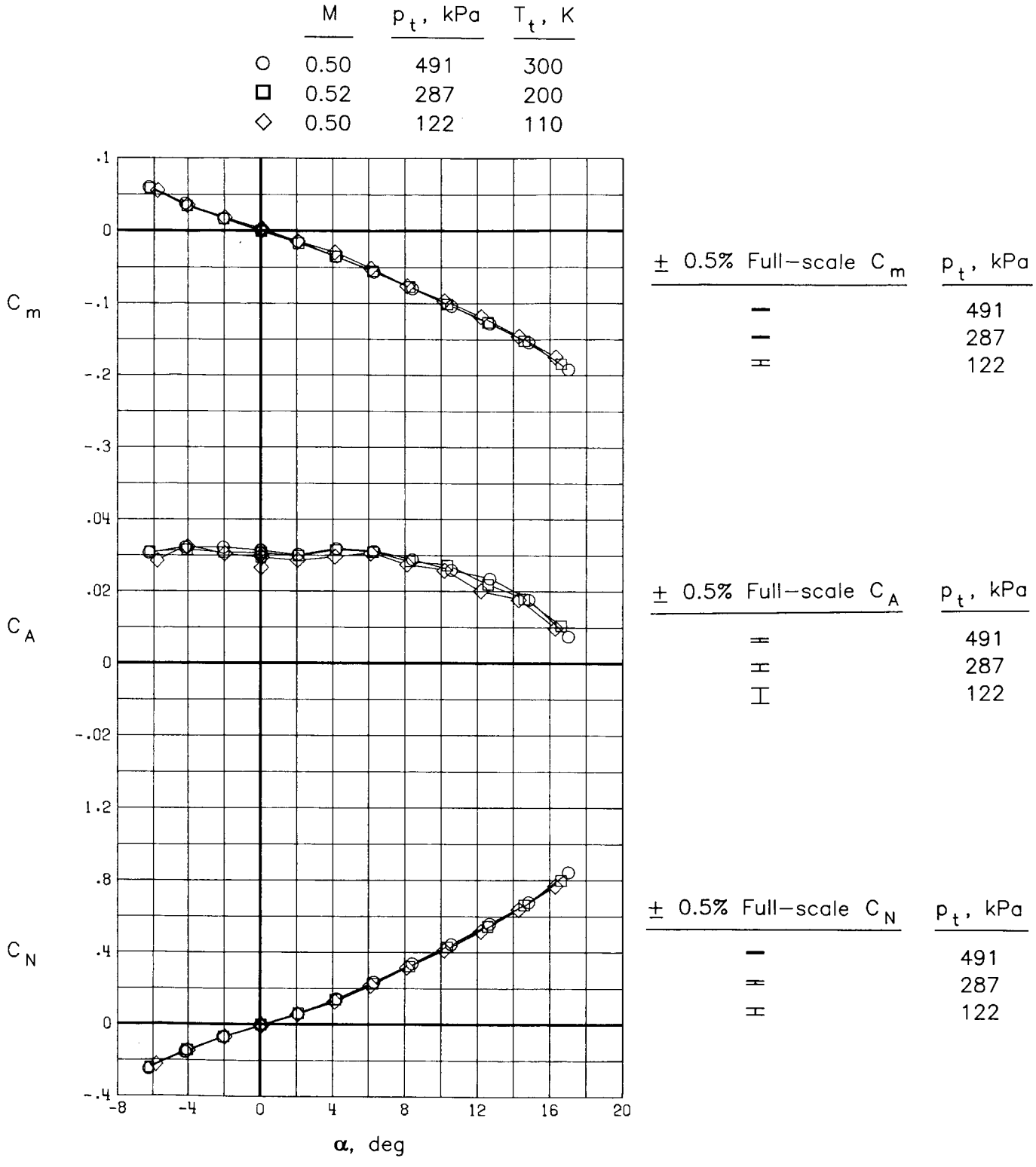

(b) $M = 0.50$ and $R = 7.60 \times 10^6$; $M = 0.52$ and $R = 7.84 \times 10^6$.

Figure 9. Concluded.

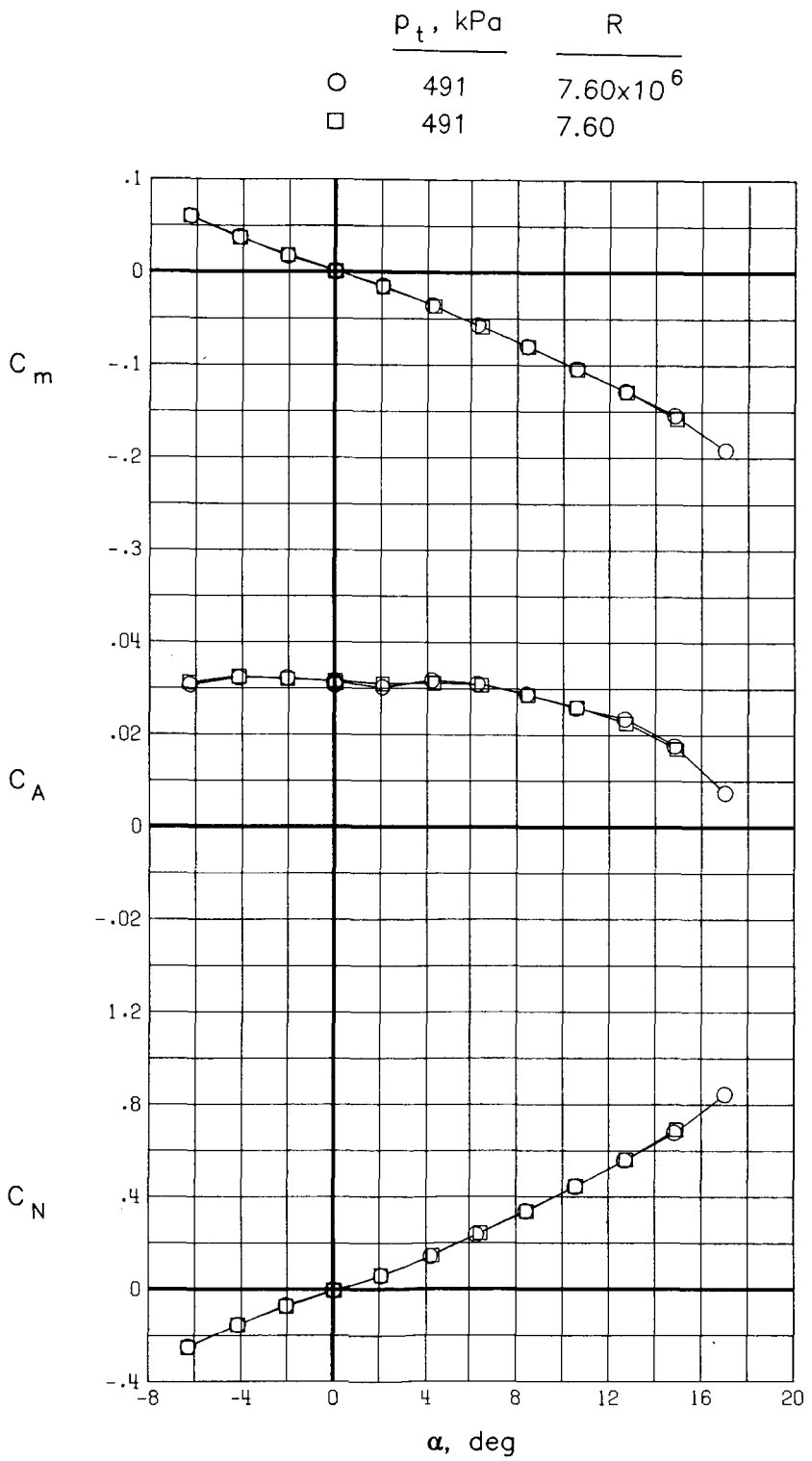

Figure 10. Comparison of results for repeat runs with convection shield on at $M = 0.5$ and $T_t = 300$ K.

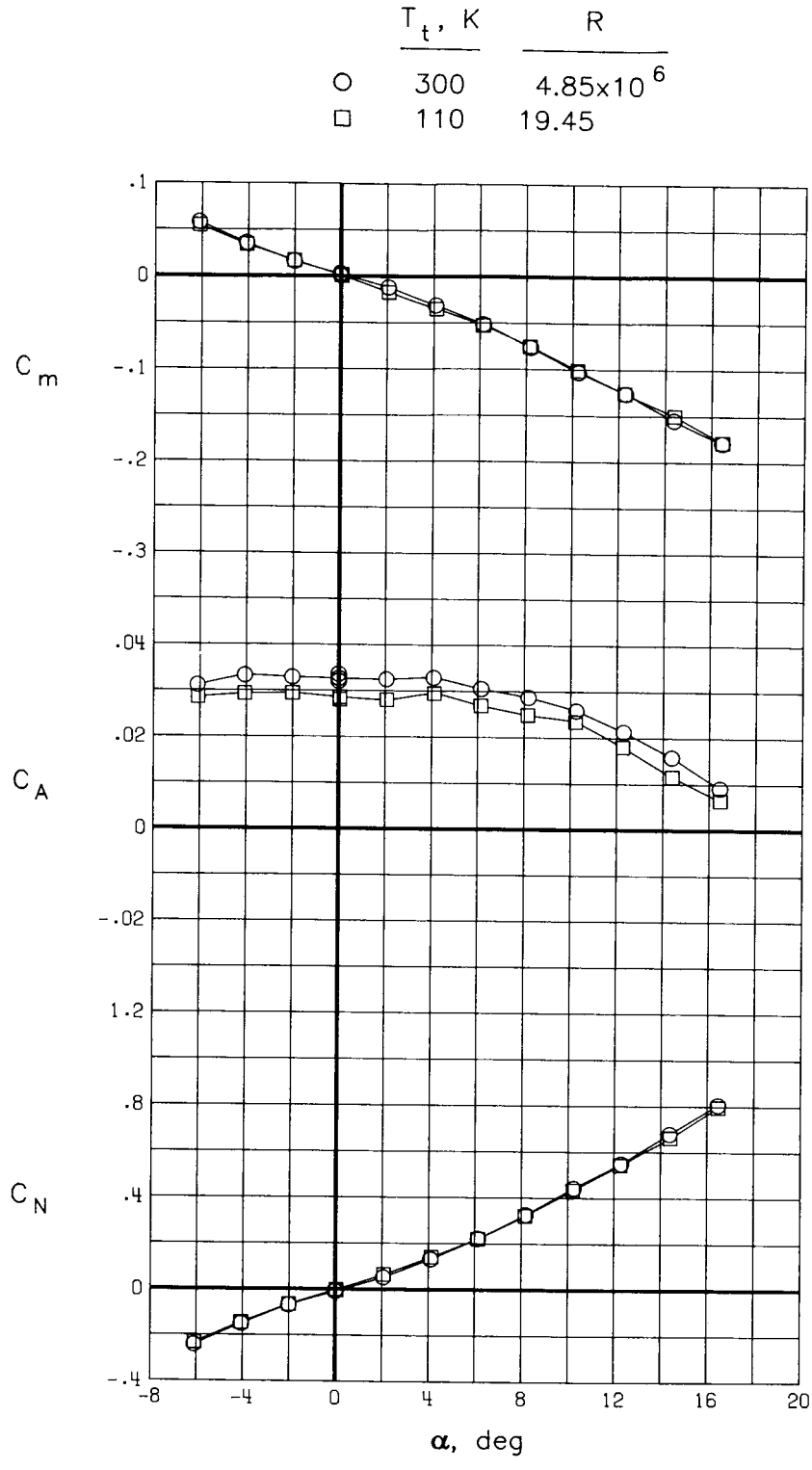

(a) $M = 0.3$; $p_t = 488$ kPa.

Figure 11. Comparison of results with convection shield on at constant pressure.

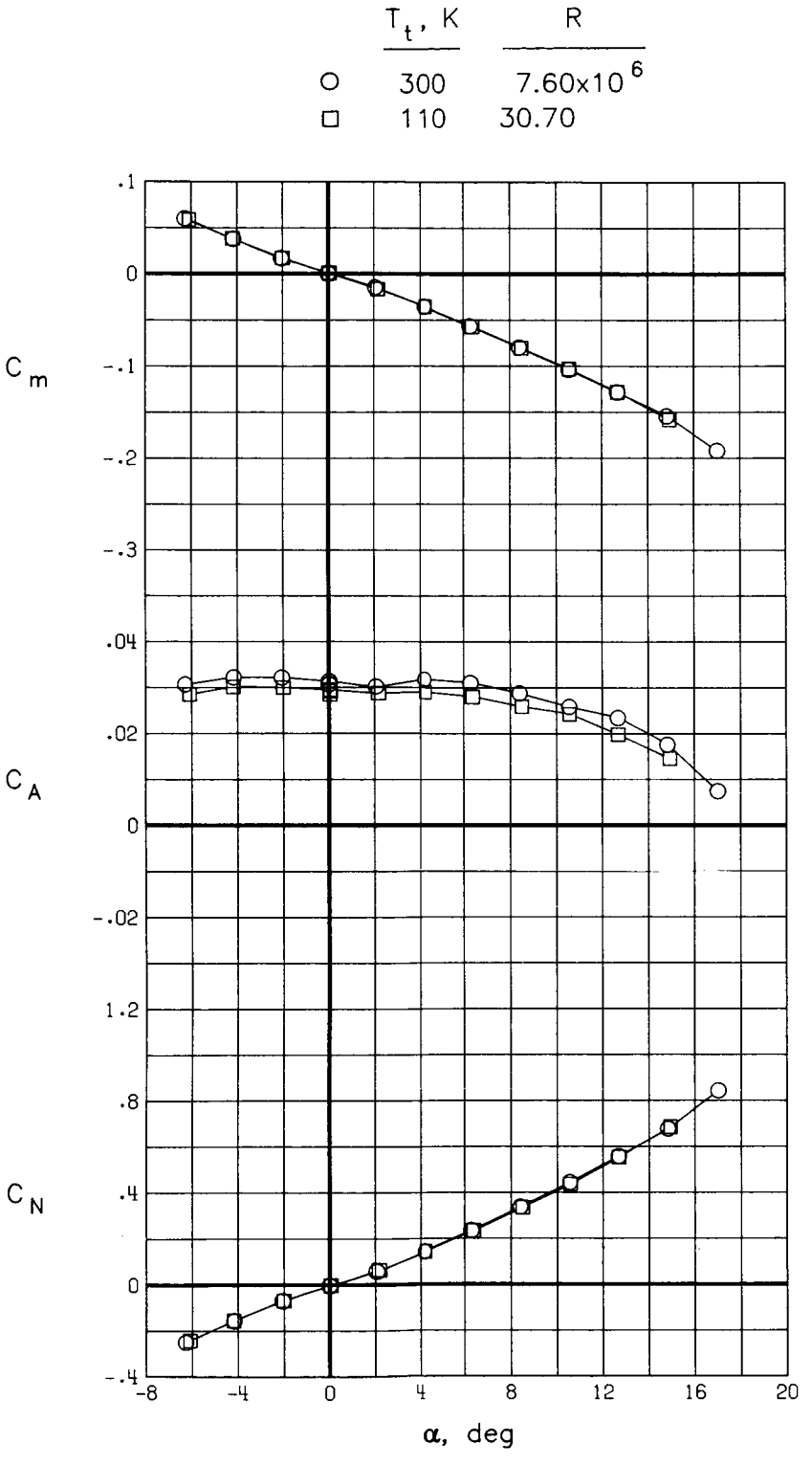

(b) $M = 0.5$; $p_t = 491$ kPa.

Figure 11. Continued.

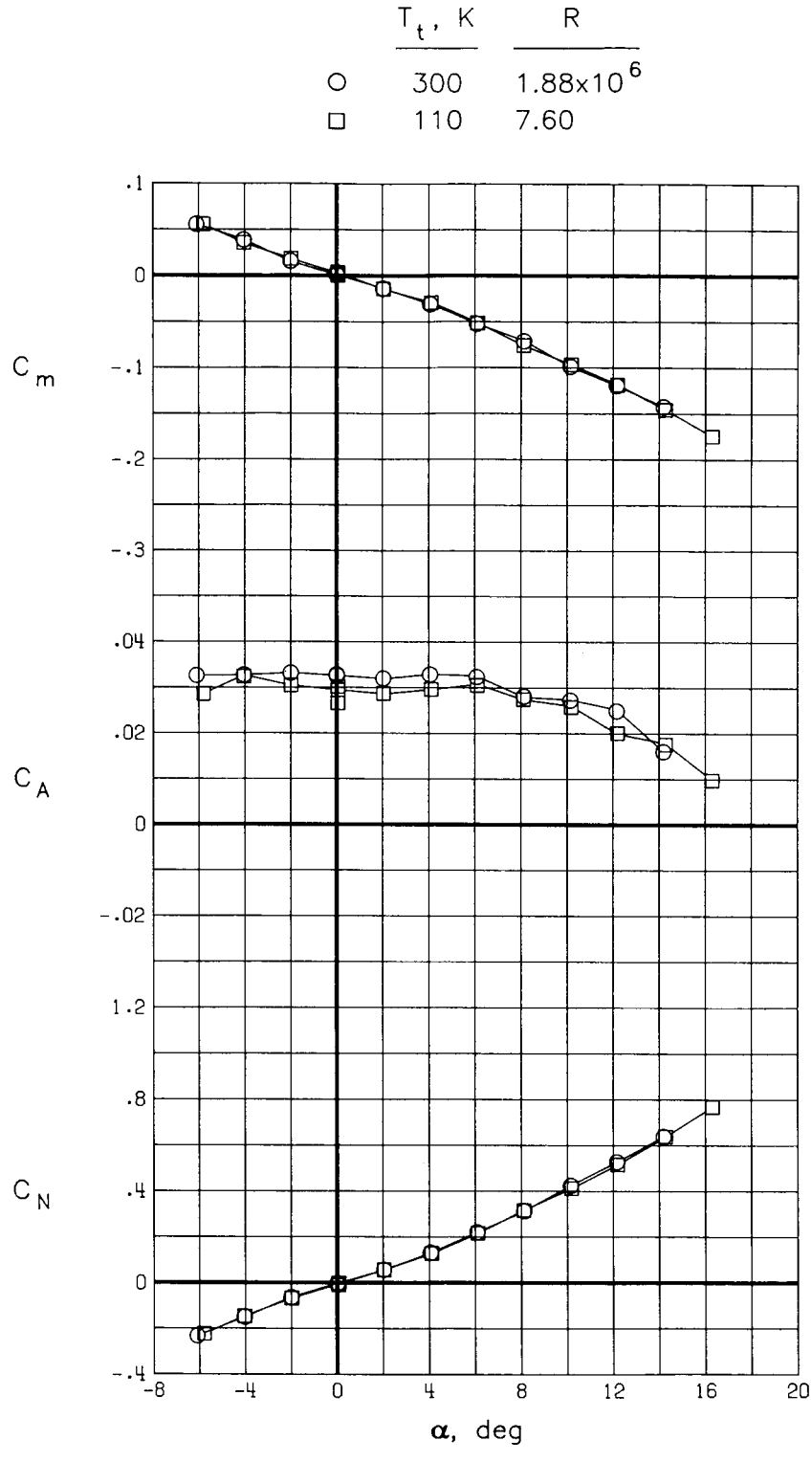

(c) $M = 0.5$; $p_t = 122$ kPa.

Figure 11. Concluded.

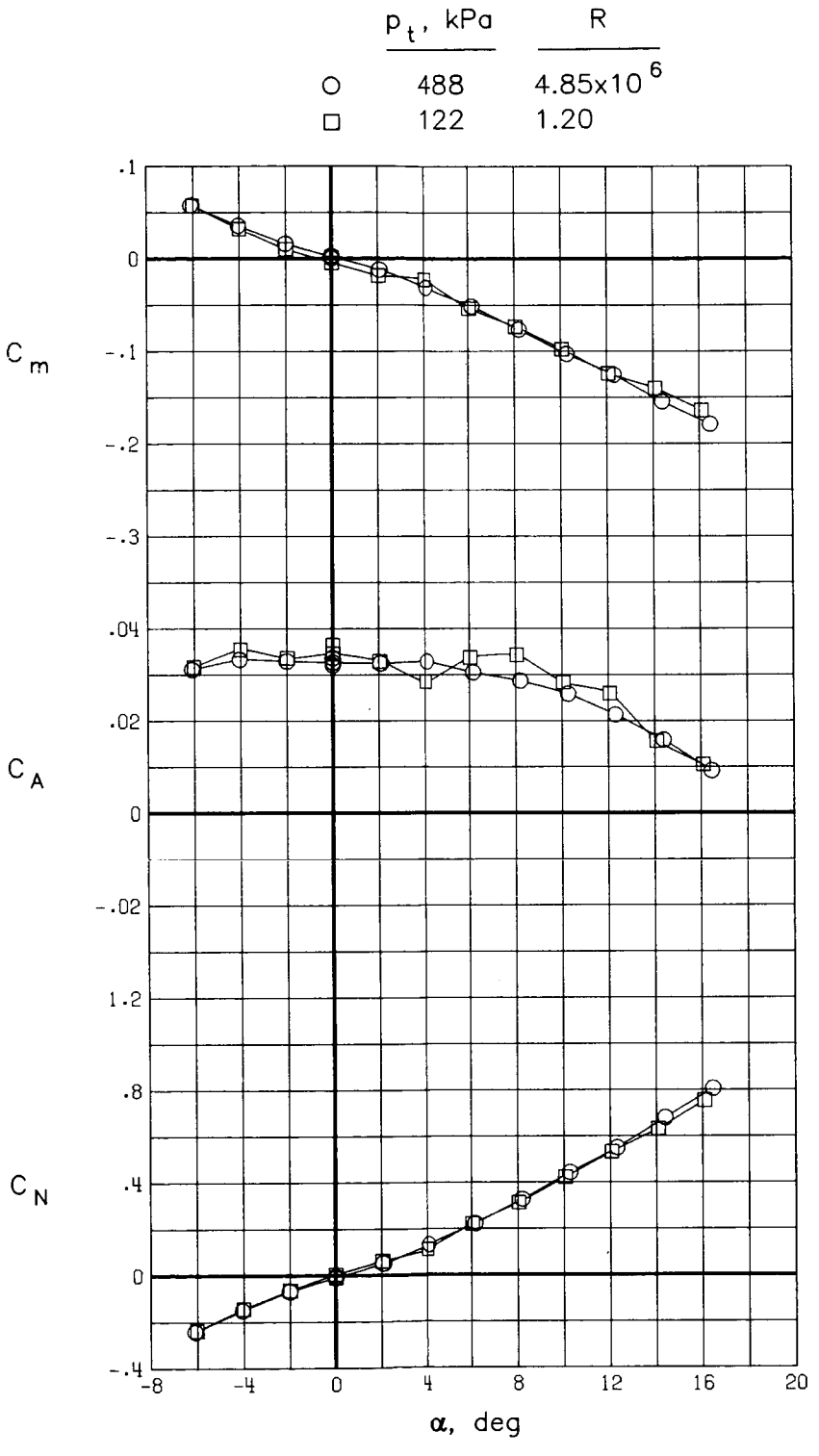

(a) $M = 0.3$.

Figure 12. Comparison of results with convection shield on at $T_t = 300$ K.

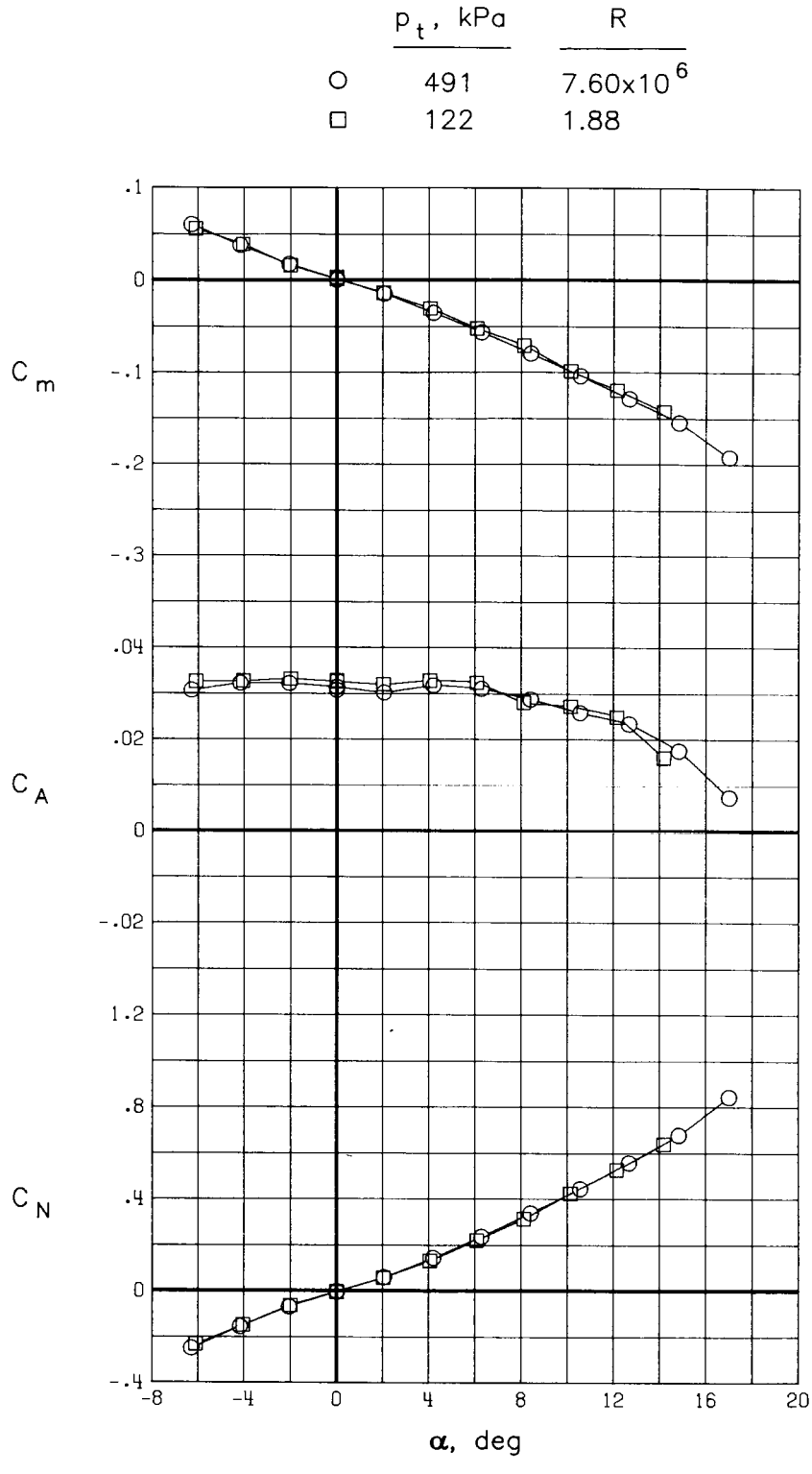

(b) $M = 0.5$.

Figure 12. Concluded.

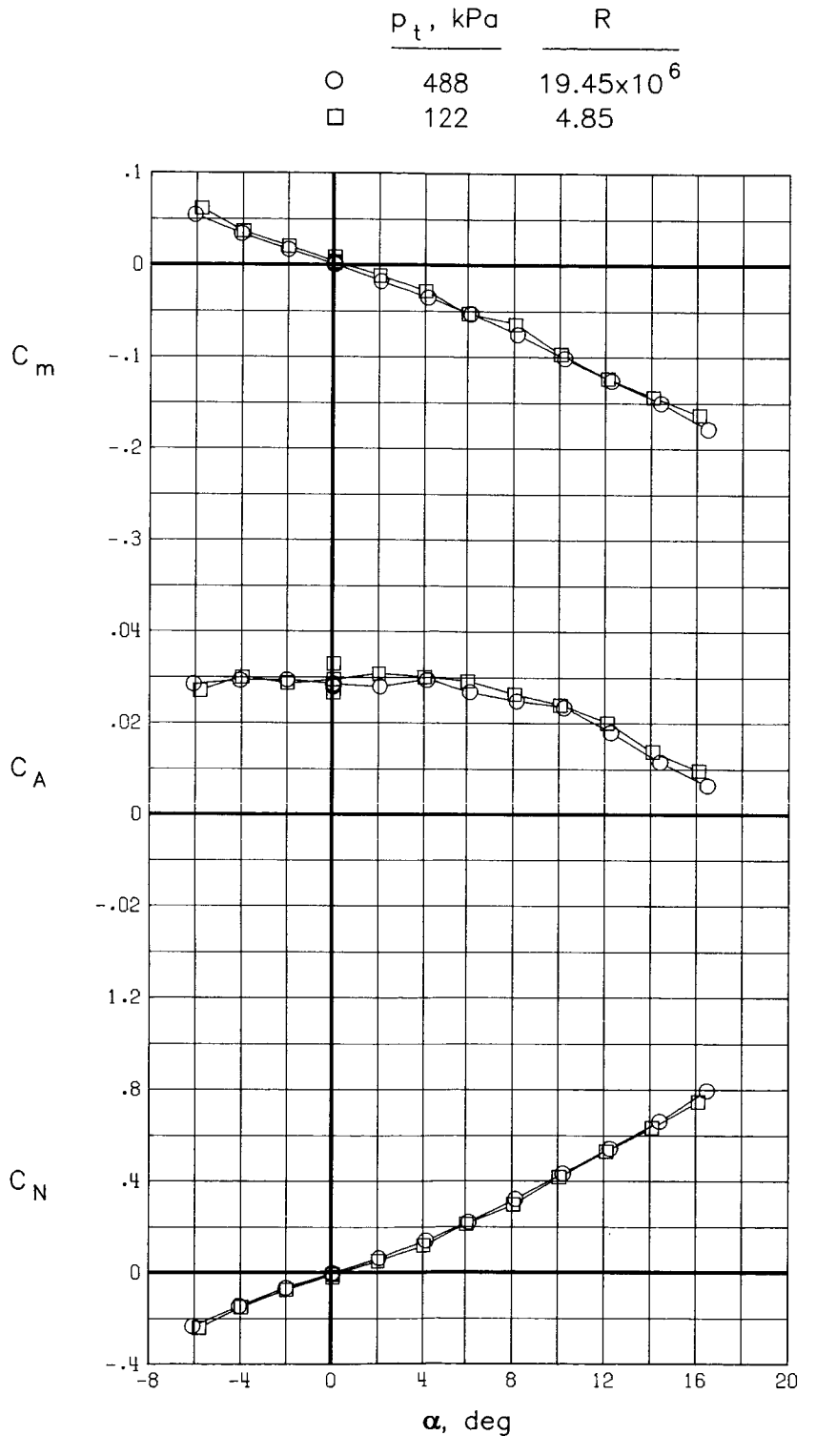

(a) $M = 0.3$.

Figure 13. Comparison of results with convection shield on at $T_t = 110$ K.

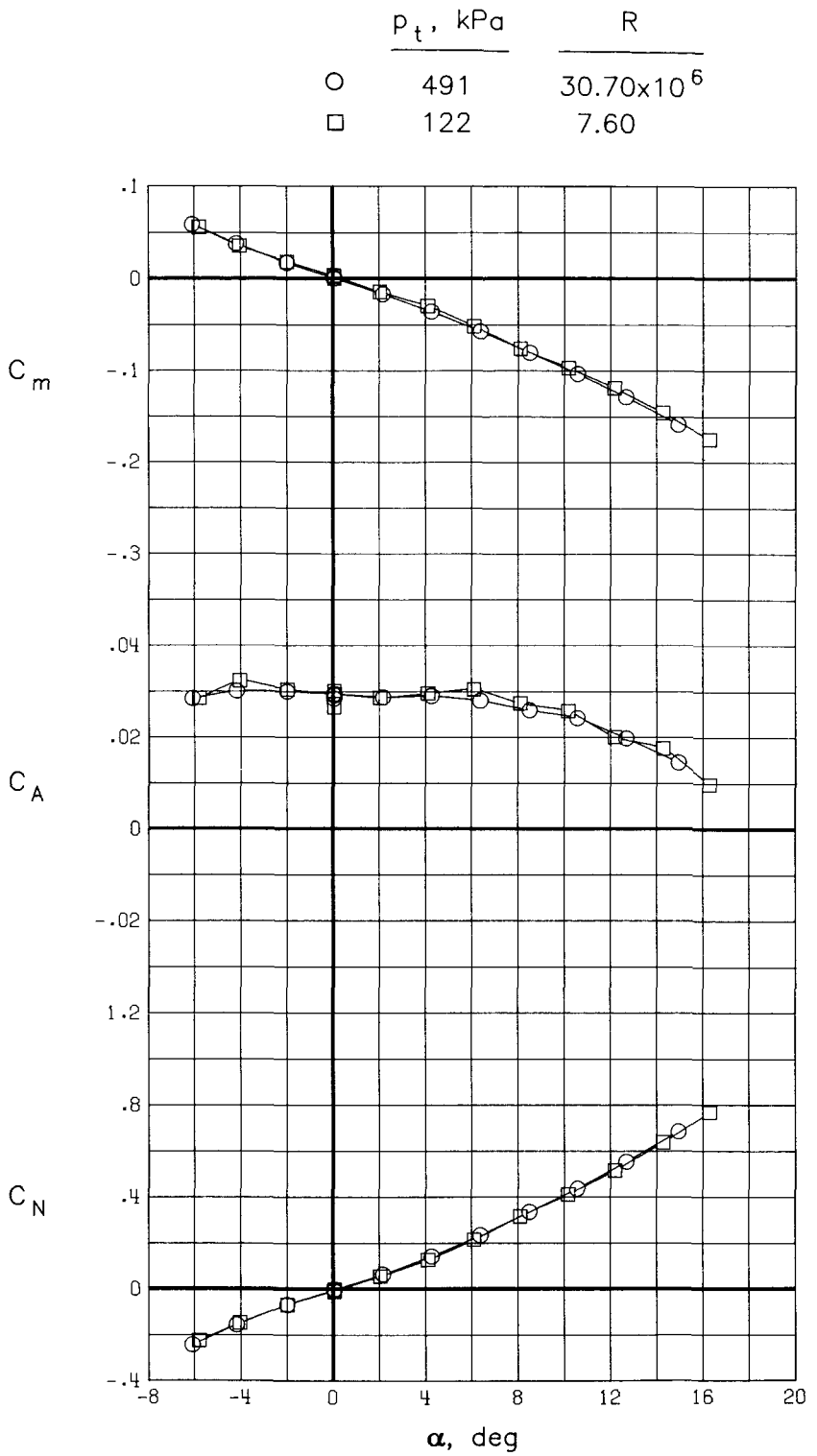

(b) $M = 0.5$.

Figure 13. Concluded.

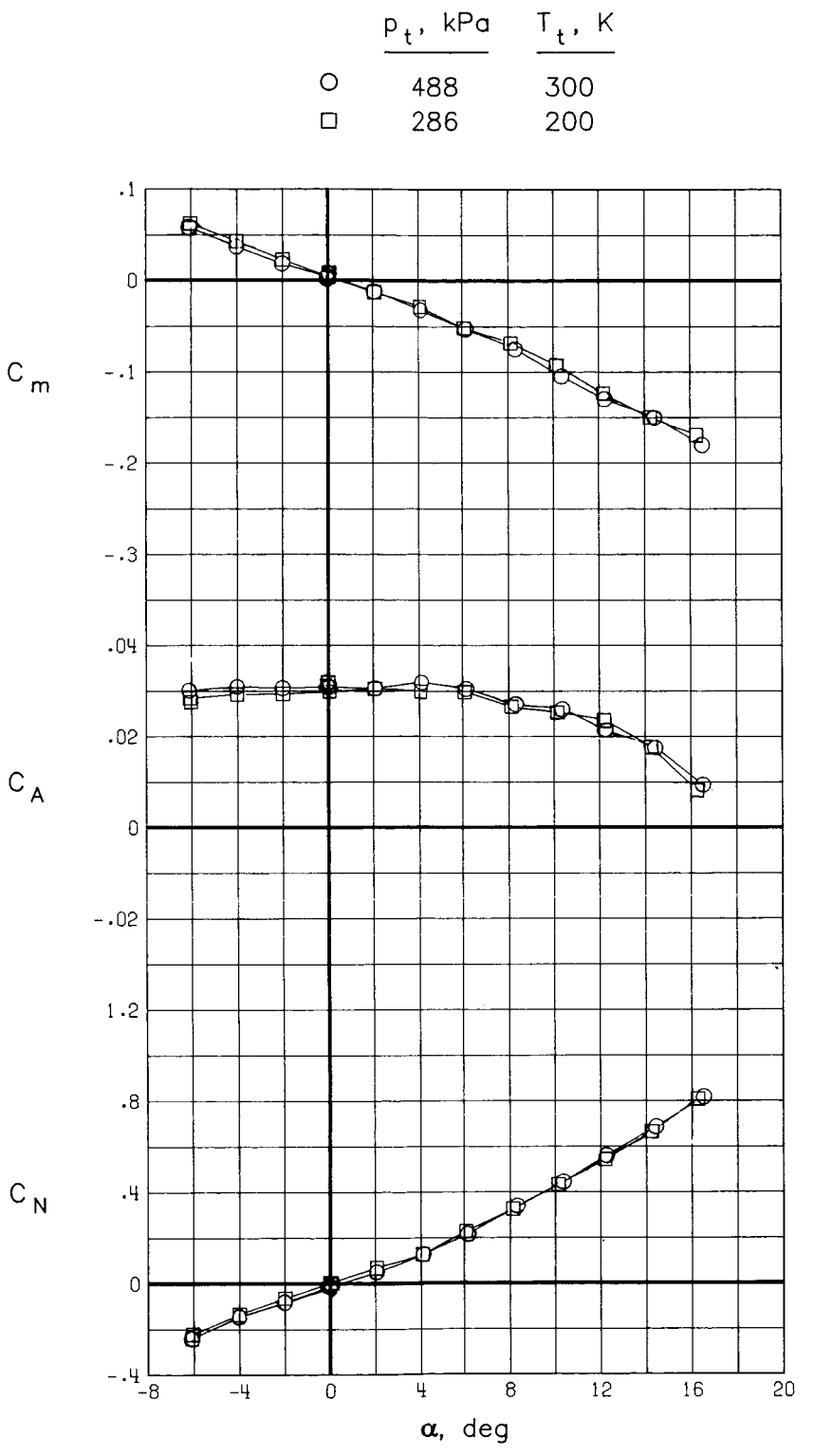

(a) $M = 0.3$; $R = 4.85 \times 10^6$.

Figure 14. Comparison of results with convection shield off at approximately constant Reynolds number.

	M	p_t, kPa	T_t, K	R
○	0.50	491	300	7.60×10^6
□	0.52	287	200	7.84
◇	0.50	122	110	7.60

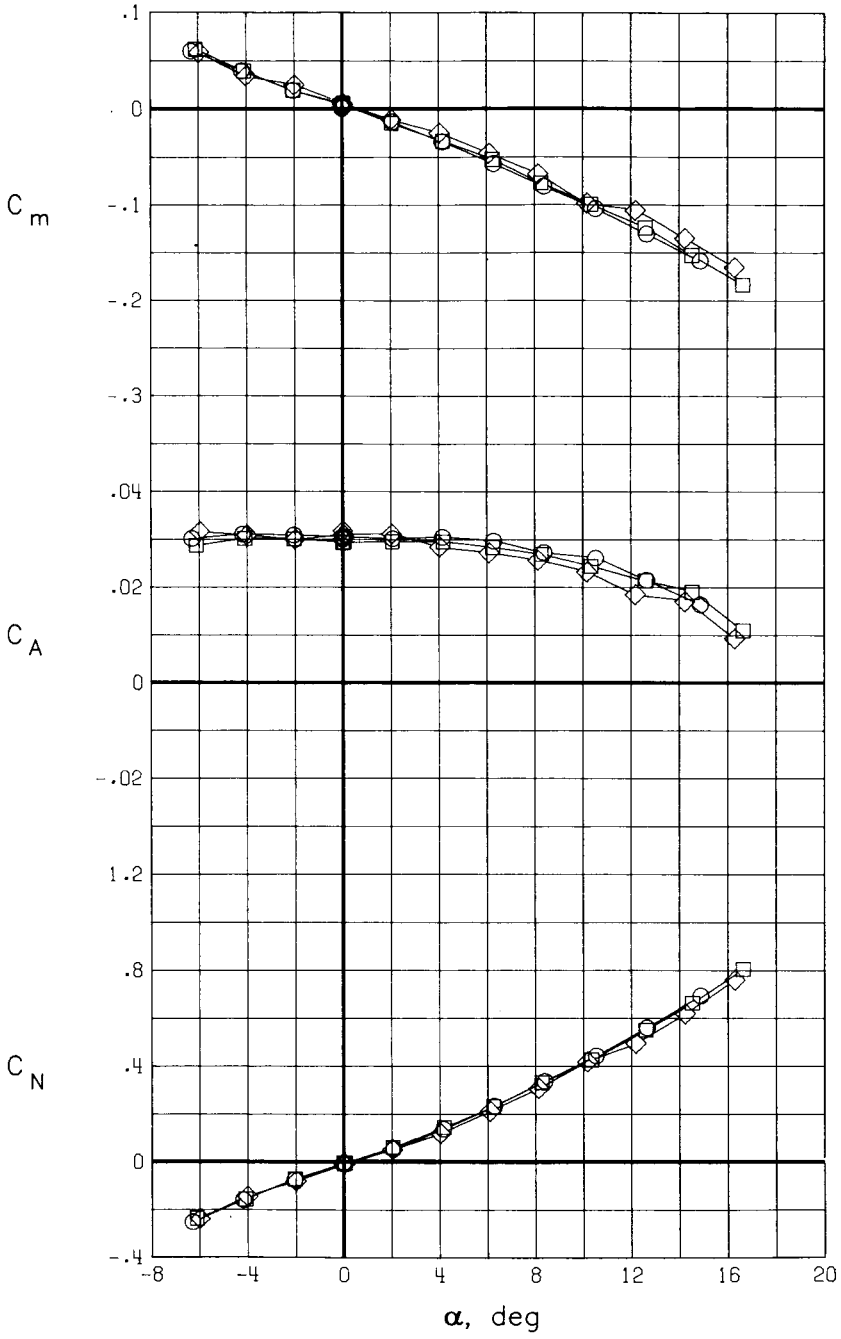

(b) $M = 0.50$ and $R = 7.60 \times 10^6$; $M = 0.52$ and $R = 7.84 \times 10^6$.

Figure 14. Concluded.

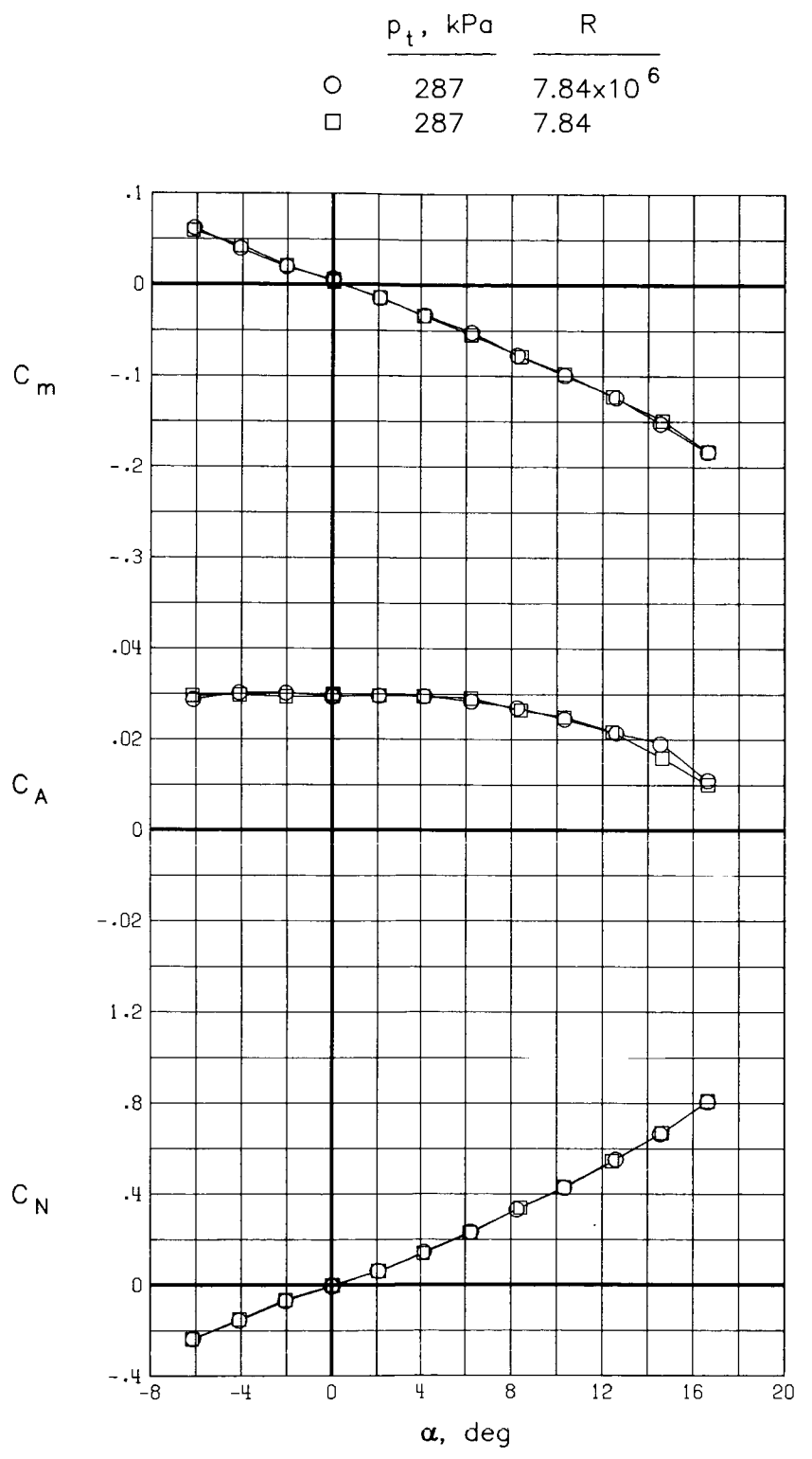

Figure 15. Comparison of results for repeat runs with convection shield off at $M = 0.52$ and $T_t = 200$ K.

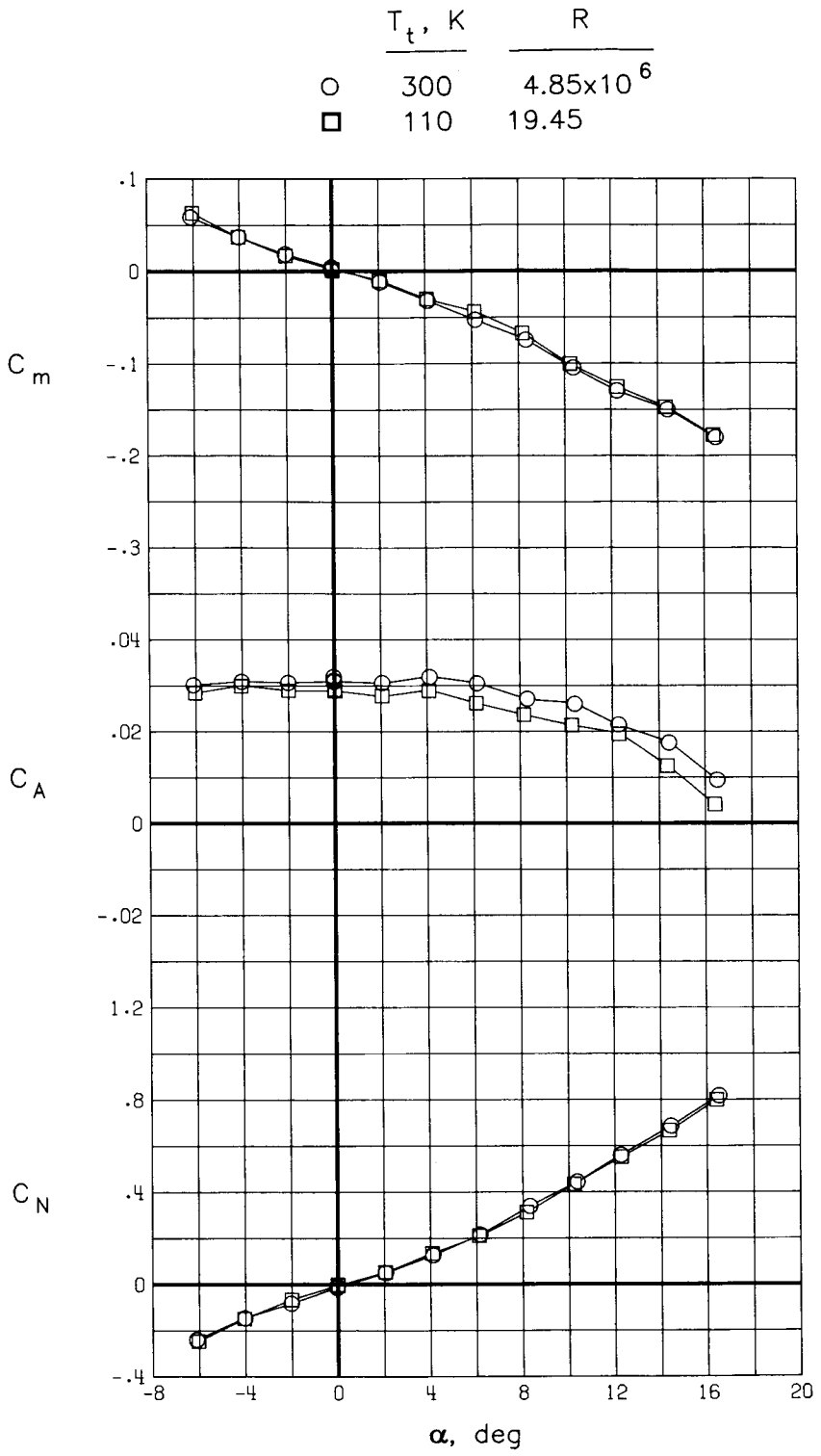

(a) $M = 0.3$; $p_t = 488$ kPa.

Figure 16. Comparison of results with convection shield off at constant pressure.

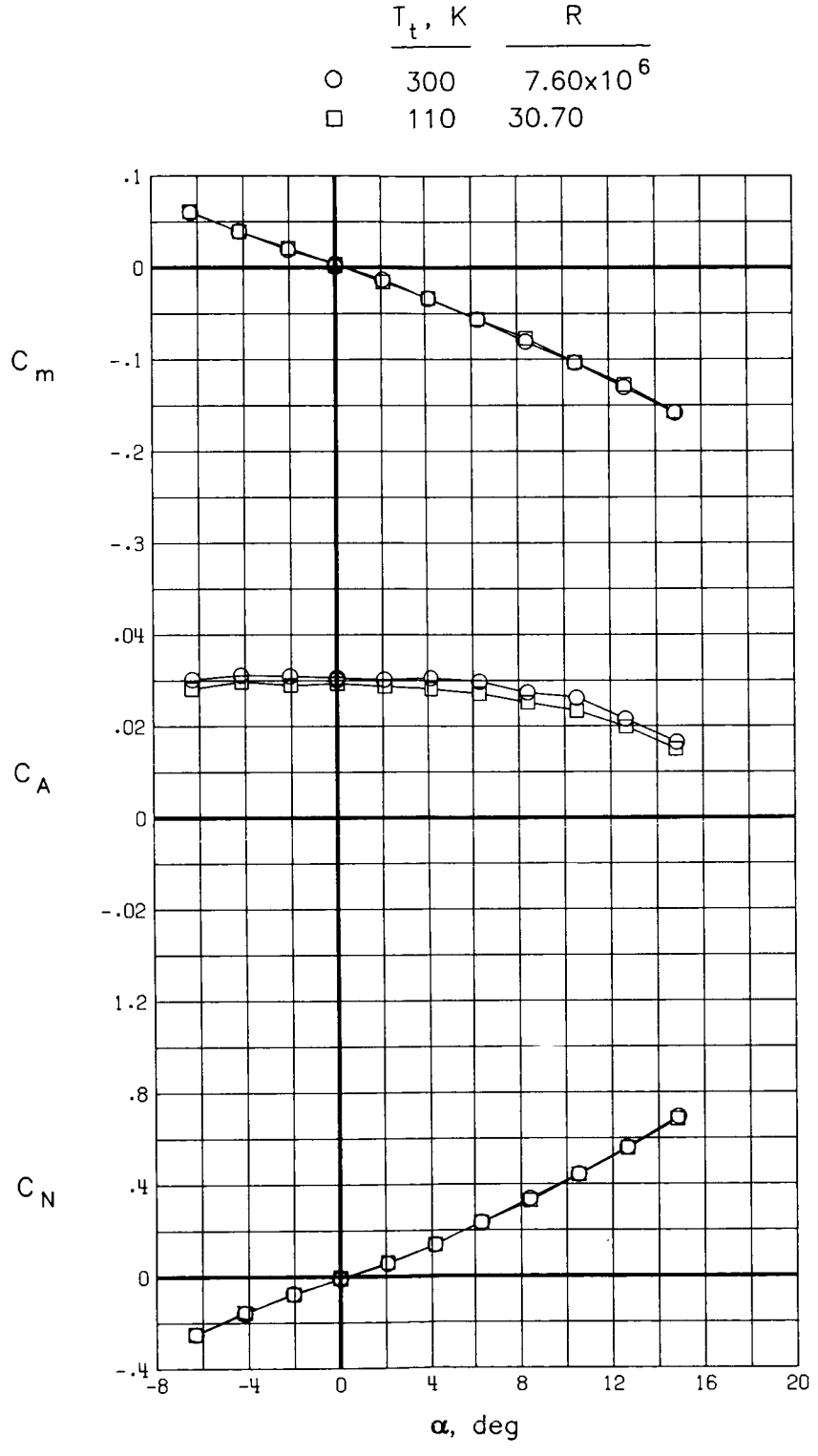

(b) $M = 0.5$; $p_t = 491$ kPa.

Figure 16. Concluded.

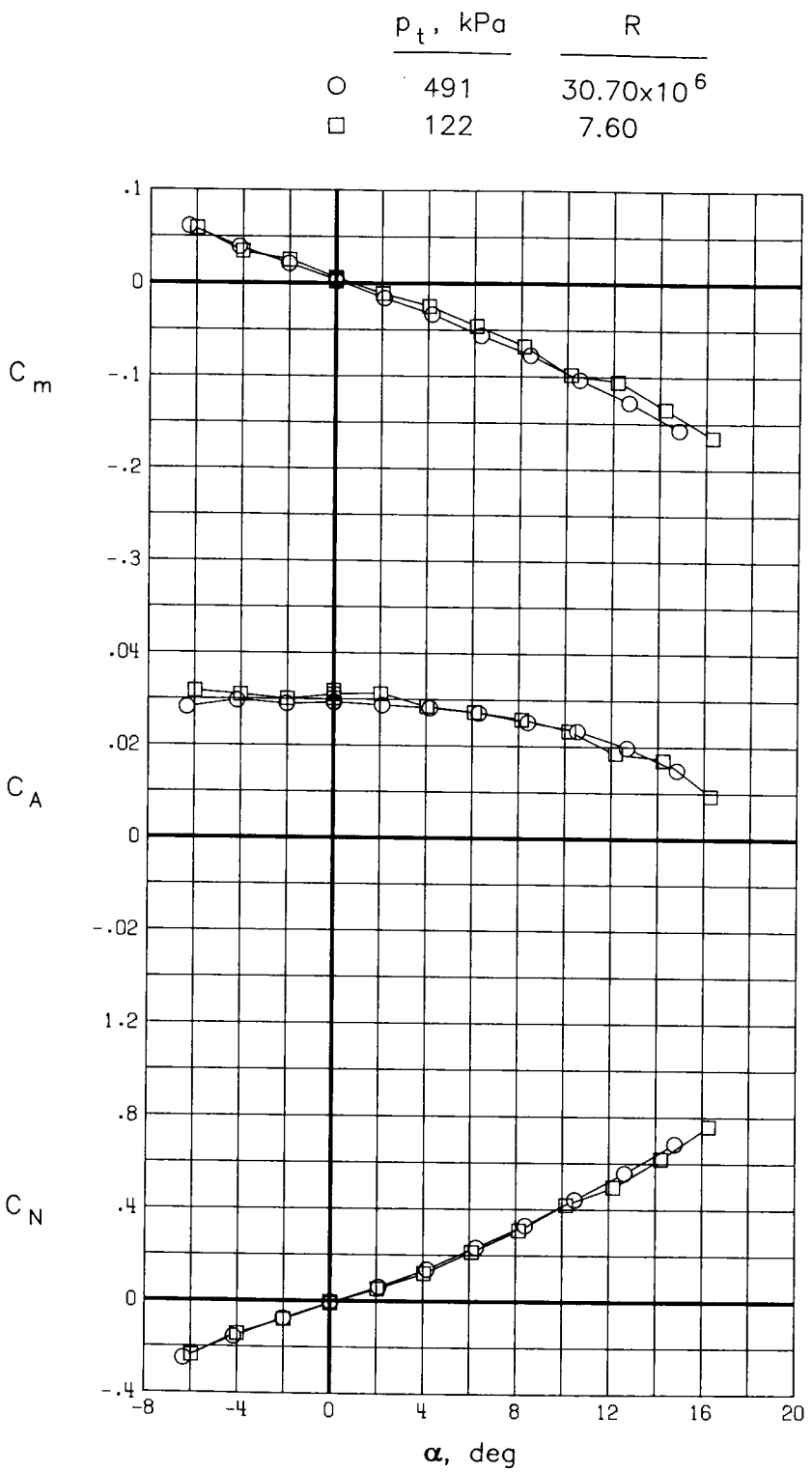

Figure 17. Comparison of results with convection shield off at $M = 0.5$ and $T_t = 110$ K.

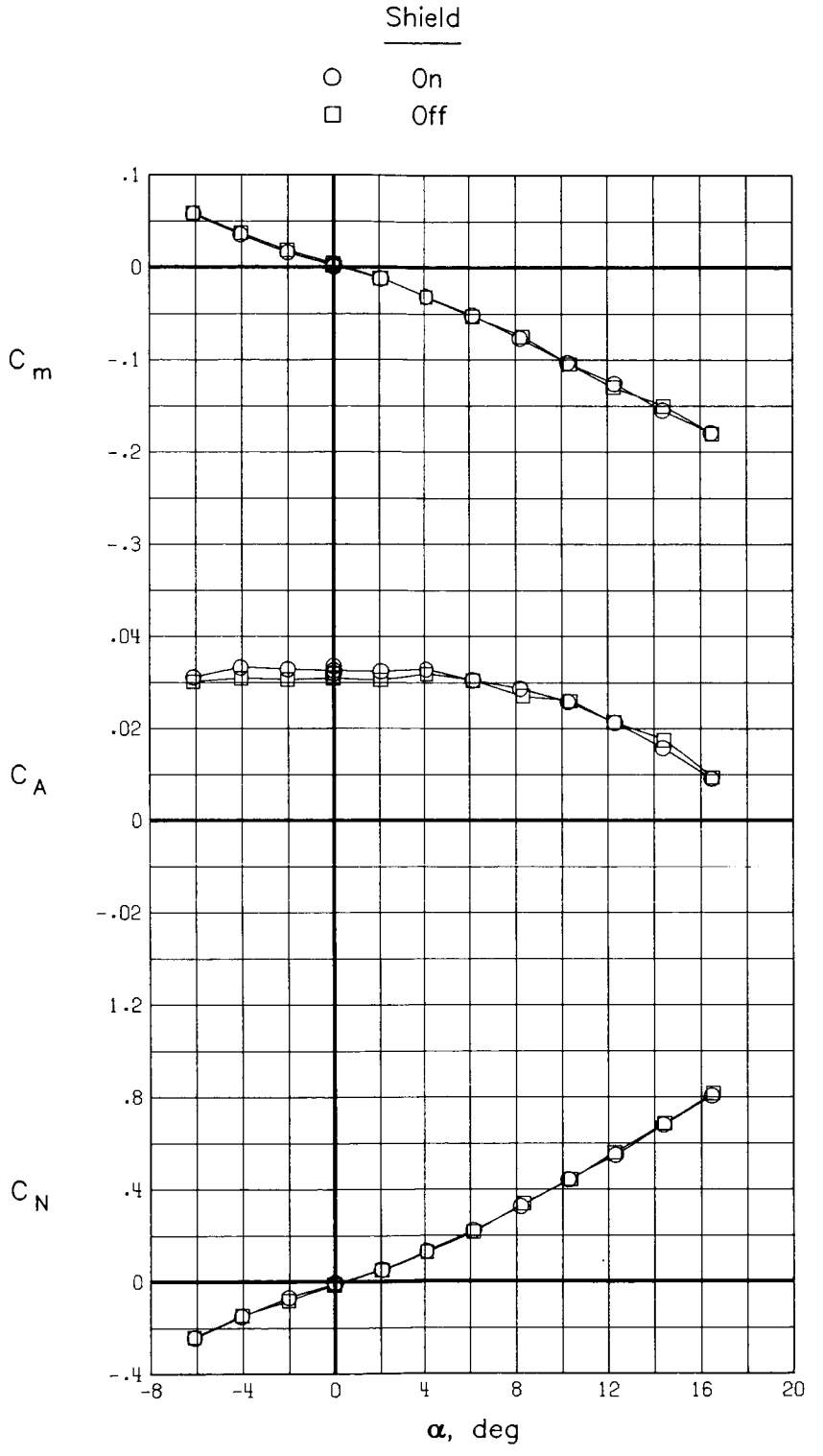

(a) $M = 0.3$; $p_t = 488$ kPa; and $R = 4.85 \times 10^6$.

Figure 18. Comparison of results with convection shield on and off at $T_t = 300$ K.

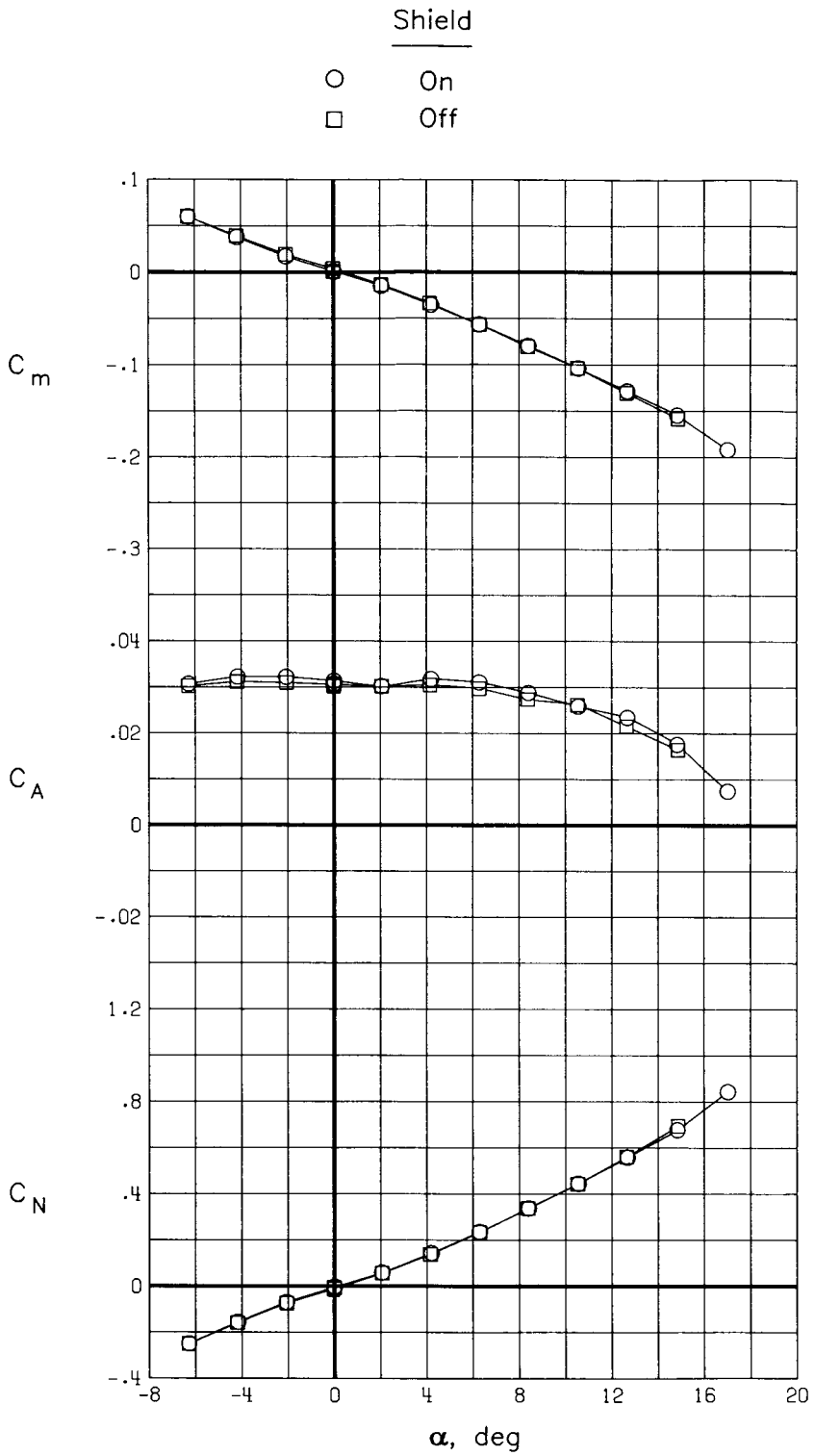

(b) $M = 0.5$; $p_t = 491$ kPa; and $R = 7.60 \times 10^6$.

Figure 18. Concluded.

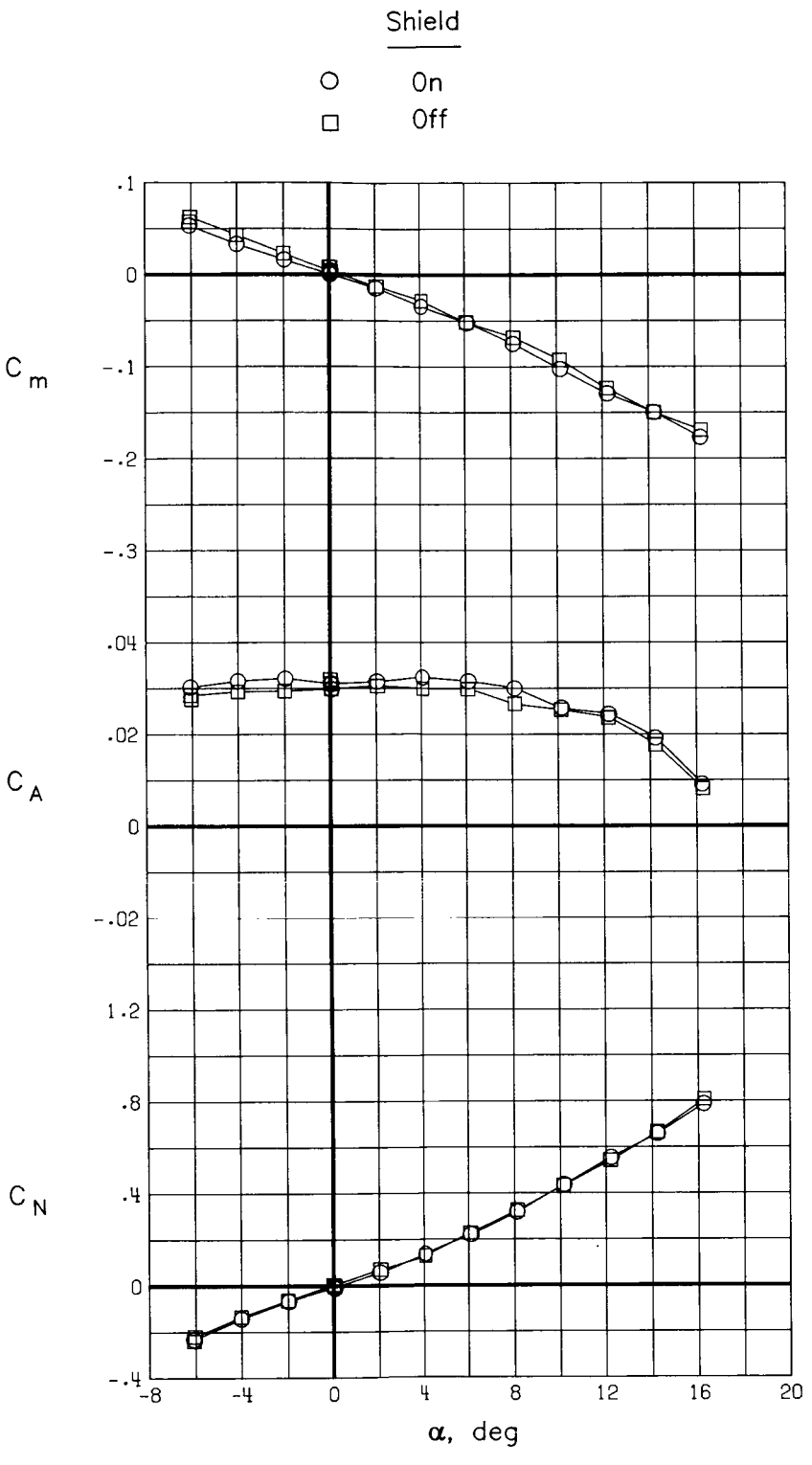

(a) $M = 0.3$; $p_t = 286$ kPa; and $R = 4.85 \times 10^6$.

Figure 19. Comparison of results with convection shield on and off at $T_t = 200$ K.

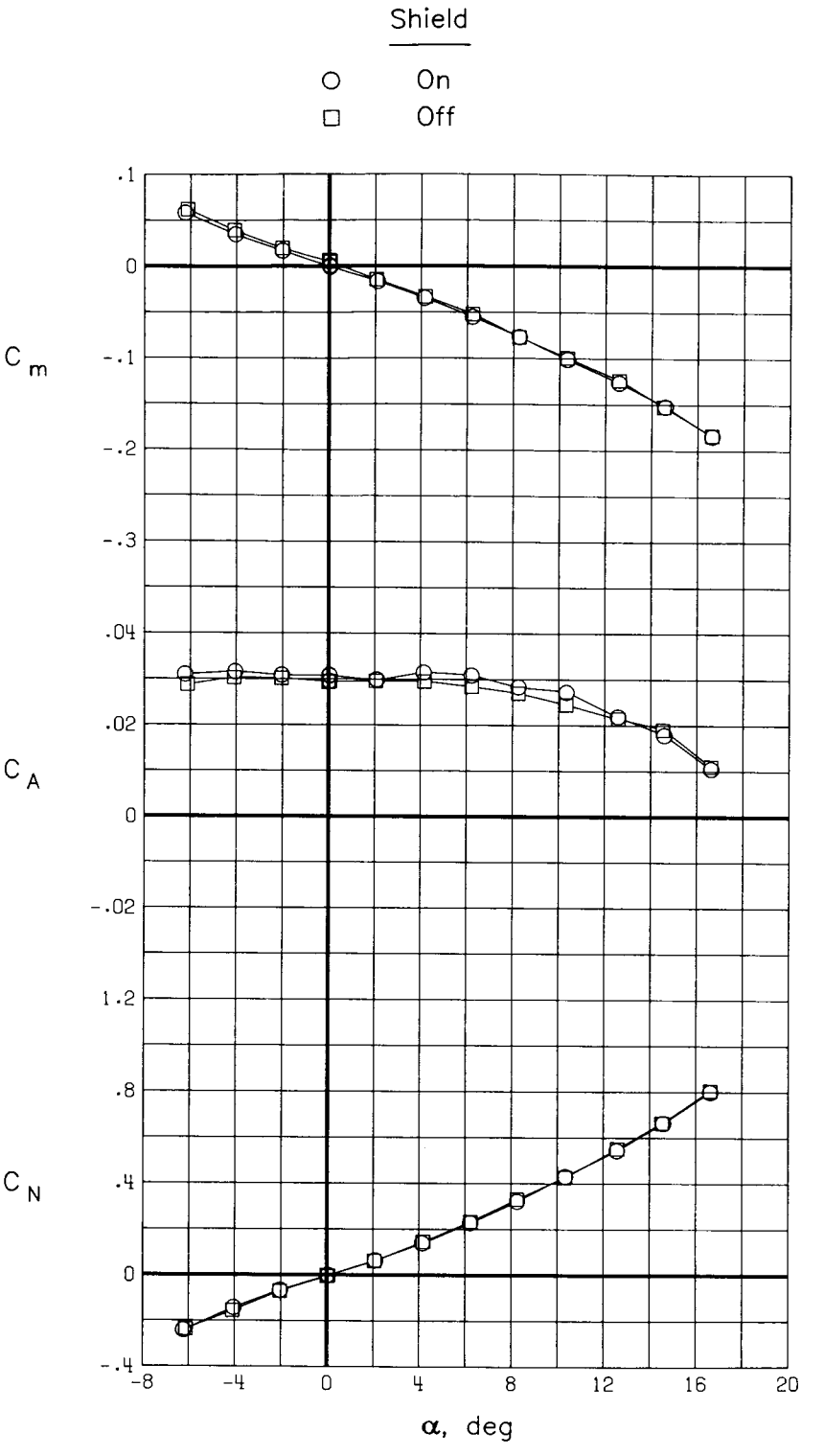

(b) $M = 0.52$; $p_t = 287$ kPa; and $R = 7.84 \times 10^6$.

Figure 19. Concluded.

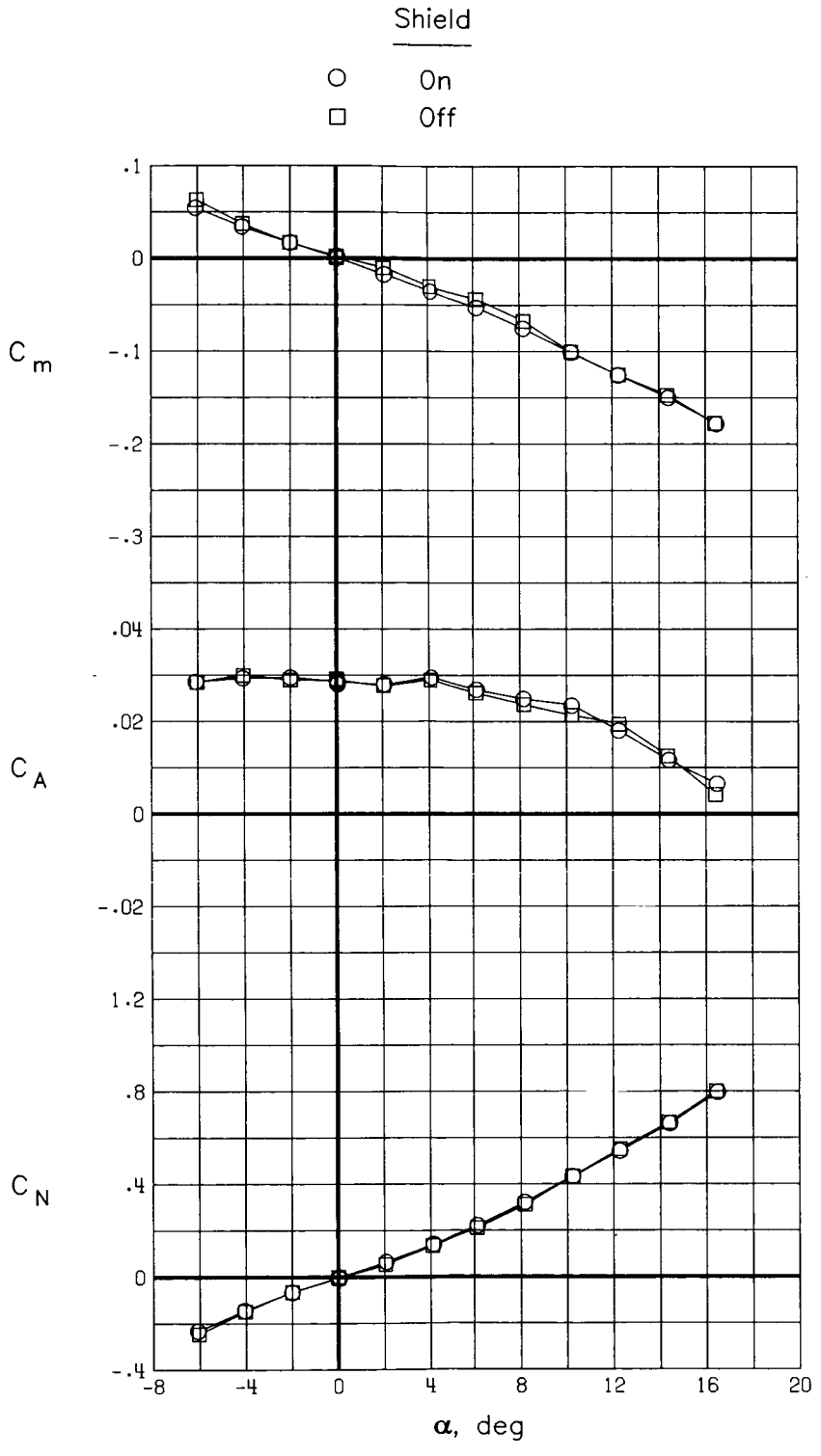

(a) $M = 0.3$; $p_t = 488$ kPa; and $R = 19.45 \times 10^6$.

Figure 20. Comparison of results with convection shield on and off at $T_t = 110$ K.

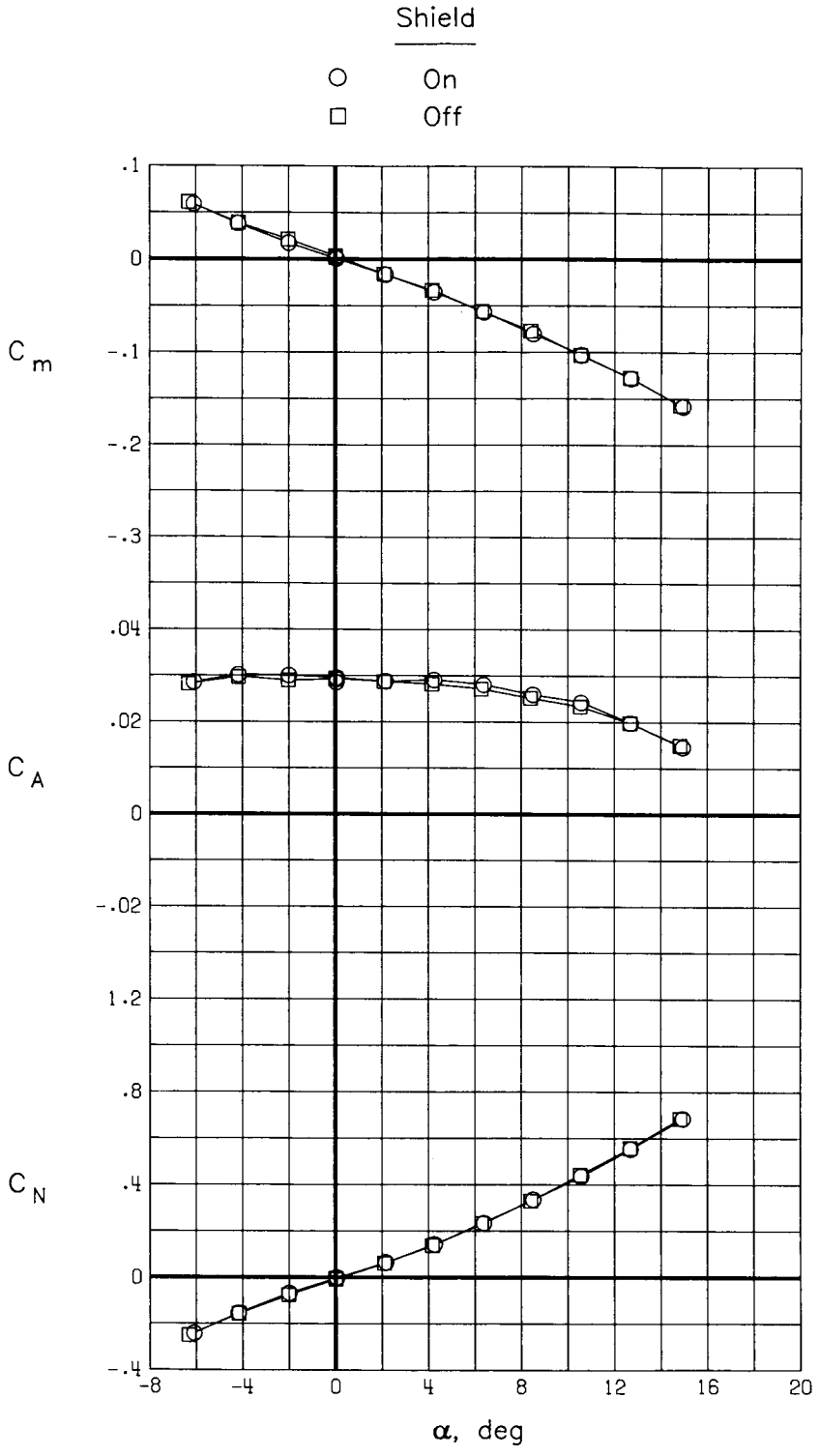

(b) $M = 0.5$; $p_t = 491$ kPa; and $R = 30.70 \times 10^6$.

Figure 20. Continued.

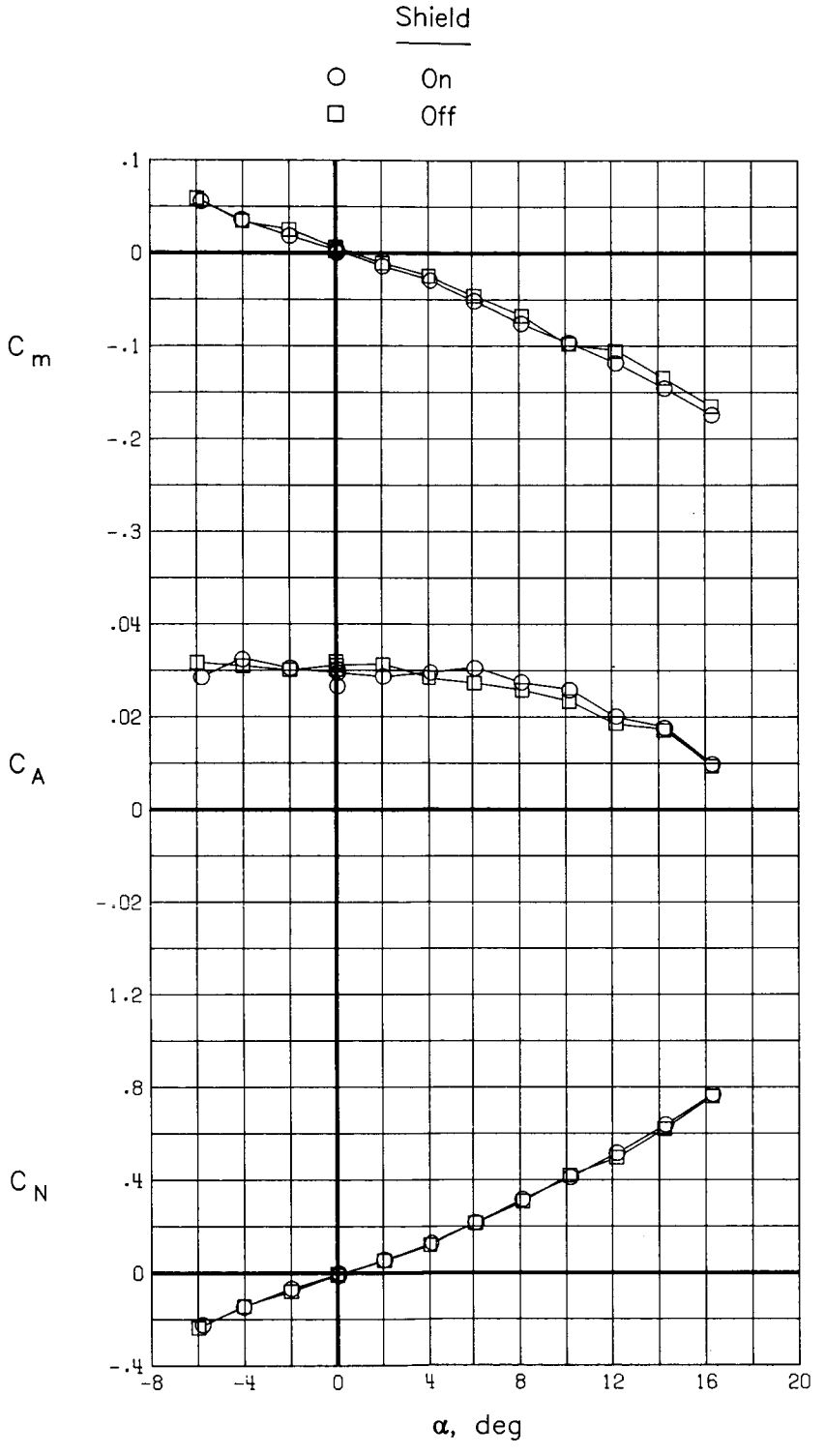

(c) $M = 0.5$; $p_t = 122$ kPa; and $R = 7.60 \times 10^6$.

Figure 20. Concluded.

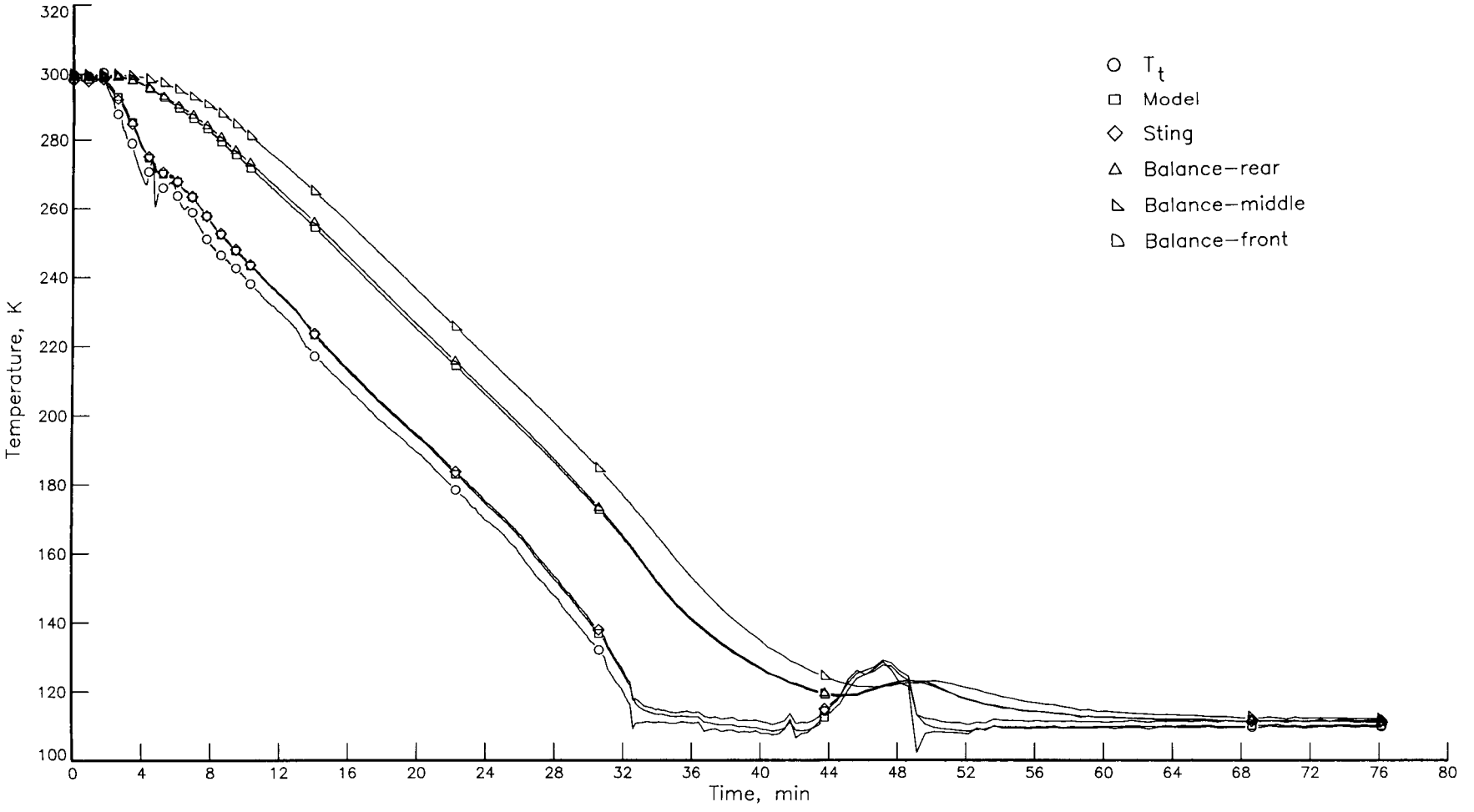

(a) $T_t = 300$ K to 110 K; $p_t = 122$ kPa.

Figure 21. Temperature response with convection shield on at $M = 0.3$. ($\alpha = 0°$ unless otherwise specified.)

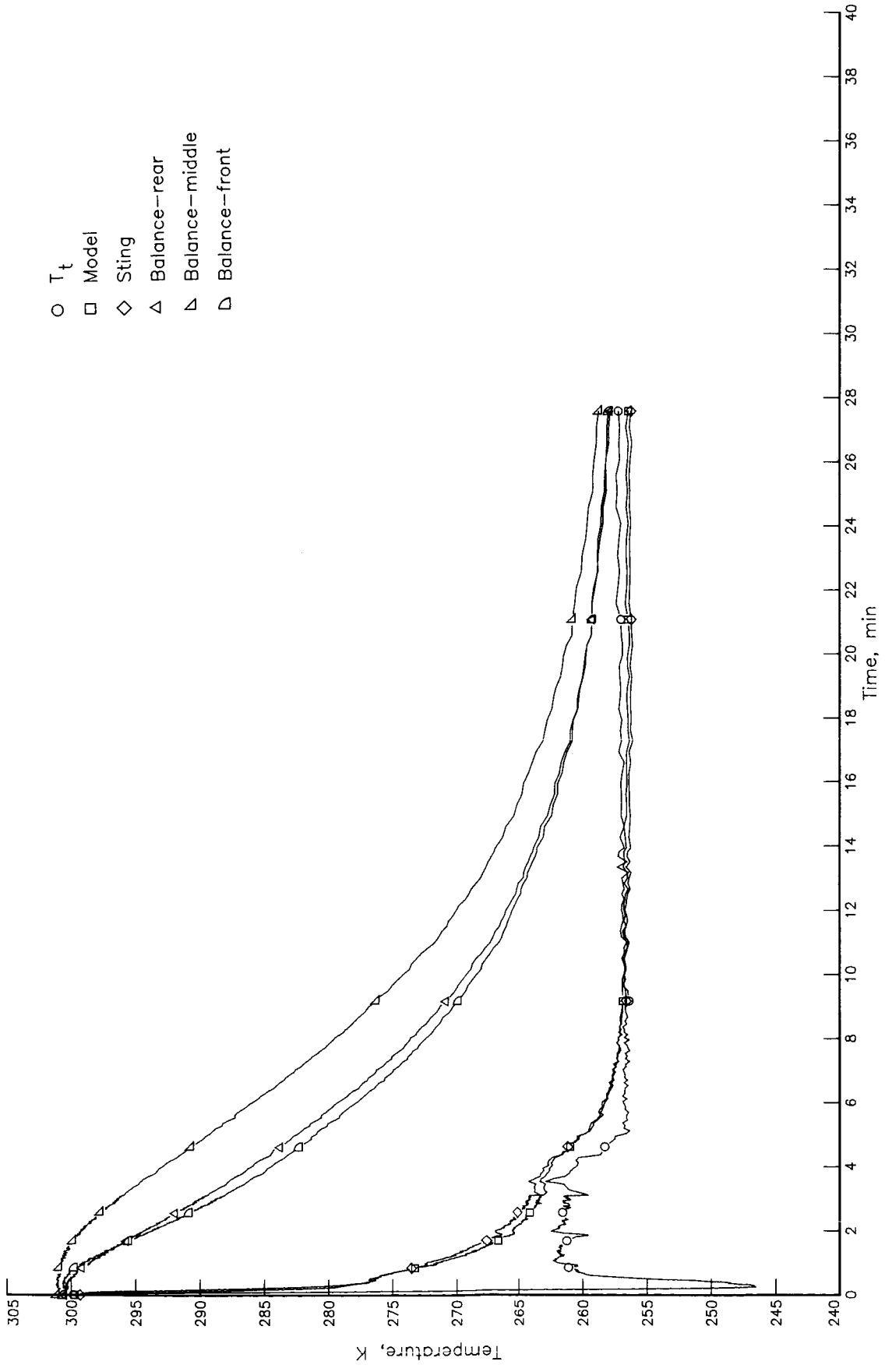

(b) $T_t = 300$ K to 260 K; $p_t = 122$ kPa.

Figure 21. Continued.

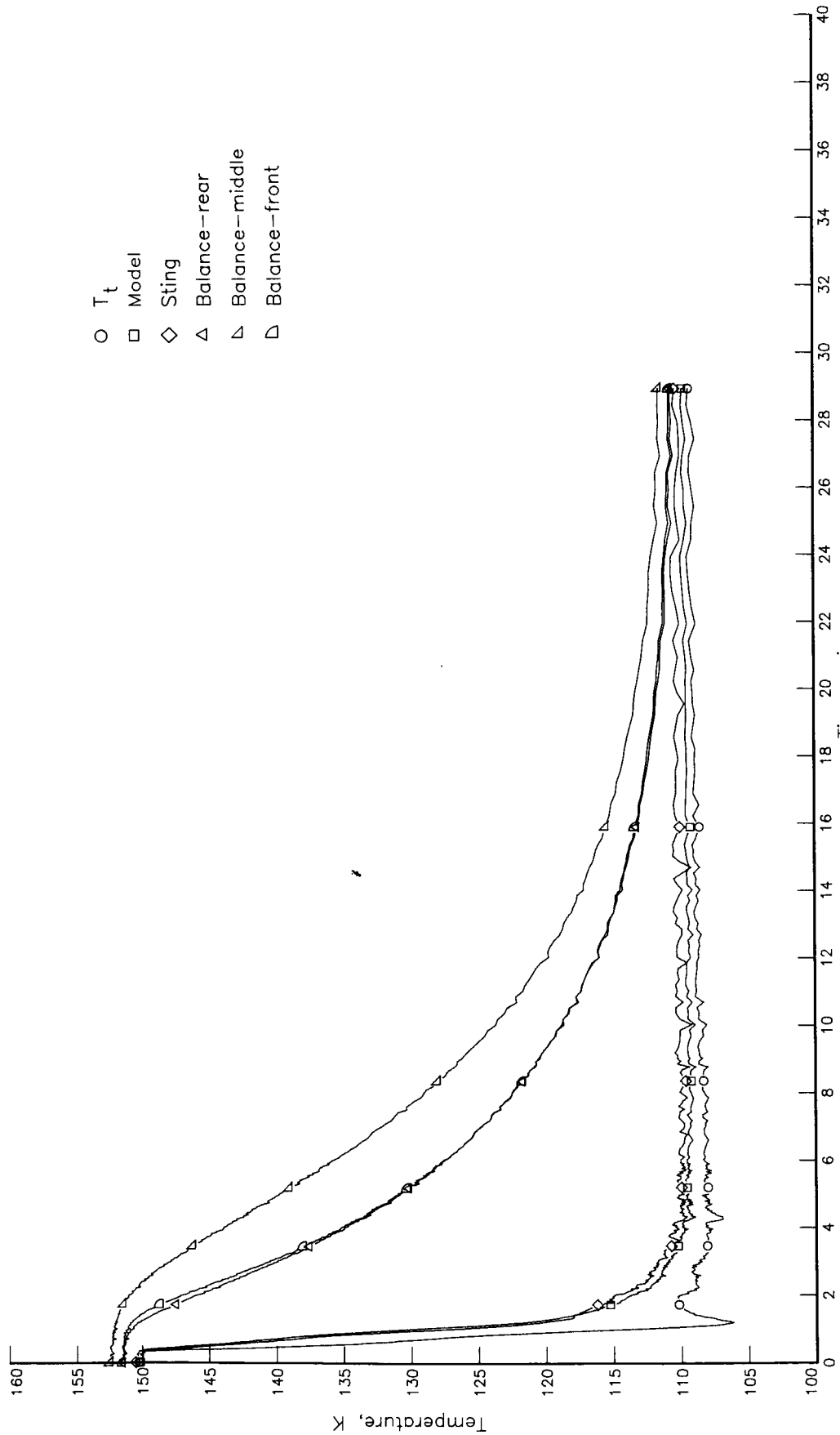

(c) $T_t = 150$ K to 110 K; $p_t = 122$ kPa.

Figure 21. Continued.

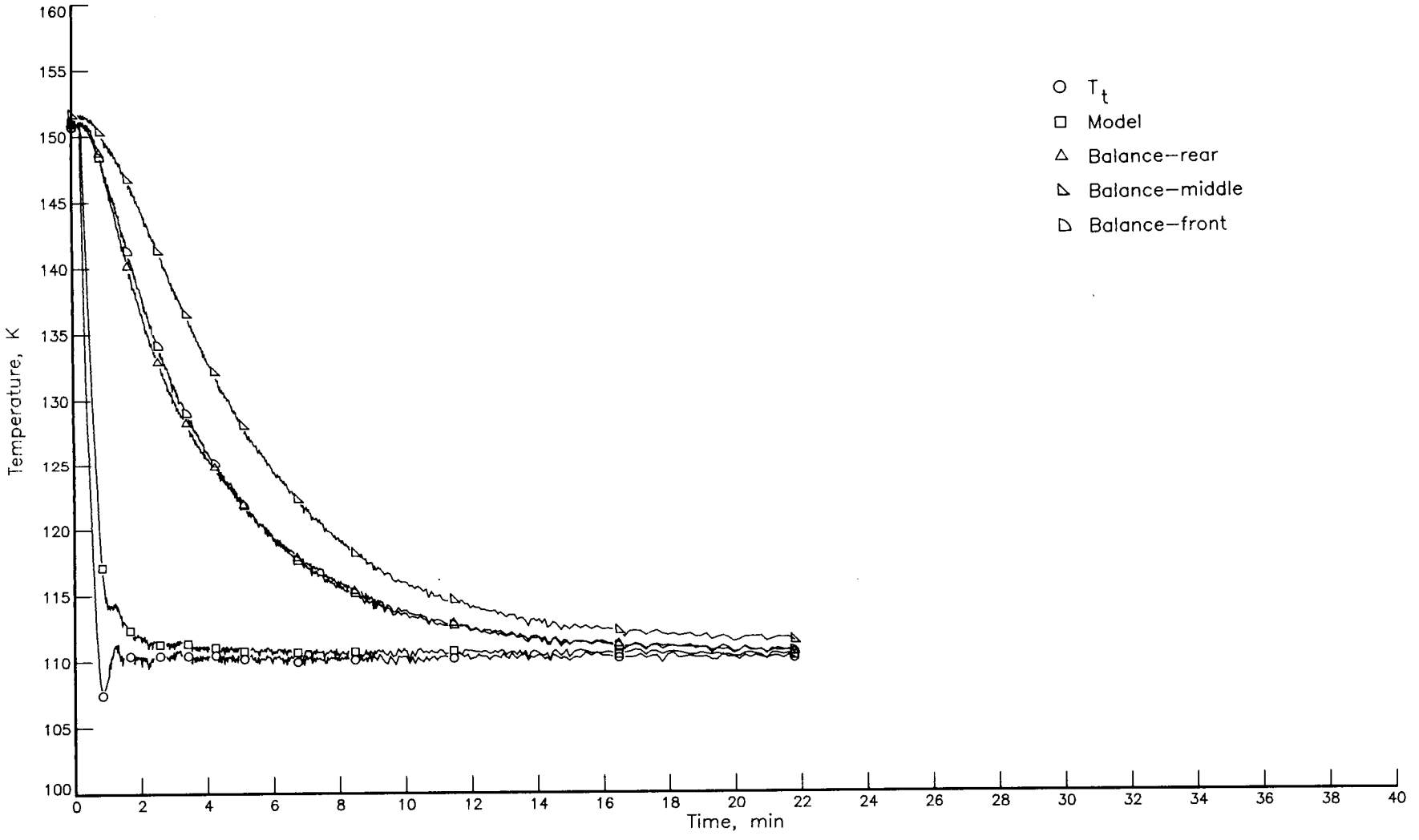

(d) $T_t = 150$ K to 110 K; $p_t = 488$ kPa.

Figure 21. Continued.

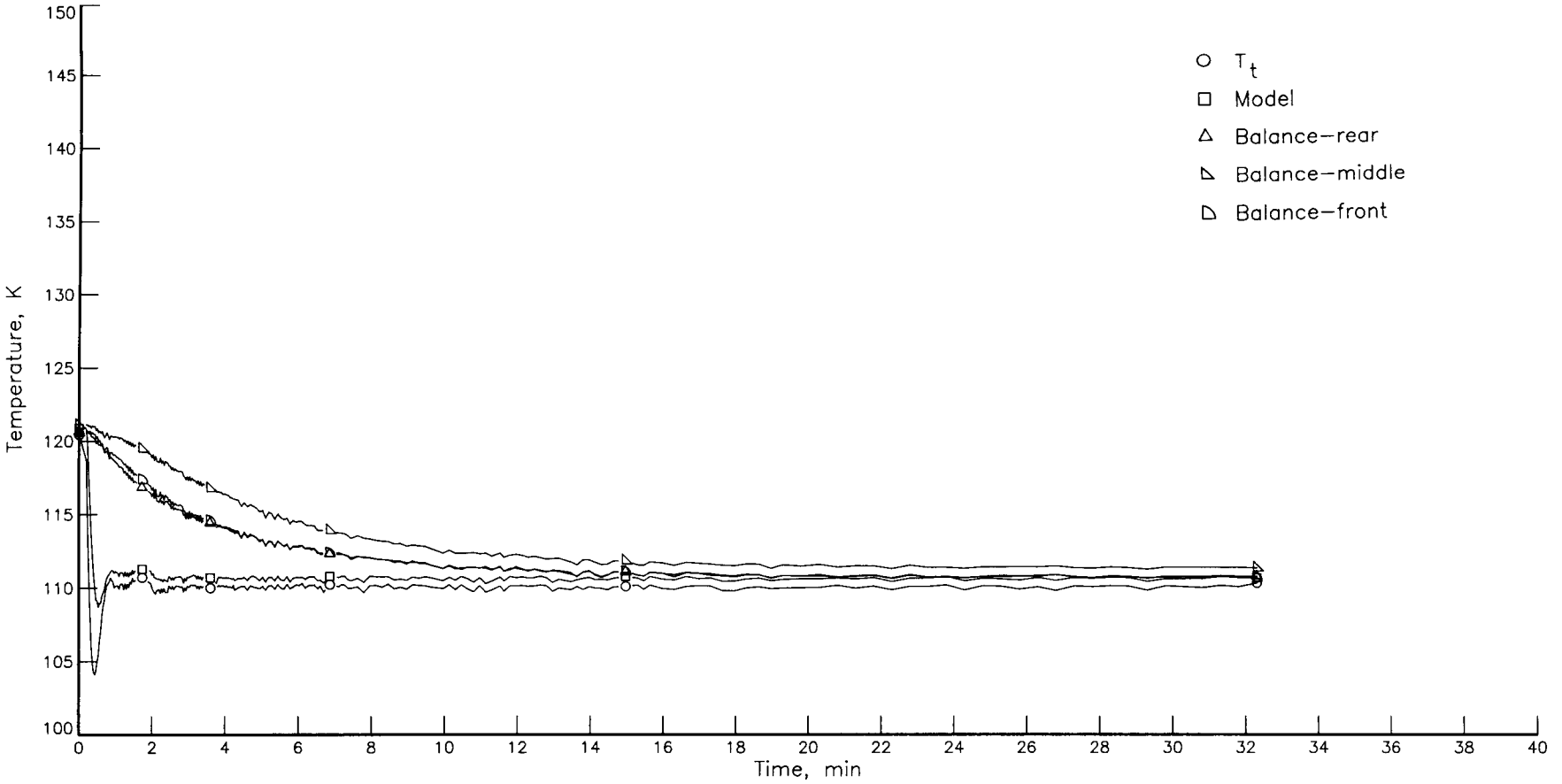

(e) $T_t = 120$ K to 110 K; $p_t = 488$ kPa.

Figure 21. Continued.

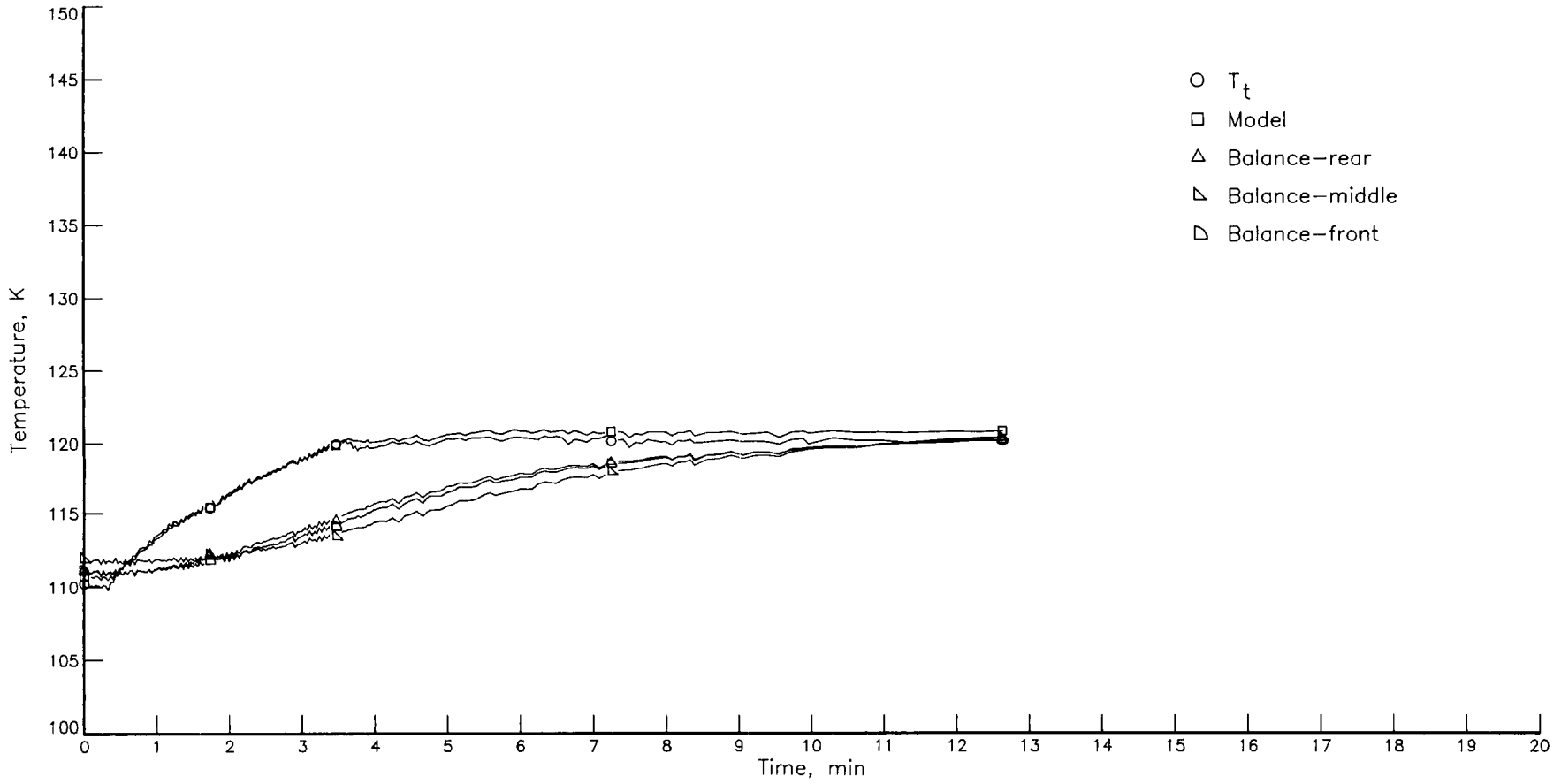

(f) $T_t = 110$ K to 120 K; $p_t = 488$ kPa.

Figure 21. Continued.

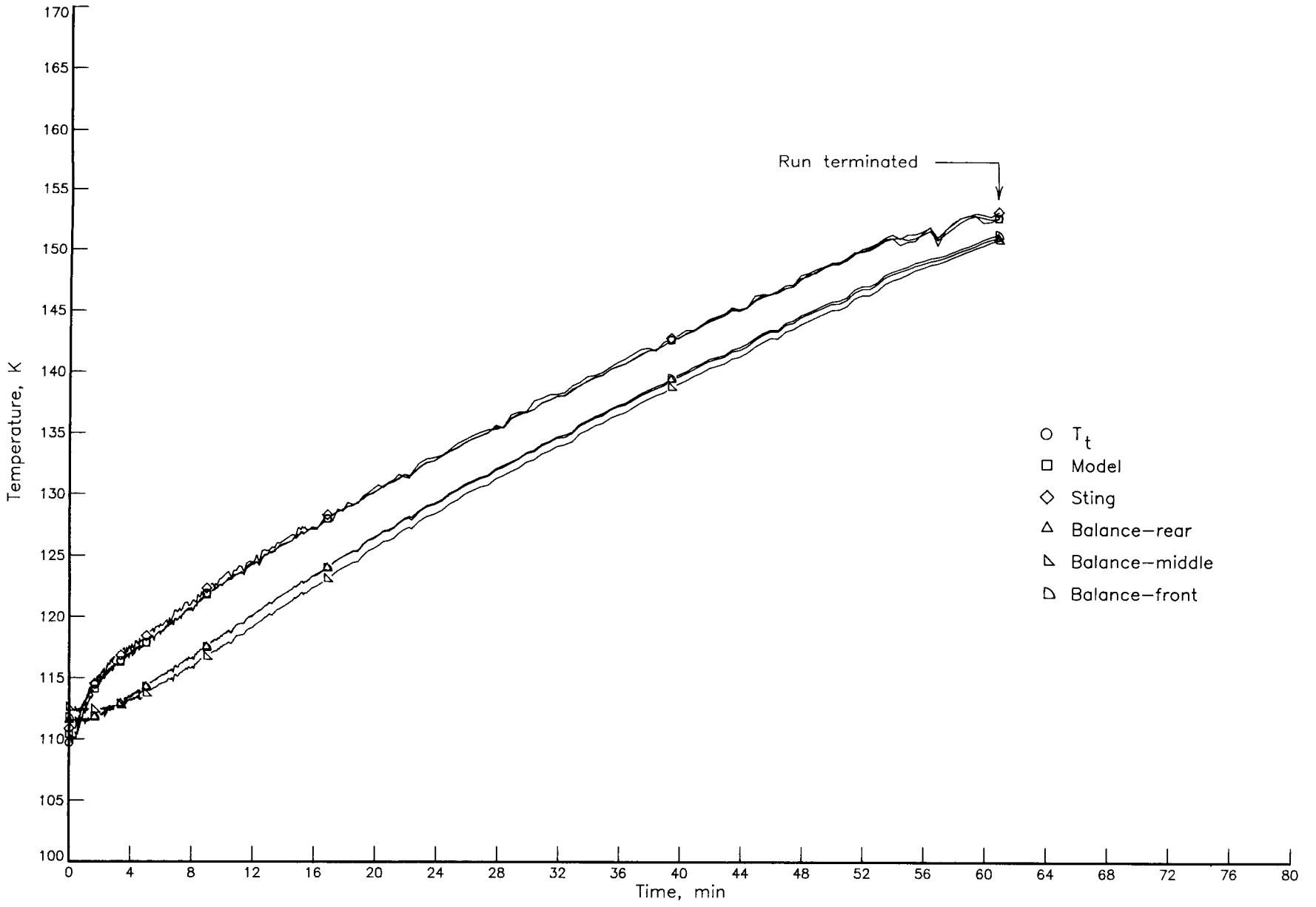

(g) $T_t = 110$ K to 150 K; $p_t = 122$ kPa.

Figure 21. Continued.

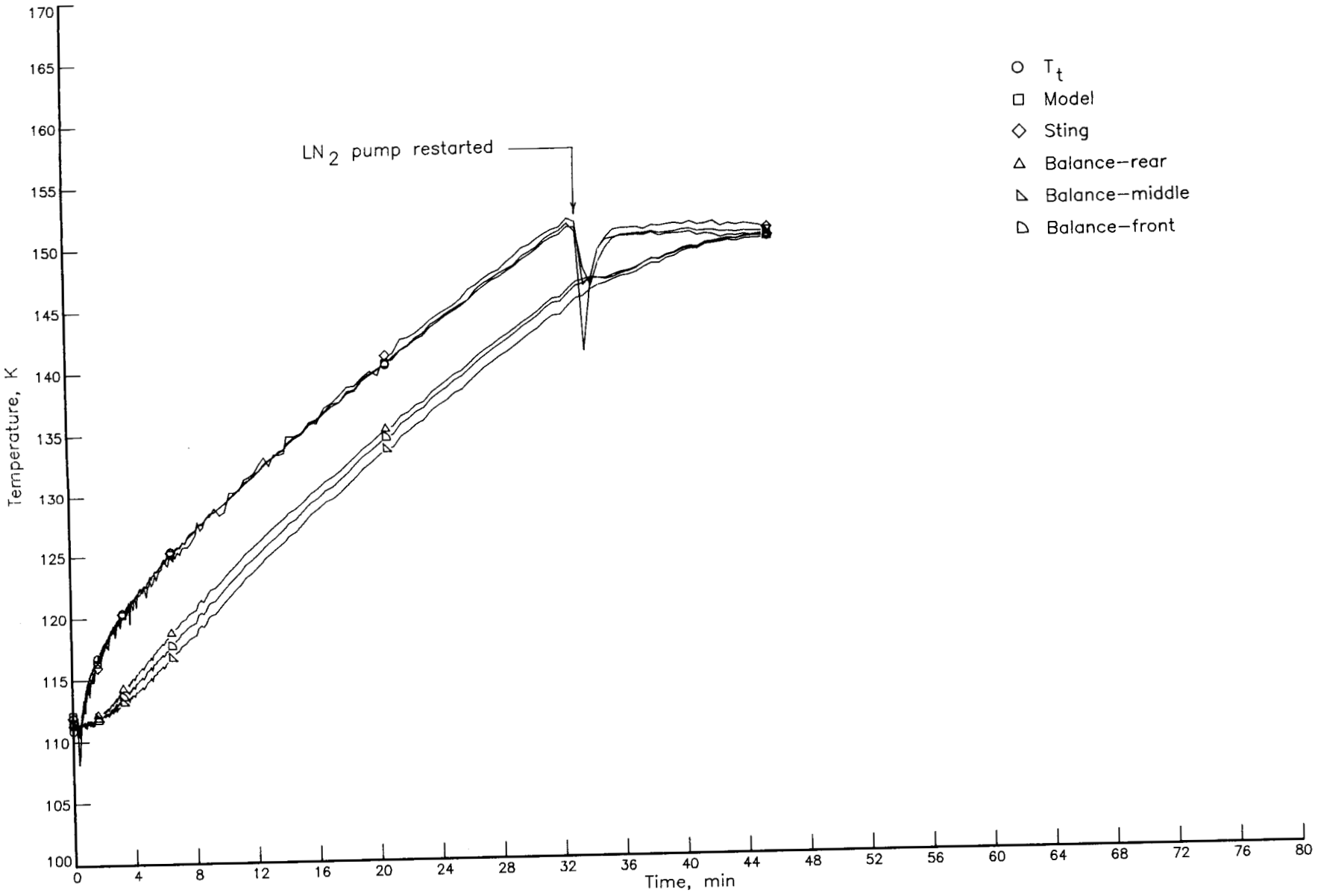

(h) $T_t = 110$ K to 150 K; $p_t = 122$ kPa; $\alpha = 15°$.

Figure 21. Continued.

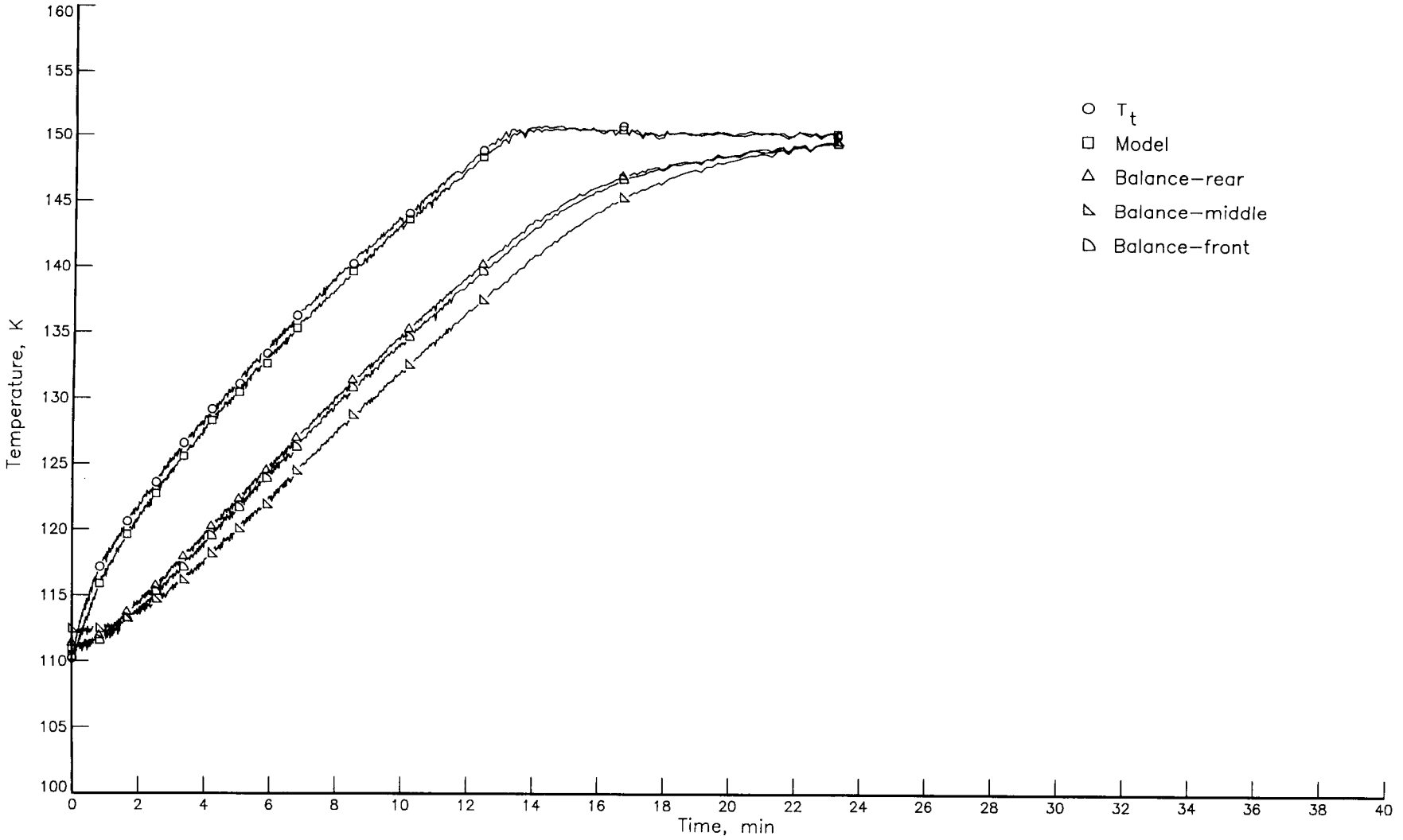

(i) $T_t = 110$ K to 150 K; $p_t = 488$ kPa.

Figure 21. Continued.

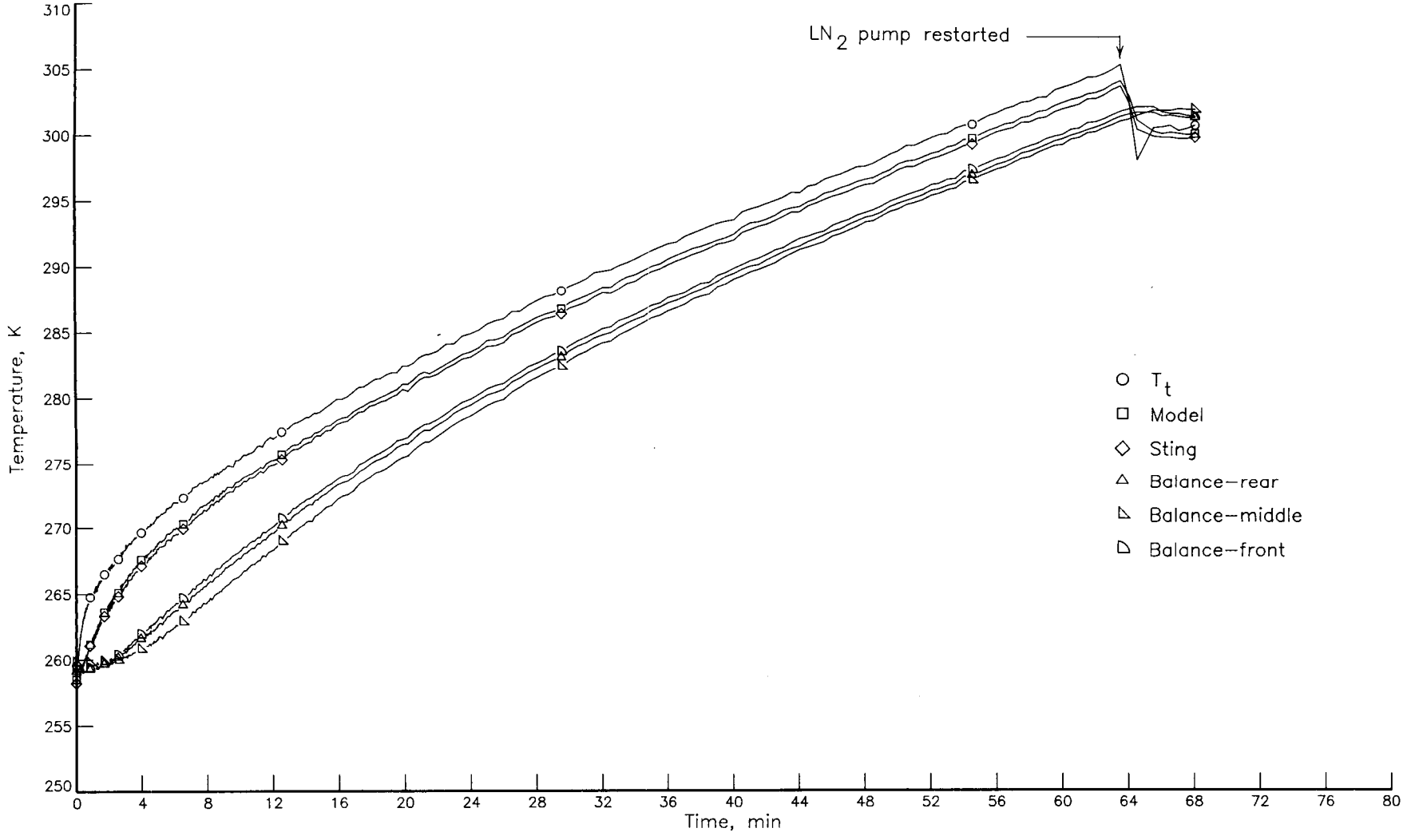

(j) T_t = 260 K to 300 K; p_t = 122 kPa.

Figure 21. Concluded.

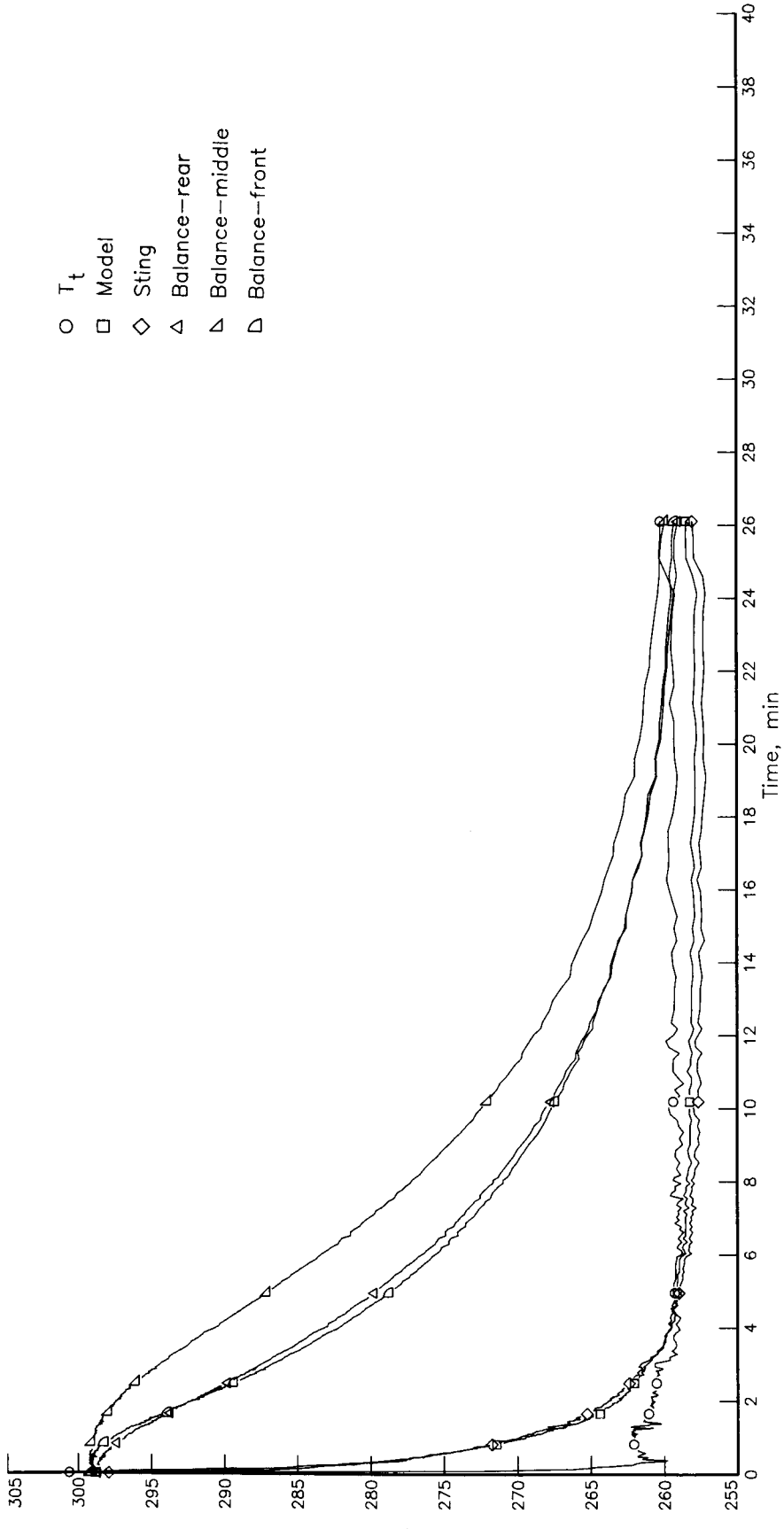

(a) $T_t = 300$ K to 260 K; $p_t = 122$ kPa.

Figure 22. Temperature response with convection shield on at $M = 0.5$. ($\alpha = 0°$ unless otherwise specified.)

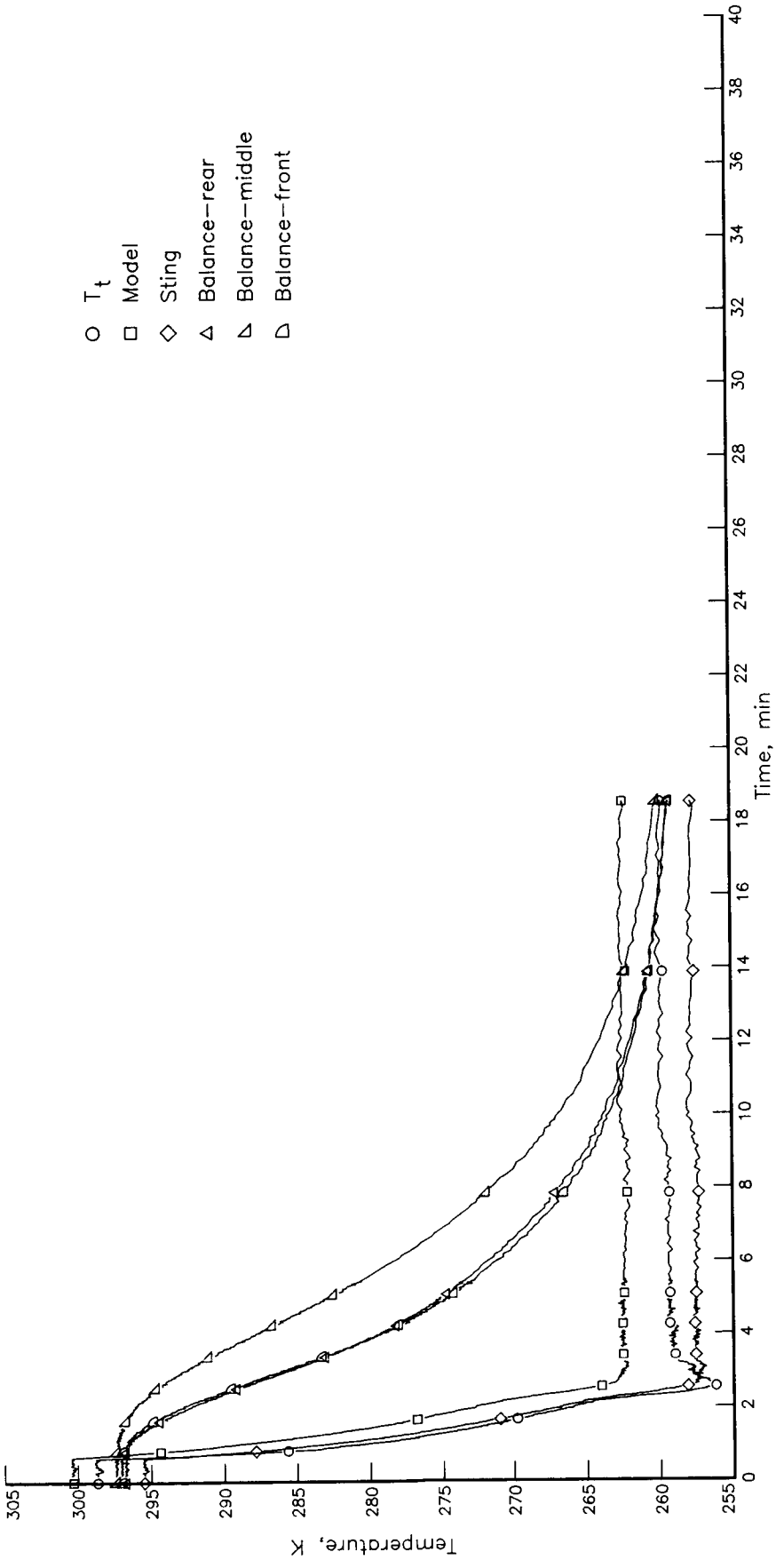

(b) $T_t = 300$ K to 260 K; $p_t = 491$ kPa.

Figure 22. Continued.

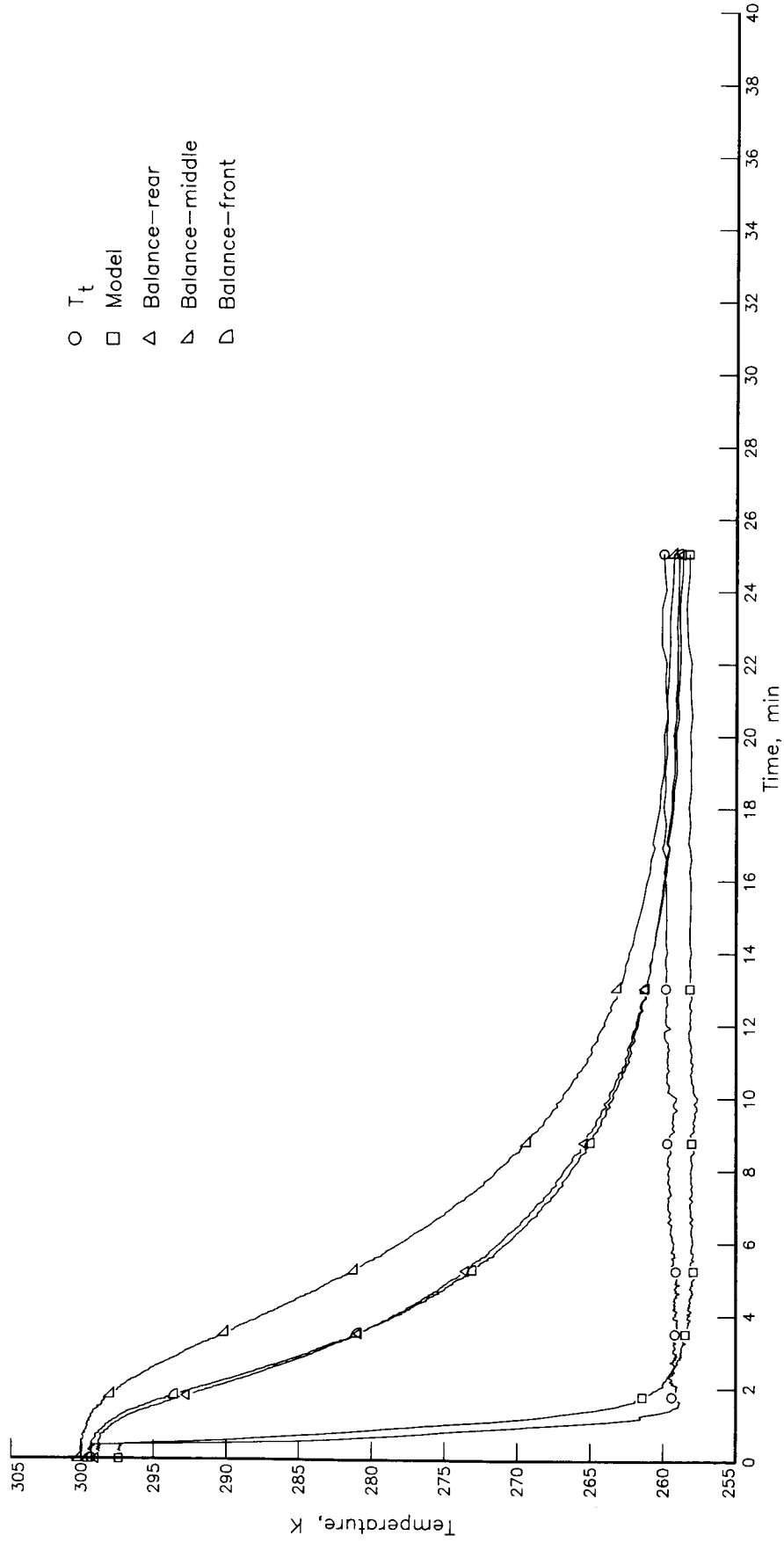

(c) $T_t = 300$ K to 260 K; $p_t = 491$ kPa. (Repeat of run shown in fig. 22(b).)

Figure 22. Continued.

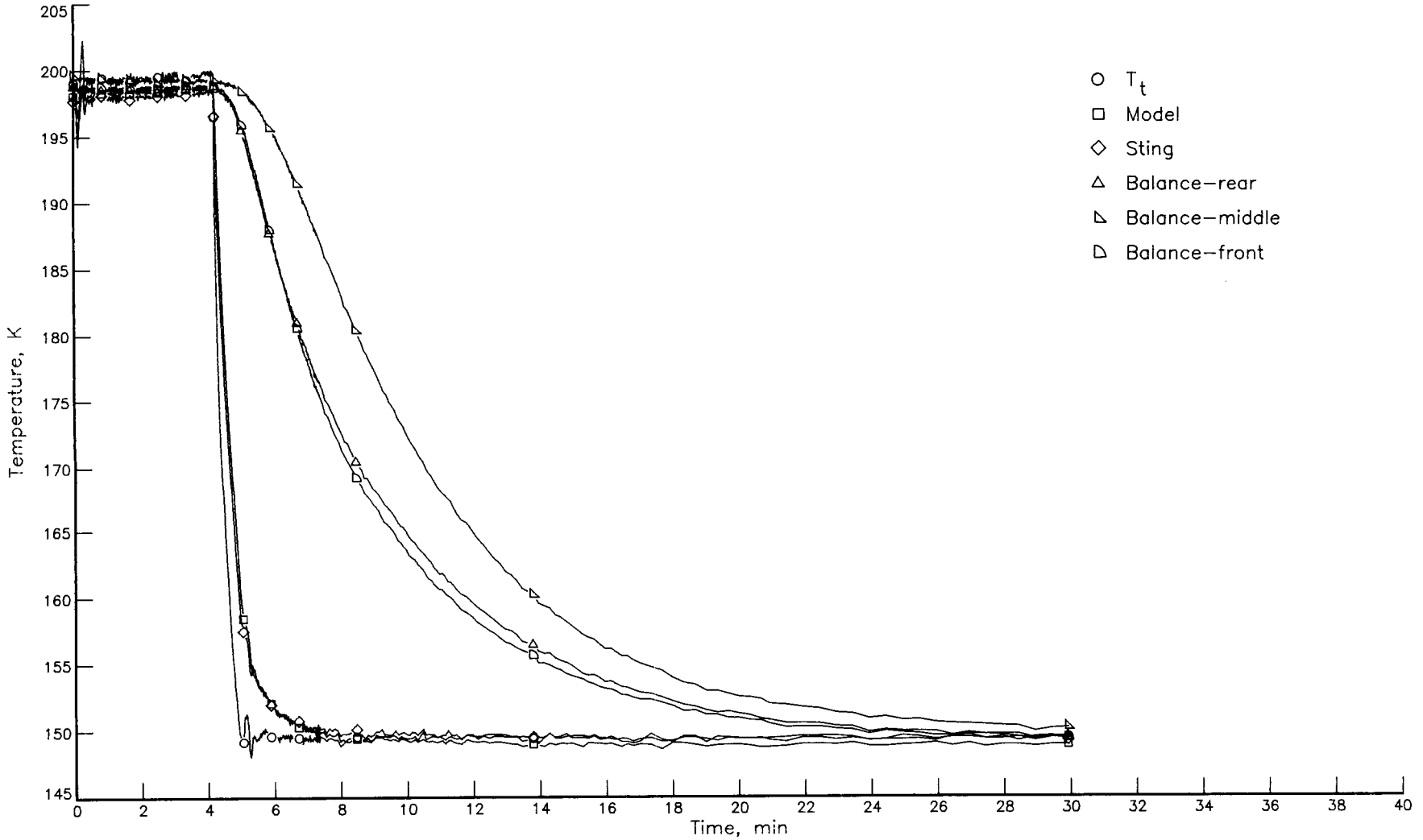

(d) $T_t = 200$ K to 150 K; $p_t = 287$ kPa.

Figure 22. Continued.

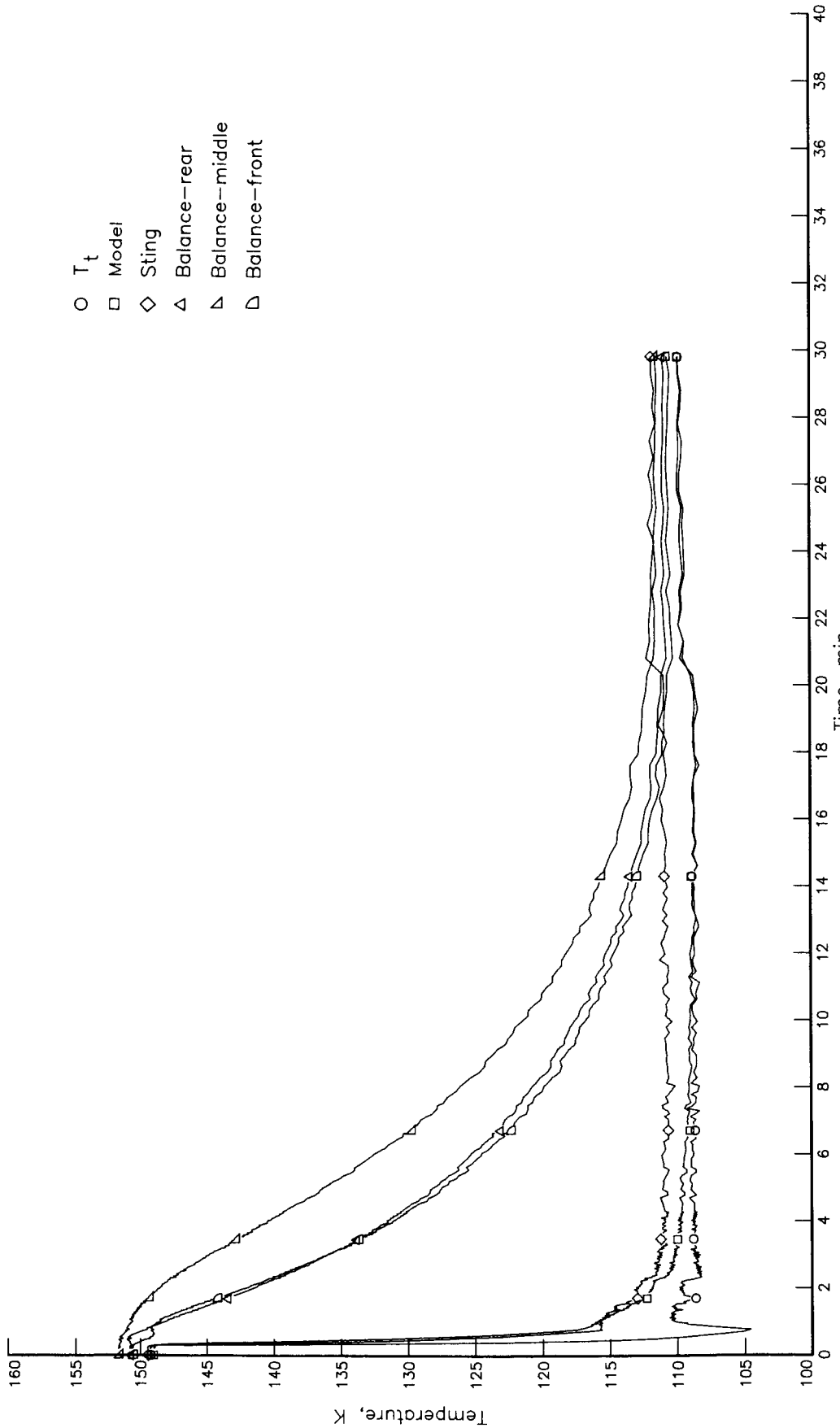

(e) $T_t = 150$ K to 110 K; $p_t = 122$ kPa.

Figure 22. Continued.

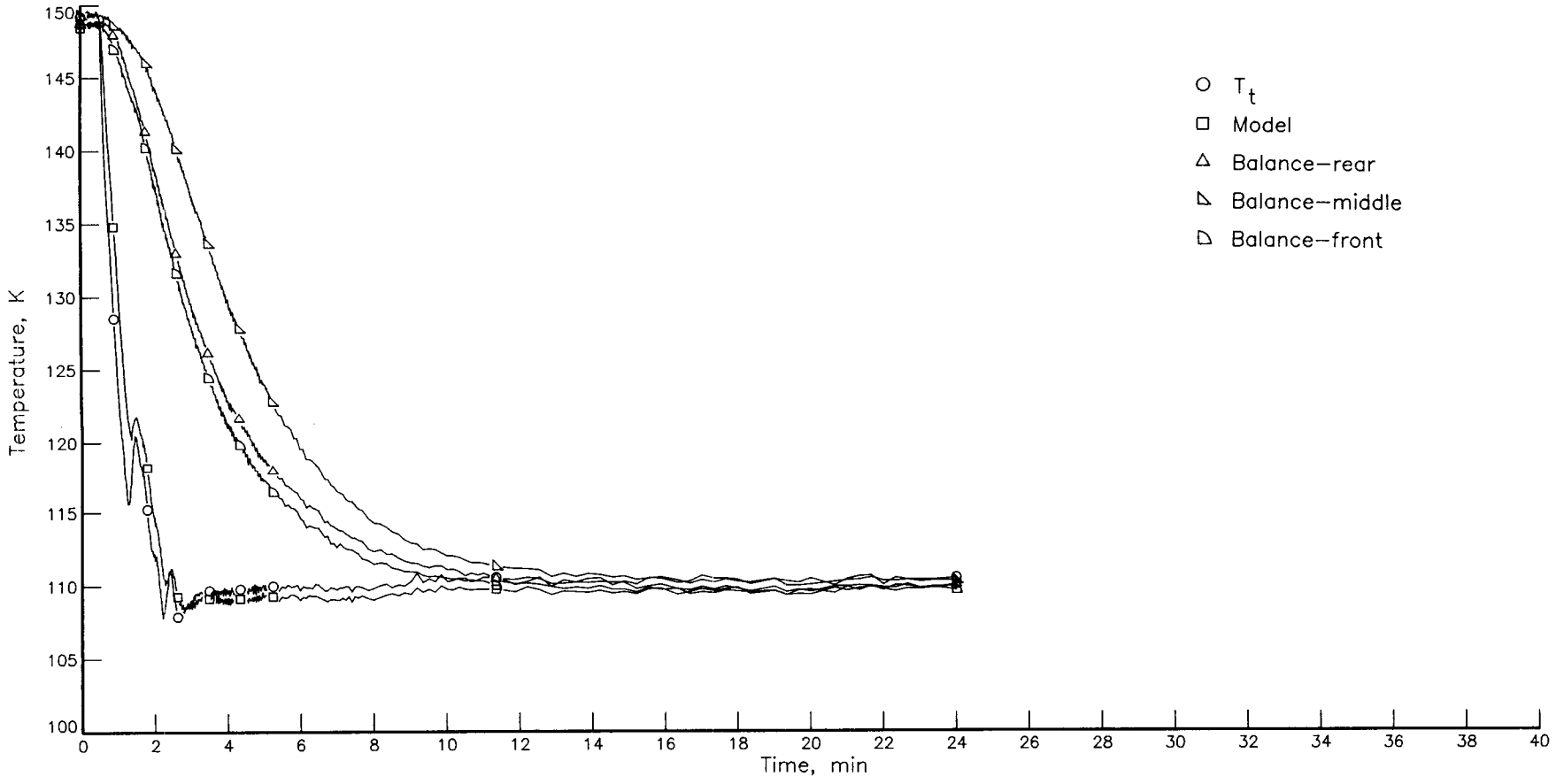

(f) $T_t = 150$ K to 110 K; $p_t = 491$ kPa.

Figure 22. Continued.

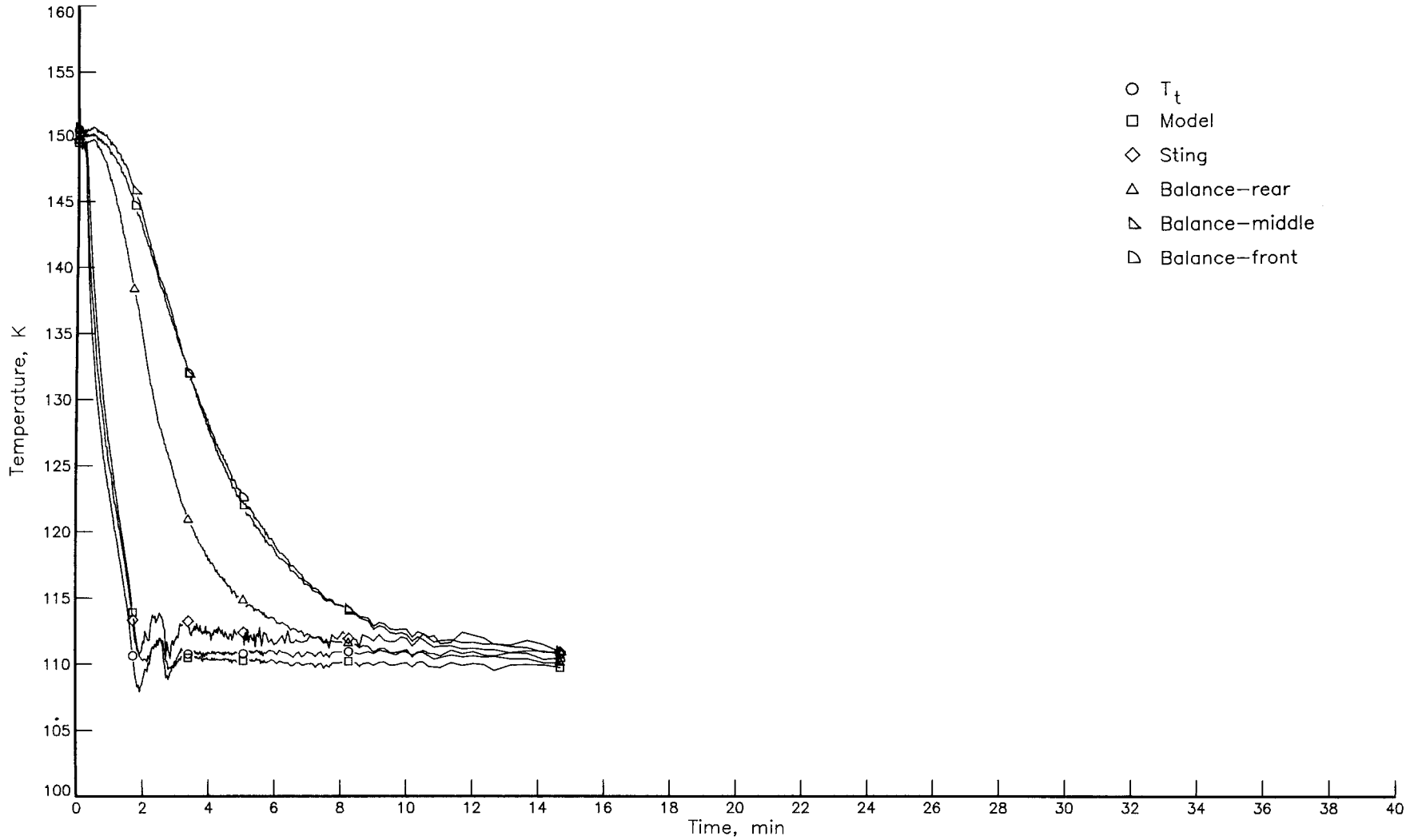

(g) $T_t = 150$ K to 110 K; $p_t = 491$ kPa; $\alpha = 15°$.

Figure 22. Continued.

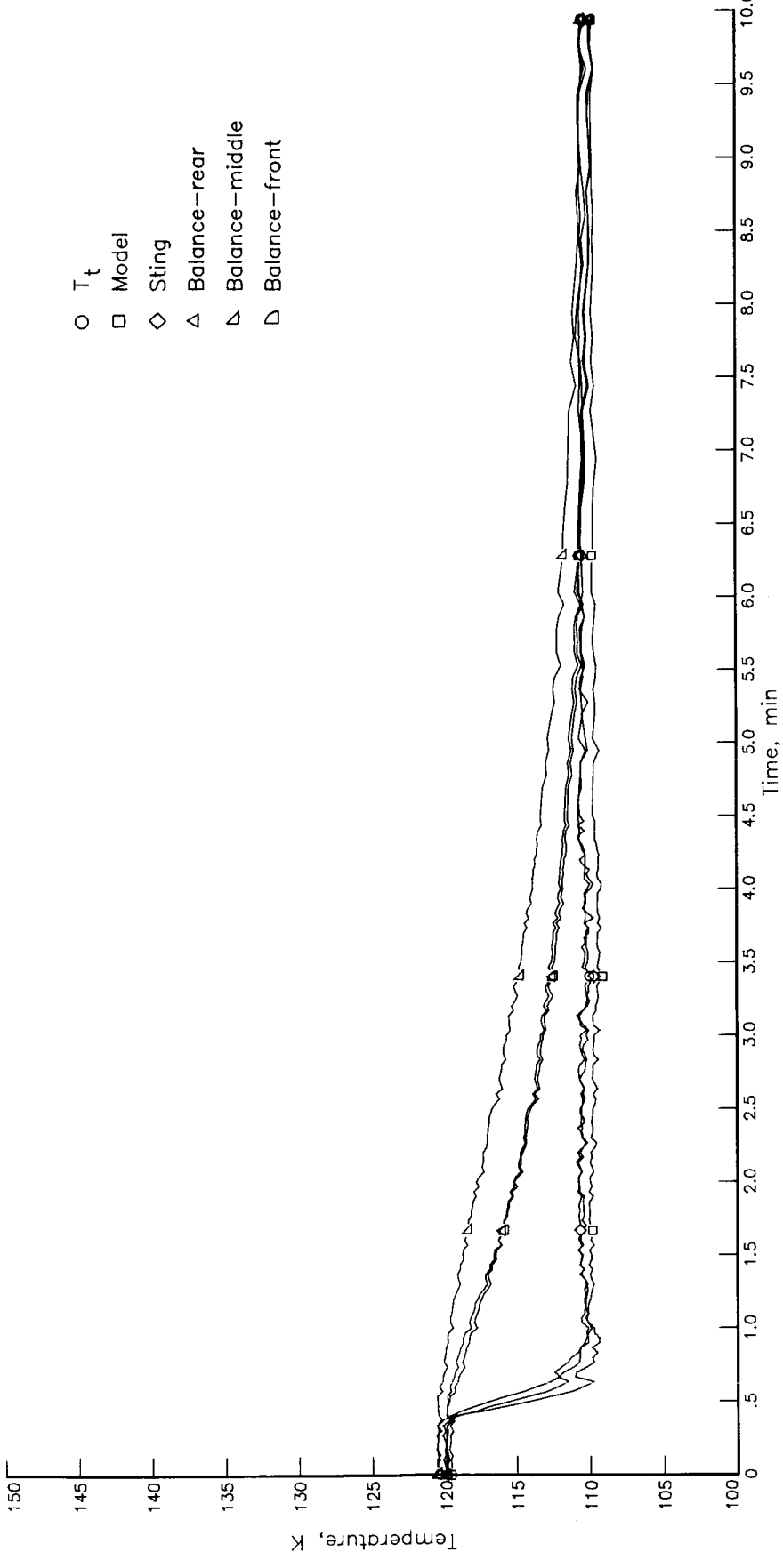

(h) $T_t = 120$ K to 110 K; $p_t = 491$ kPa.

Figure 22. Continued.

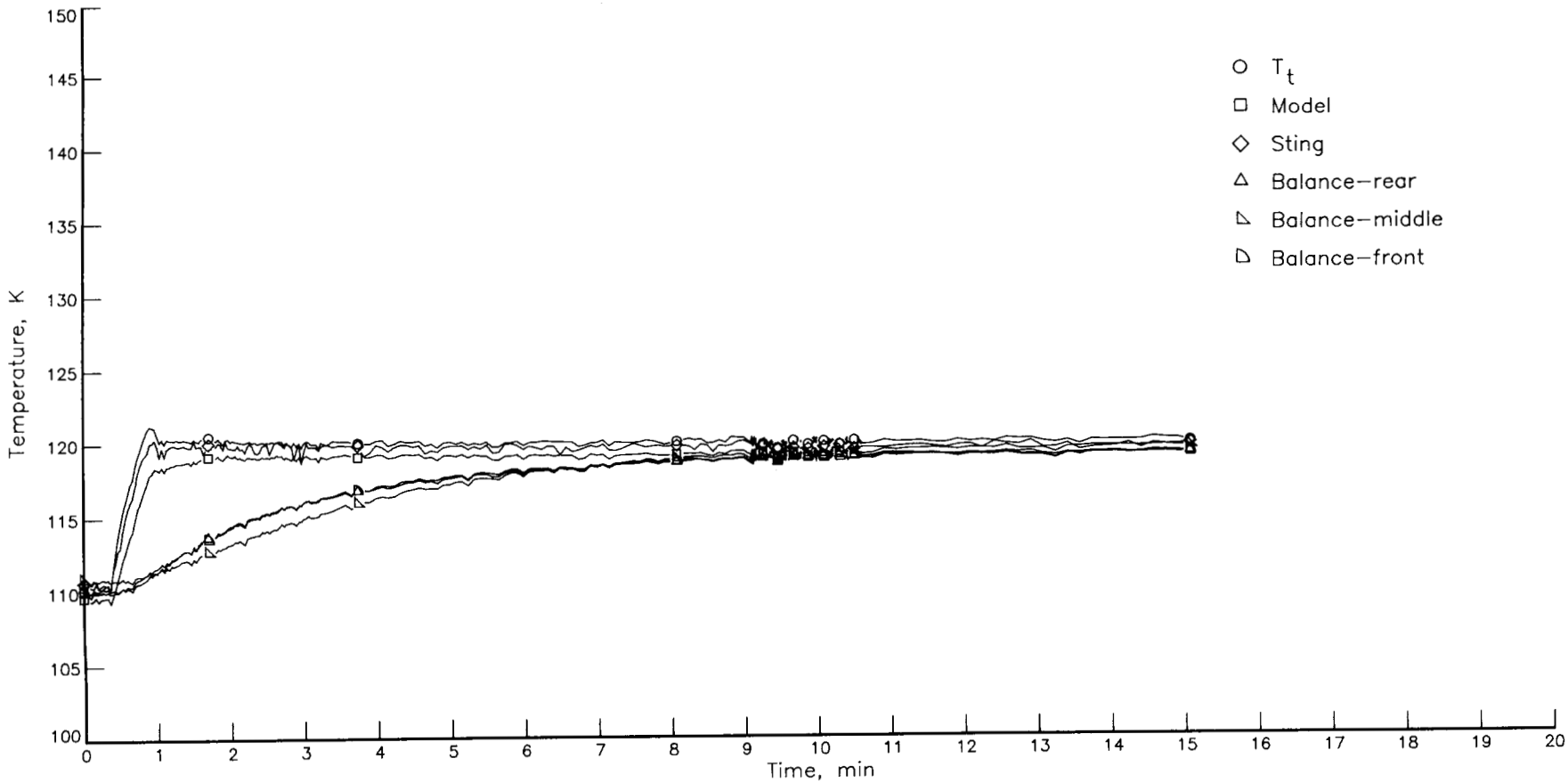

(i) $T_t = 110$ K to 120 K; $p_t = 491$ kPa.

Figure 22. Continued.

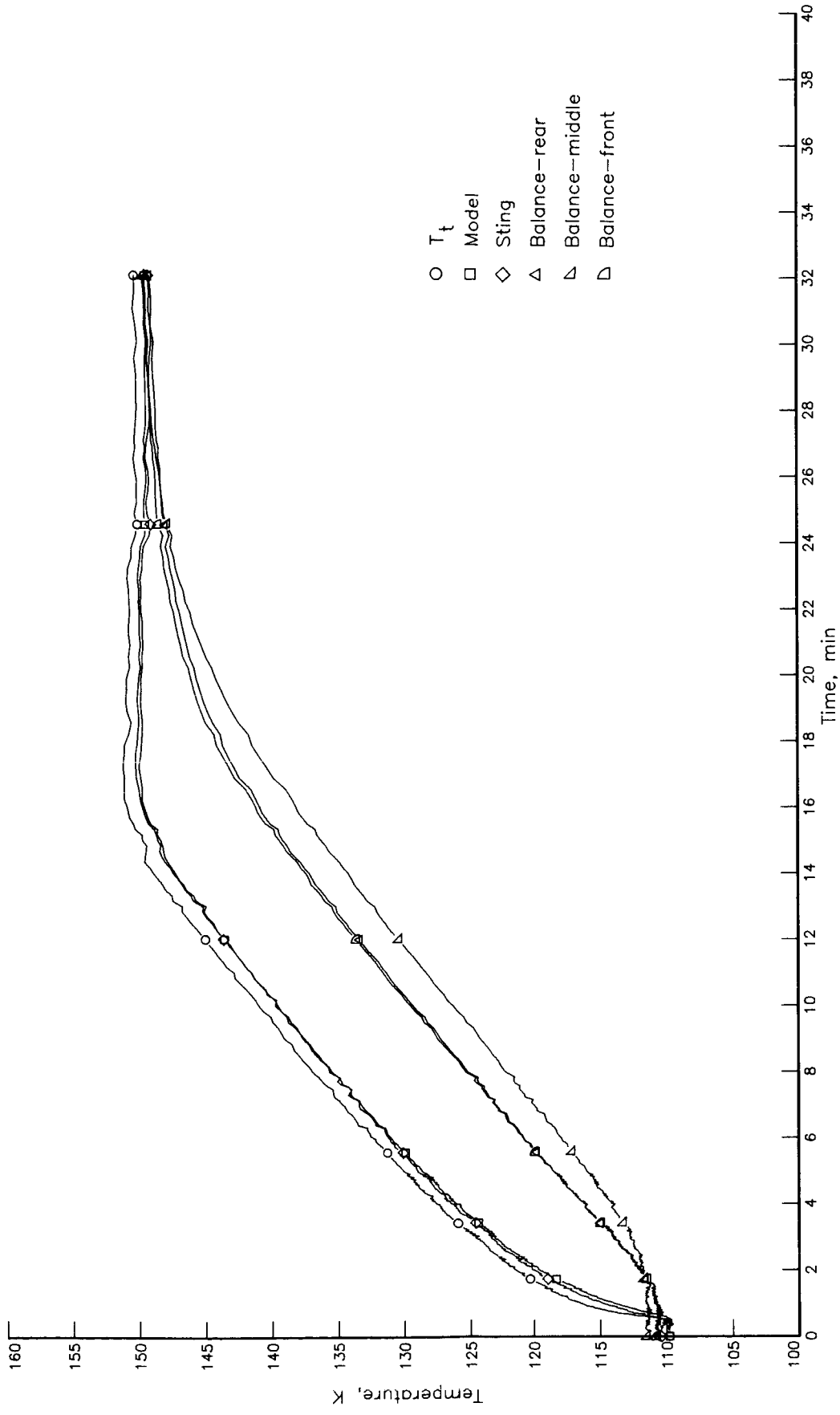

(j) $T_t = 110$ K to 150 K; $p_t = 122$ kPa.

Figure 22. Continued.

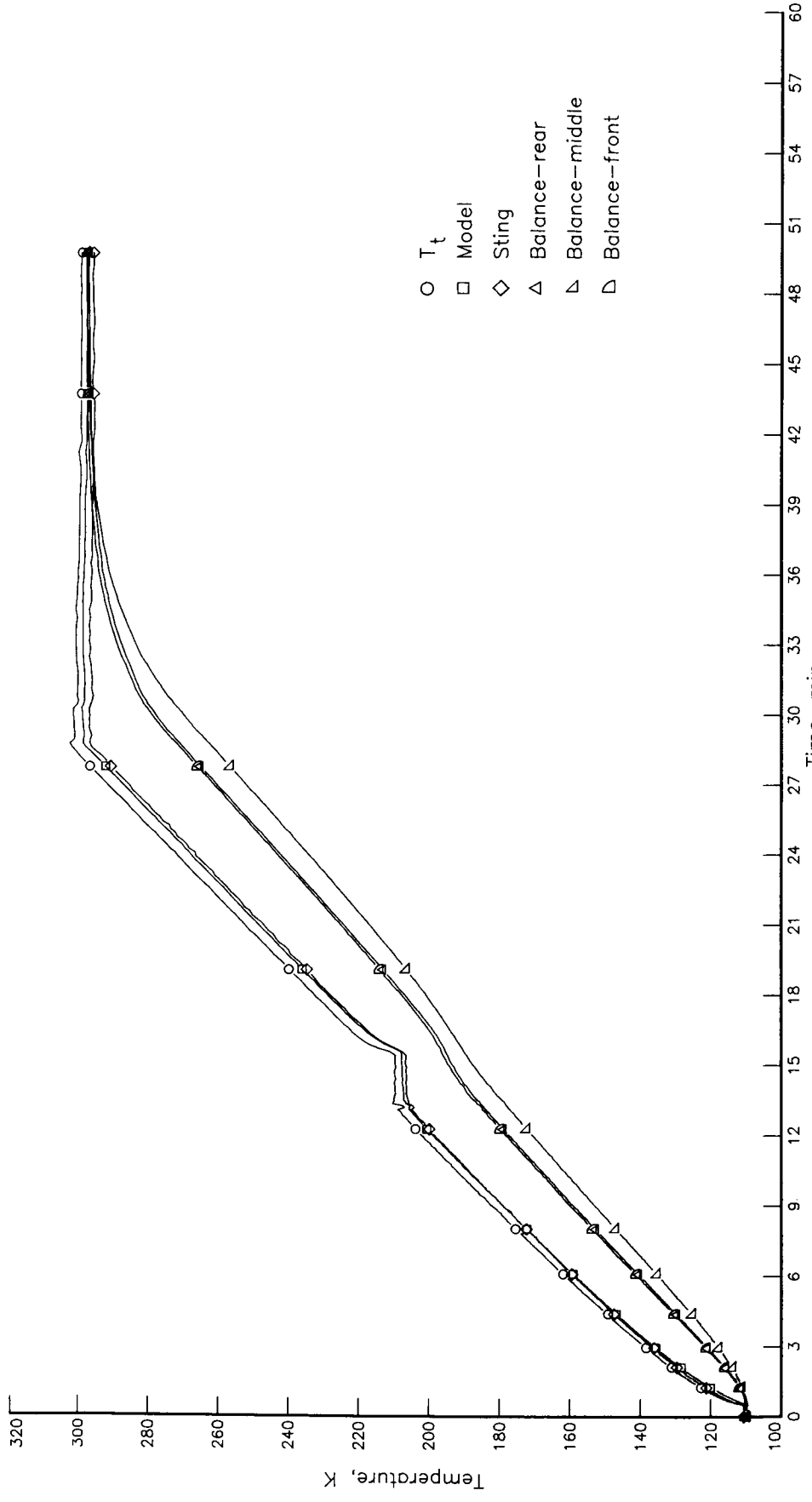

(k) $T_t = 110$ K to 300 K; $p_t = 491$ kPa.

Figure 22. Continued.

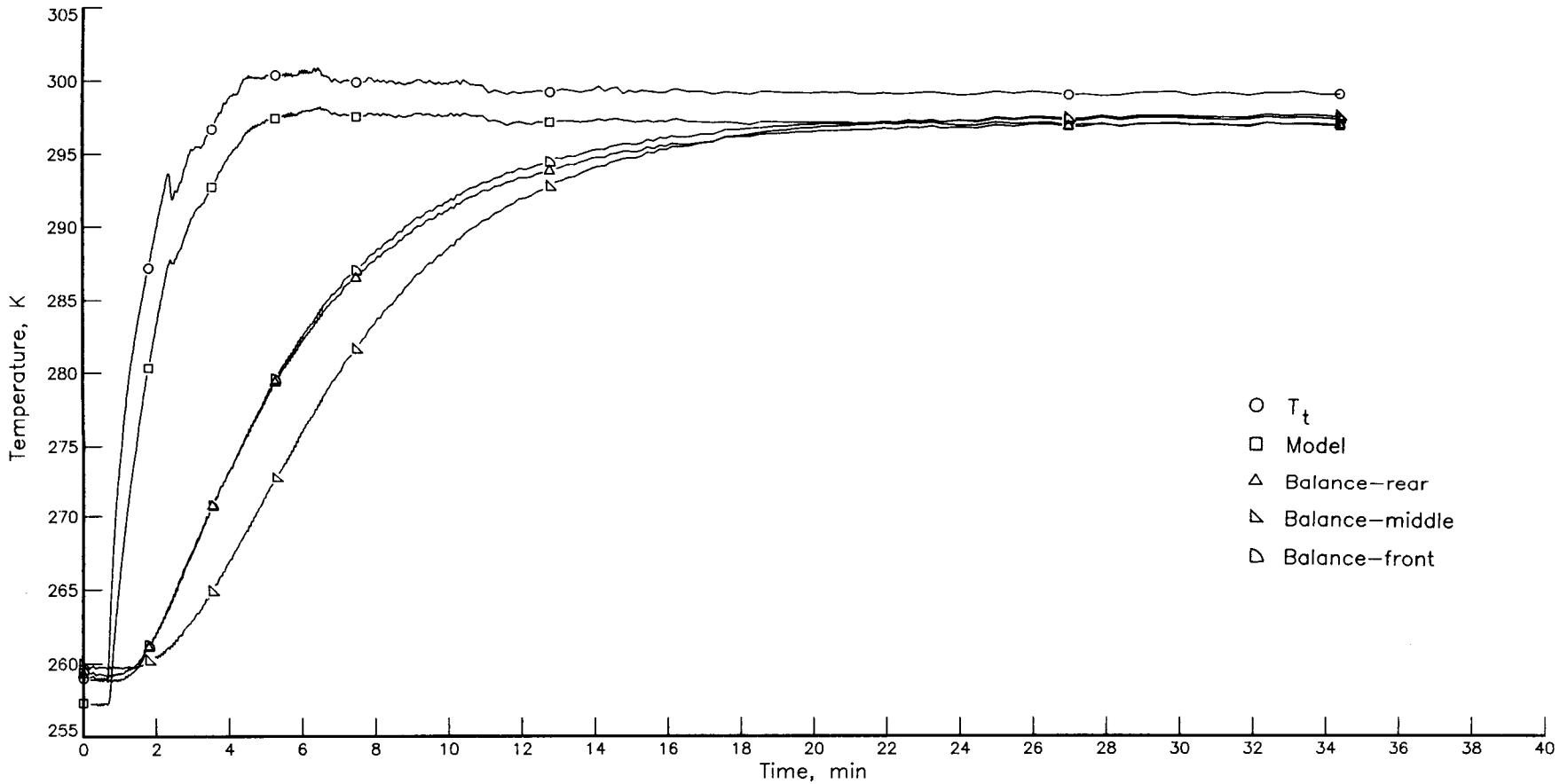

(l) $T_t = 260$ K to 300 K; $p_t = 491$ kPa.

Figure 22. Concluded.

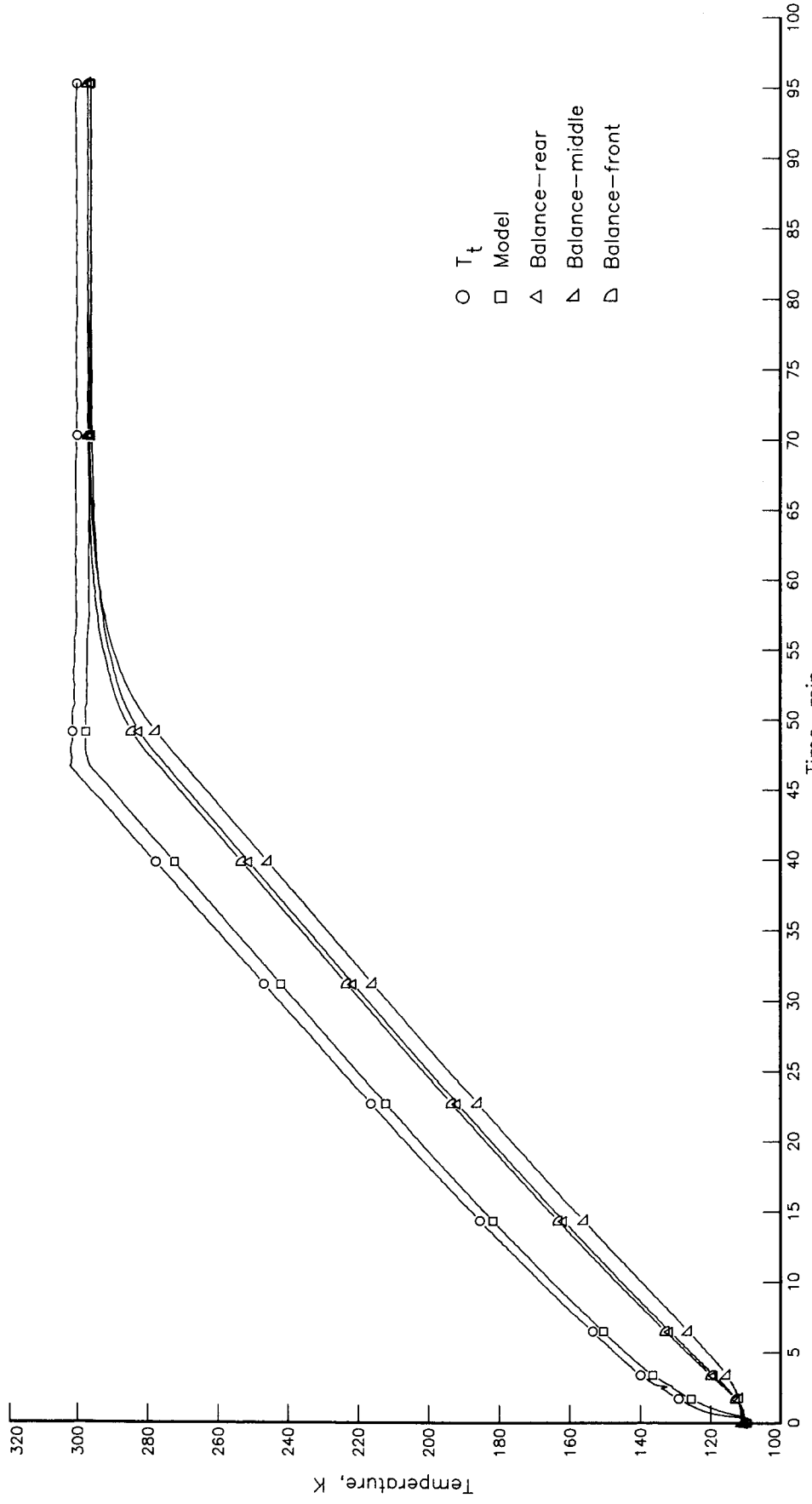

Figure 23. Temperature response with convection shield on at $M = 0.65$. $T_t = 110$ K to 300 K; $p_t = 122$ kPa; $\alpha = 0°$.

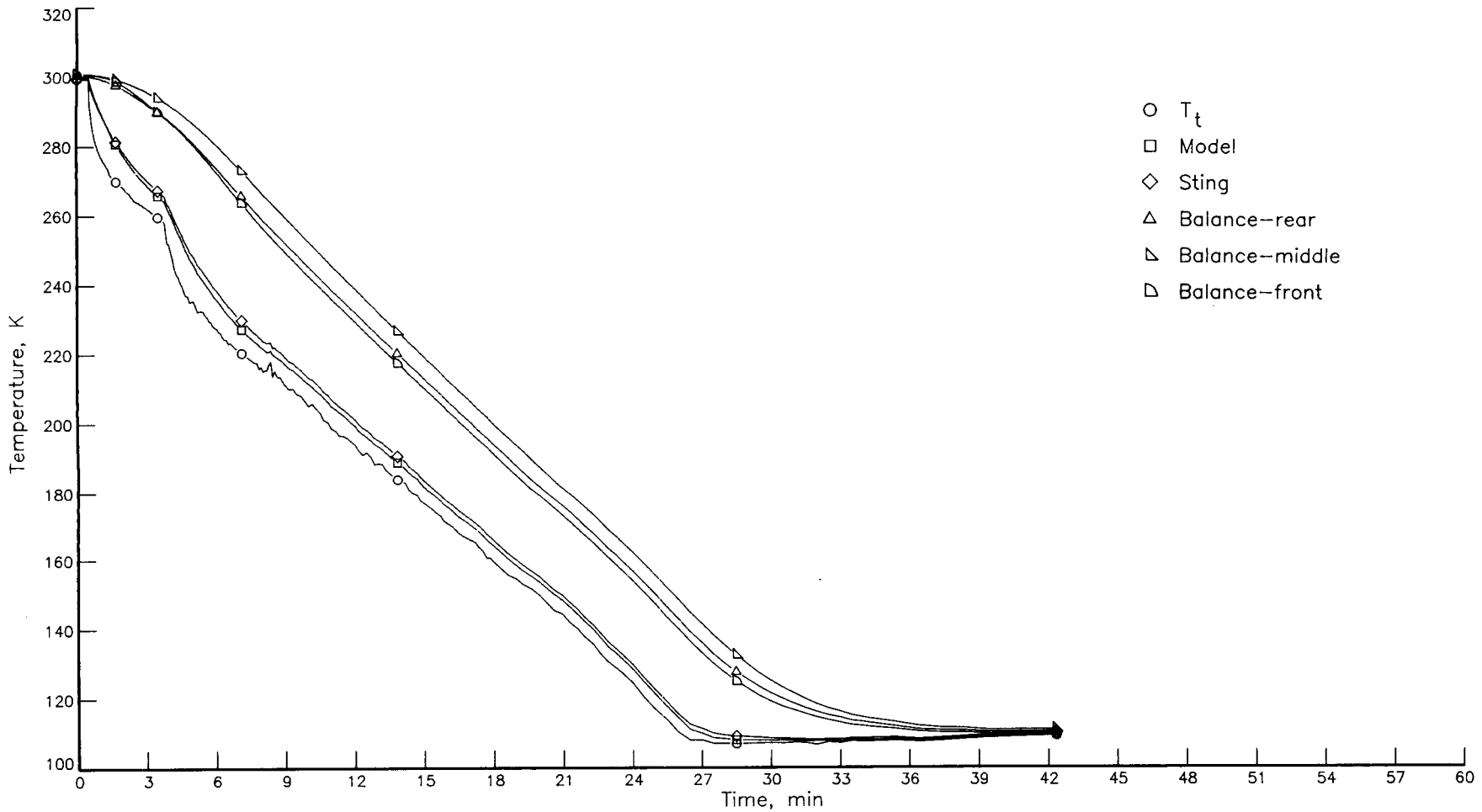

(a) $T_t = 300$ K to 110 K; $p_t = 122$ kPa.

Figure 24. Temperature response with convection shield off at $M = 0.3$. ($\alpha = 0°$ unless otherwise specified.)

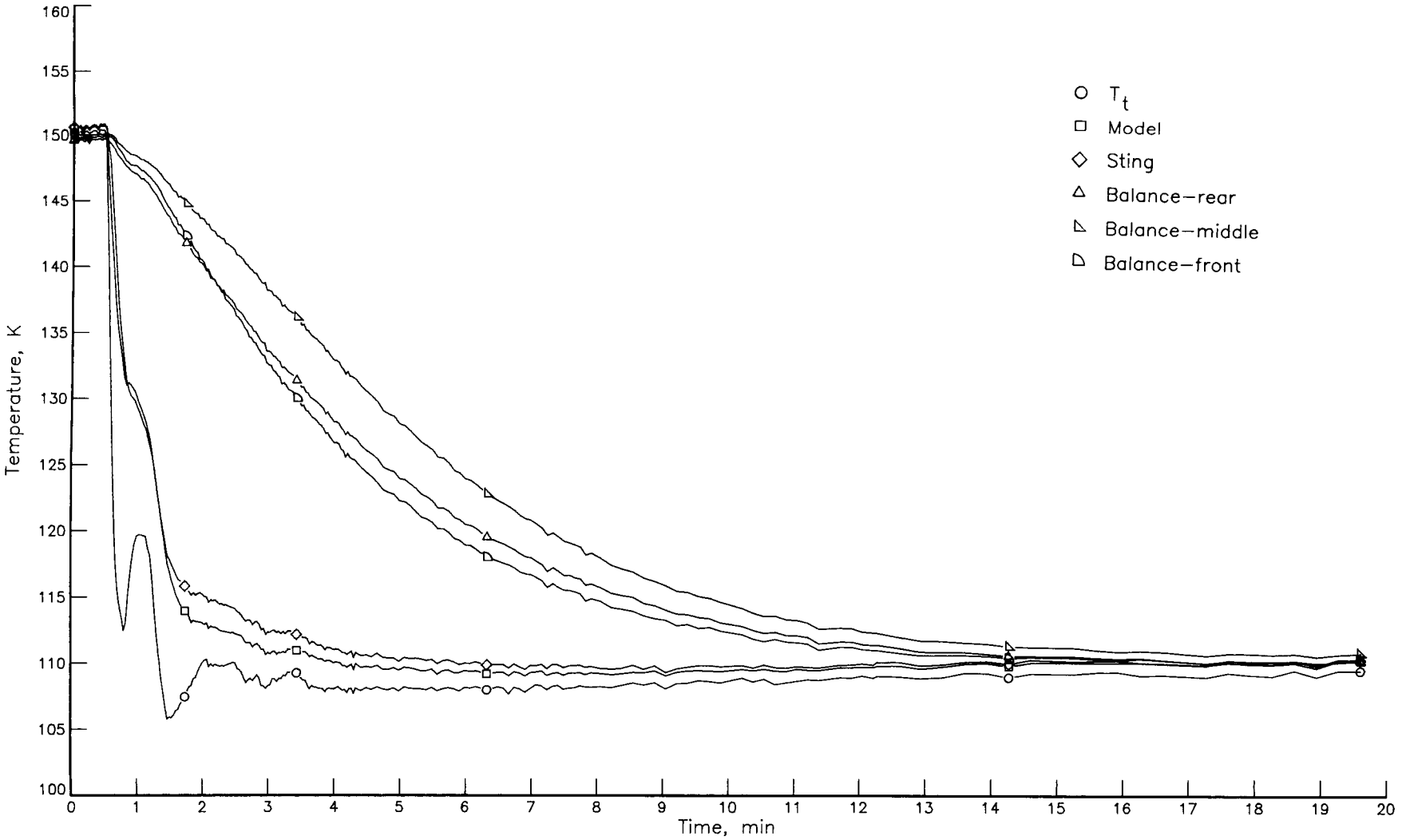

(b) $T_t = 150$ K to 110 K; $p_t = 122$ kPa.

Figure 24. Continued.

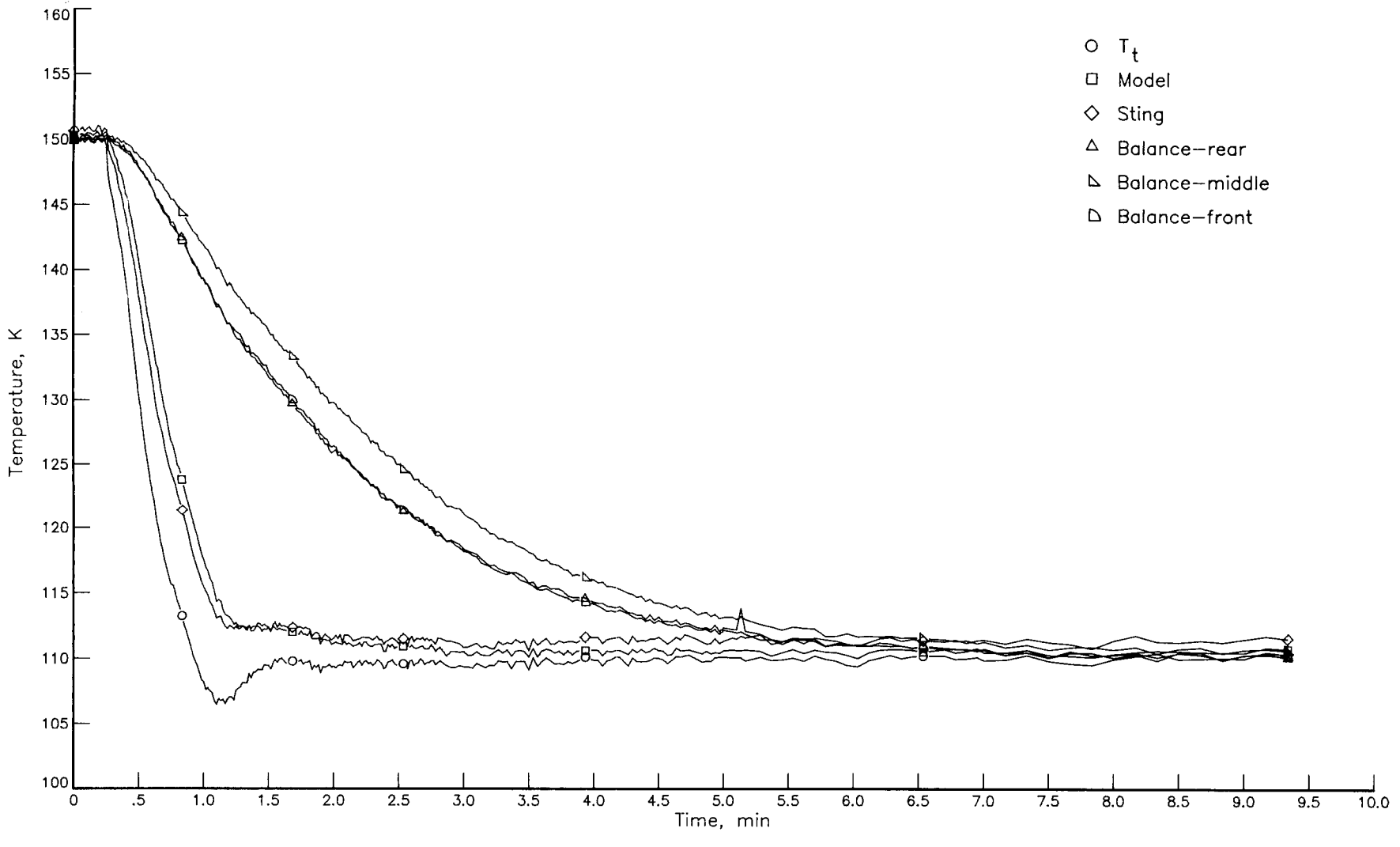

(c) $T_t = 150$ K to 110 K; $p_t = 488$ kPa.

Figure 24. Continued.

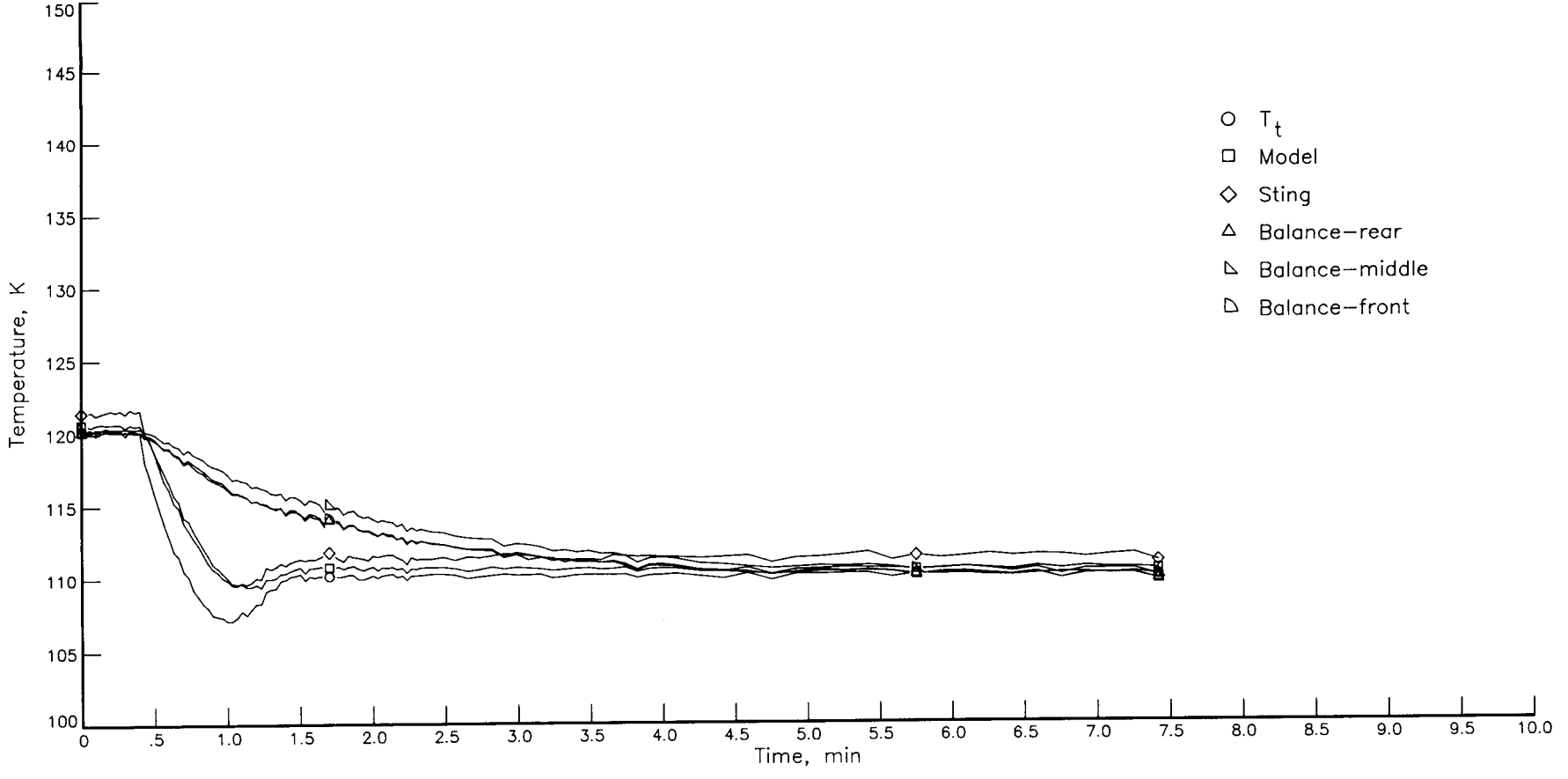

(d) $T_t = 120$ K to 110 K; $p_t = 488$ kPa.

Figure 24. Continued.

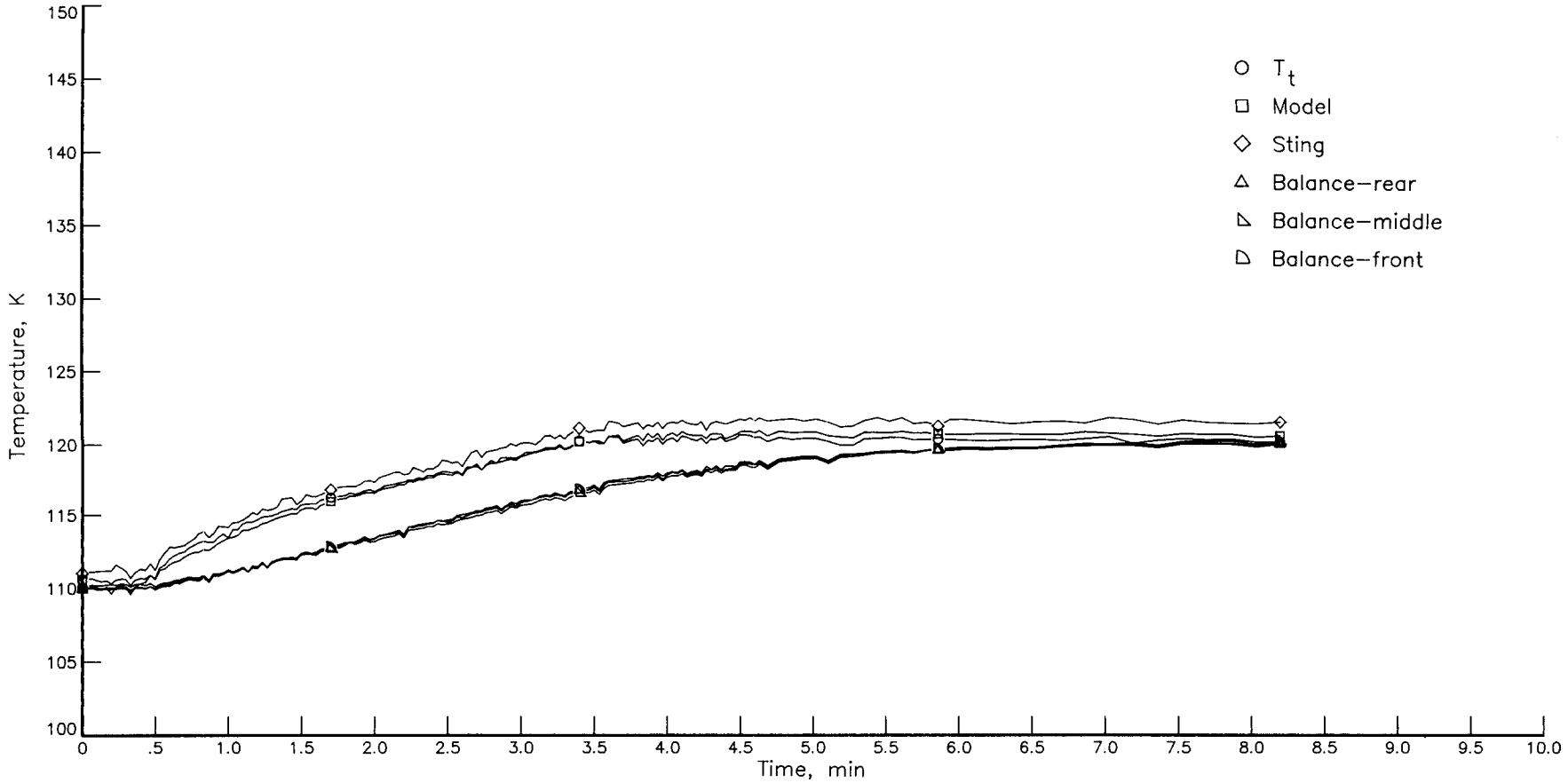

(e) $T_t = 110$ K to 120 K; $p_t = 488$ kPa.

Figure 24. Continued.

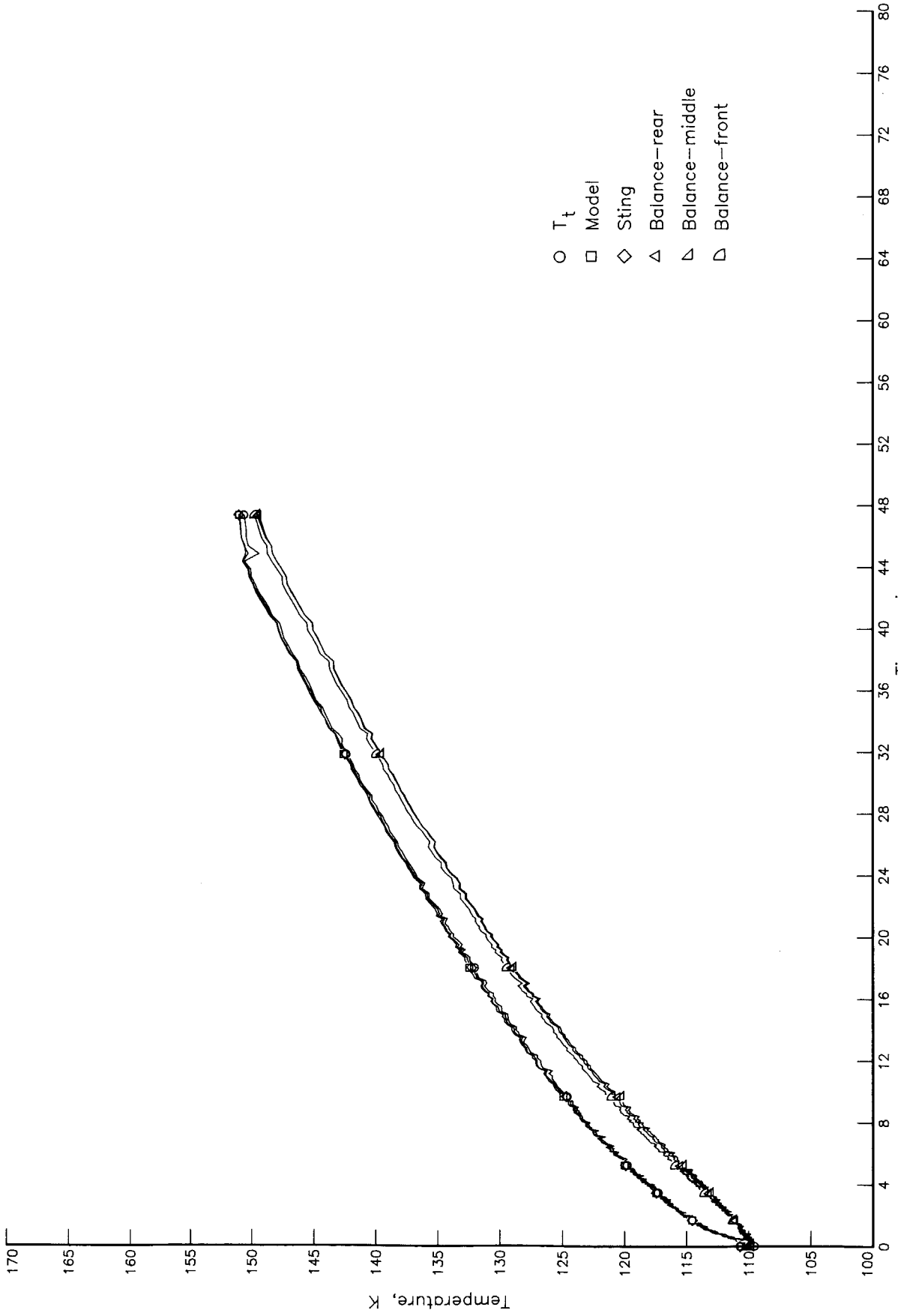

(f) $T_t = 110$ K to 150 K; $p_t = 122$ kPa.

Figure 24. Continued.

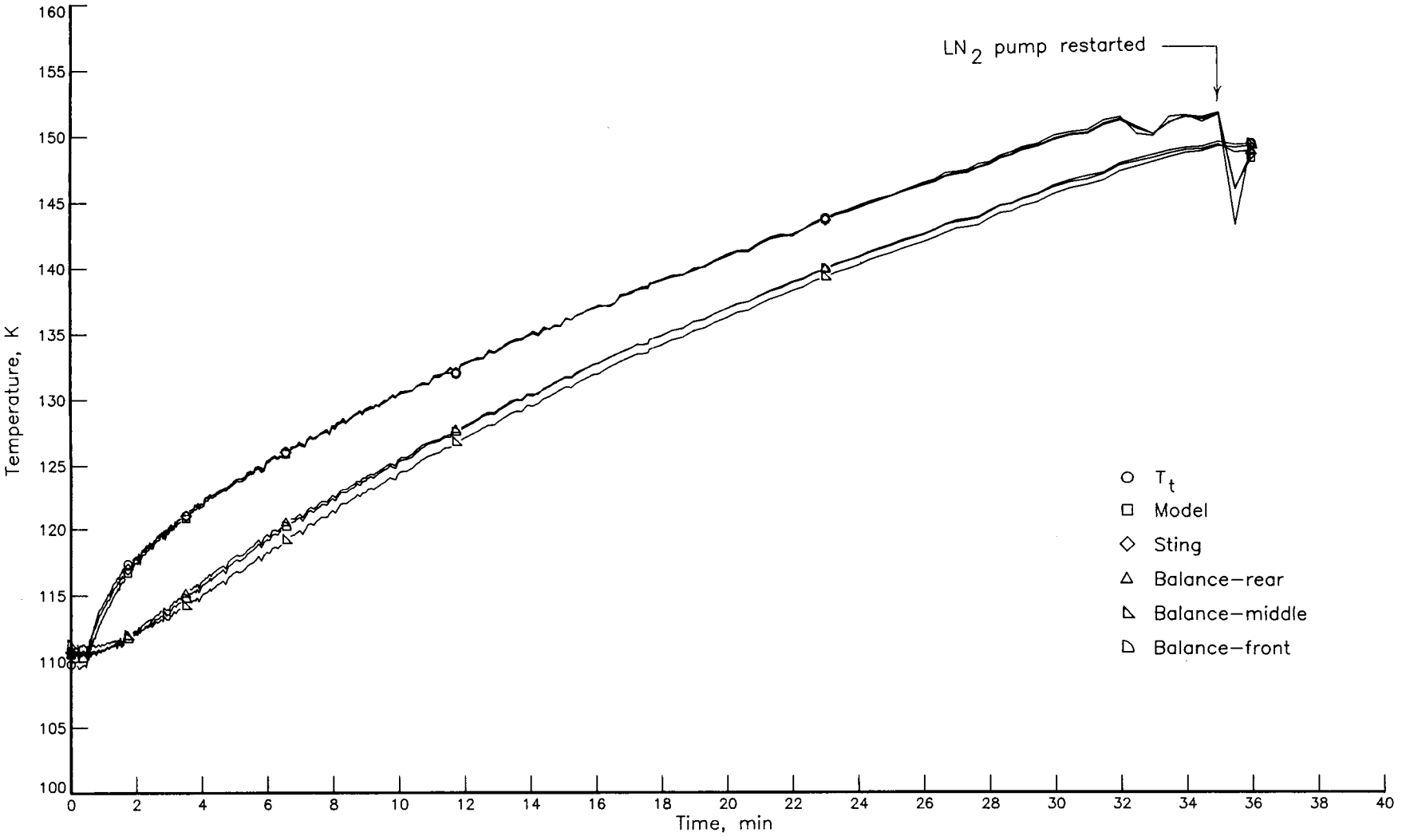

(g) $T_t = 110$ K to 150 K; $p_t = 122$ kPa; $\alpha = 15°$.

Figure 24. Continued.

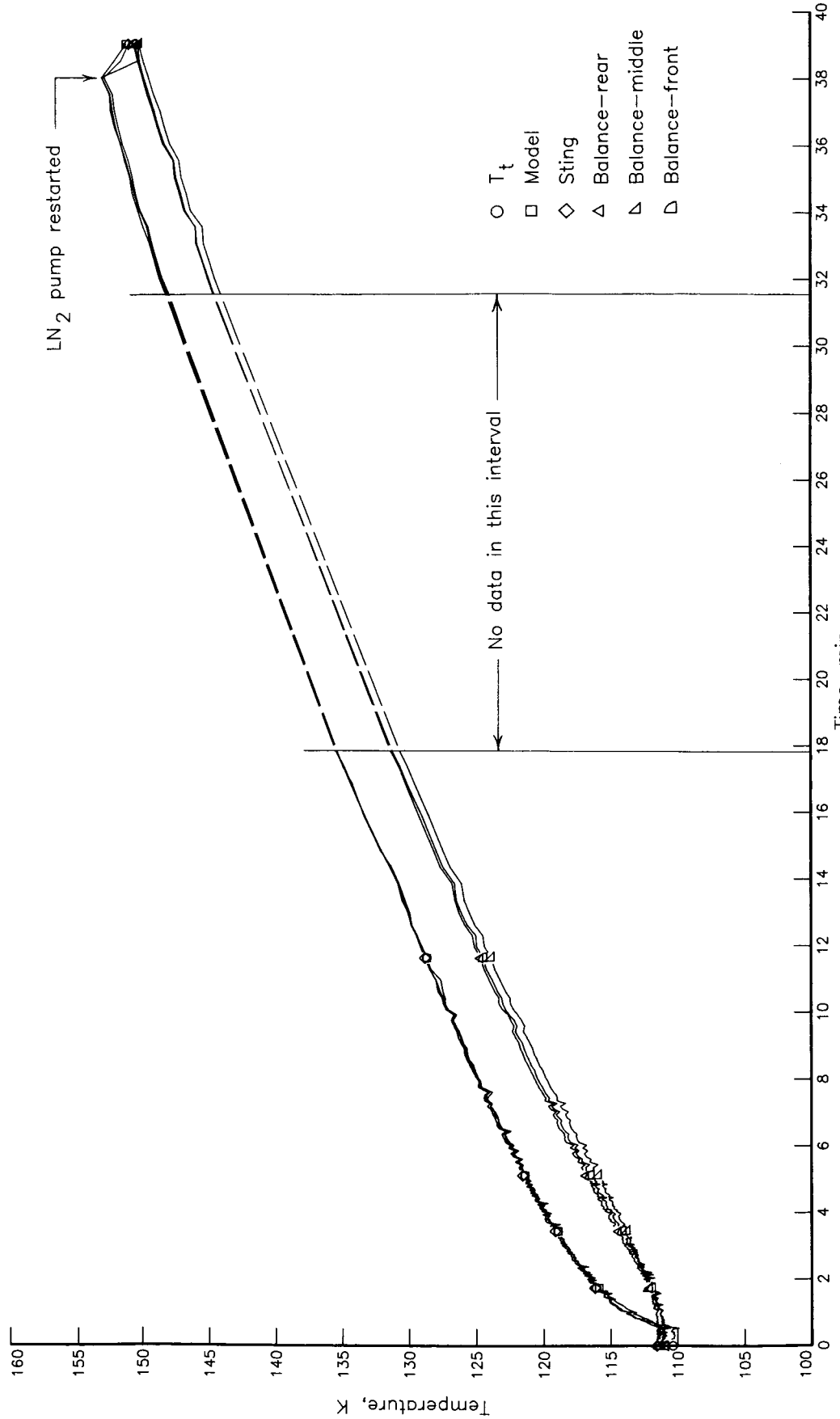

(h) $T_t = 110$ K to 150 K; $p_t = 122$ kPa; $\alpha = 15°$.

Figure 24. Continued.

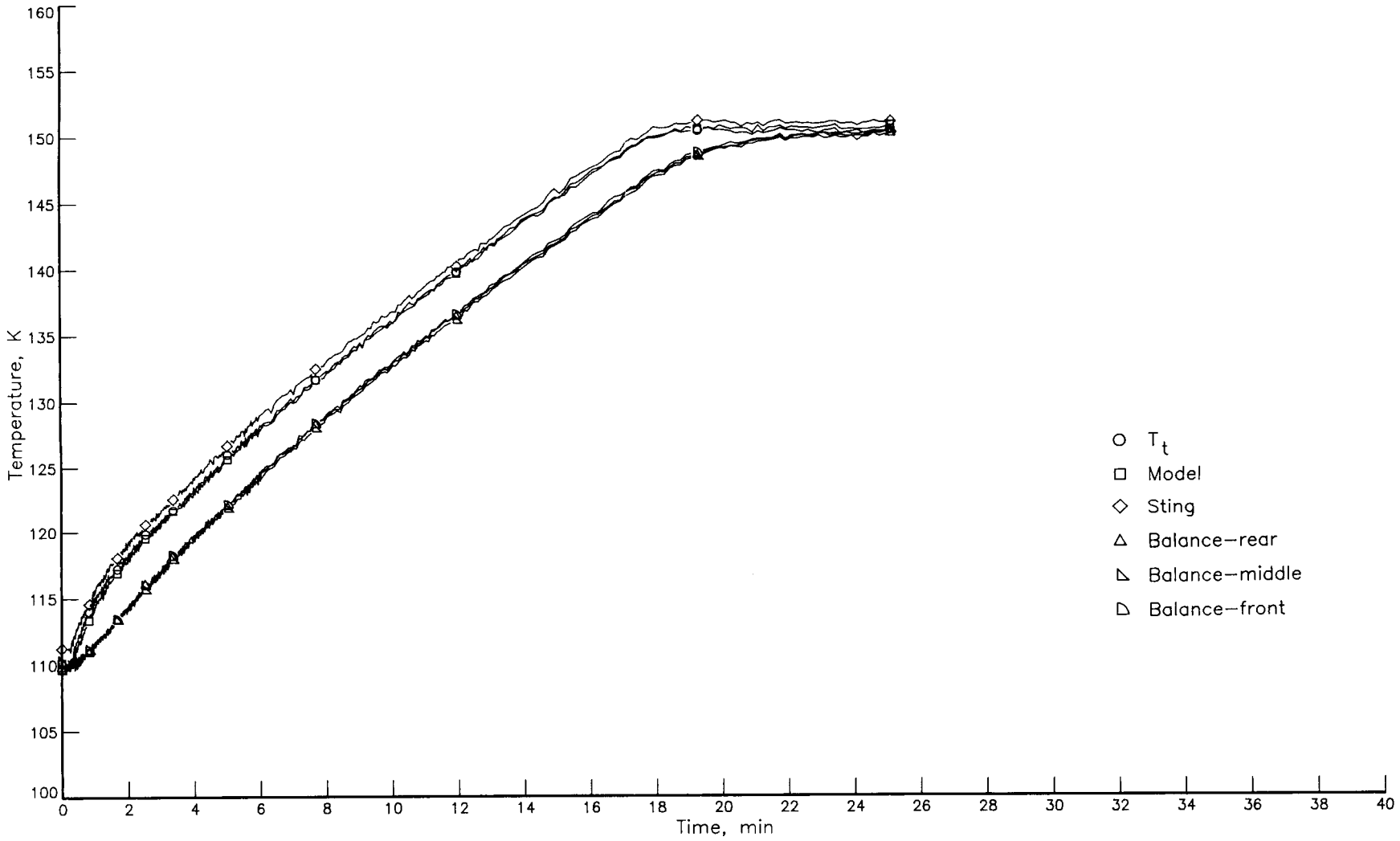

(i) $T_t = 110$ K to 150 K; $p_t = 488$ kPa.

Figure 24. Concluded.

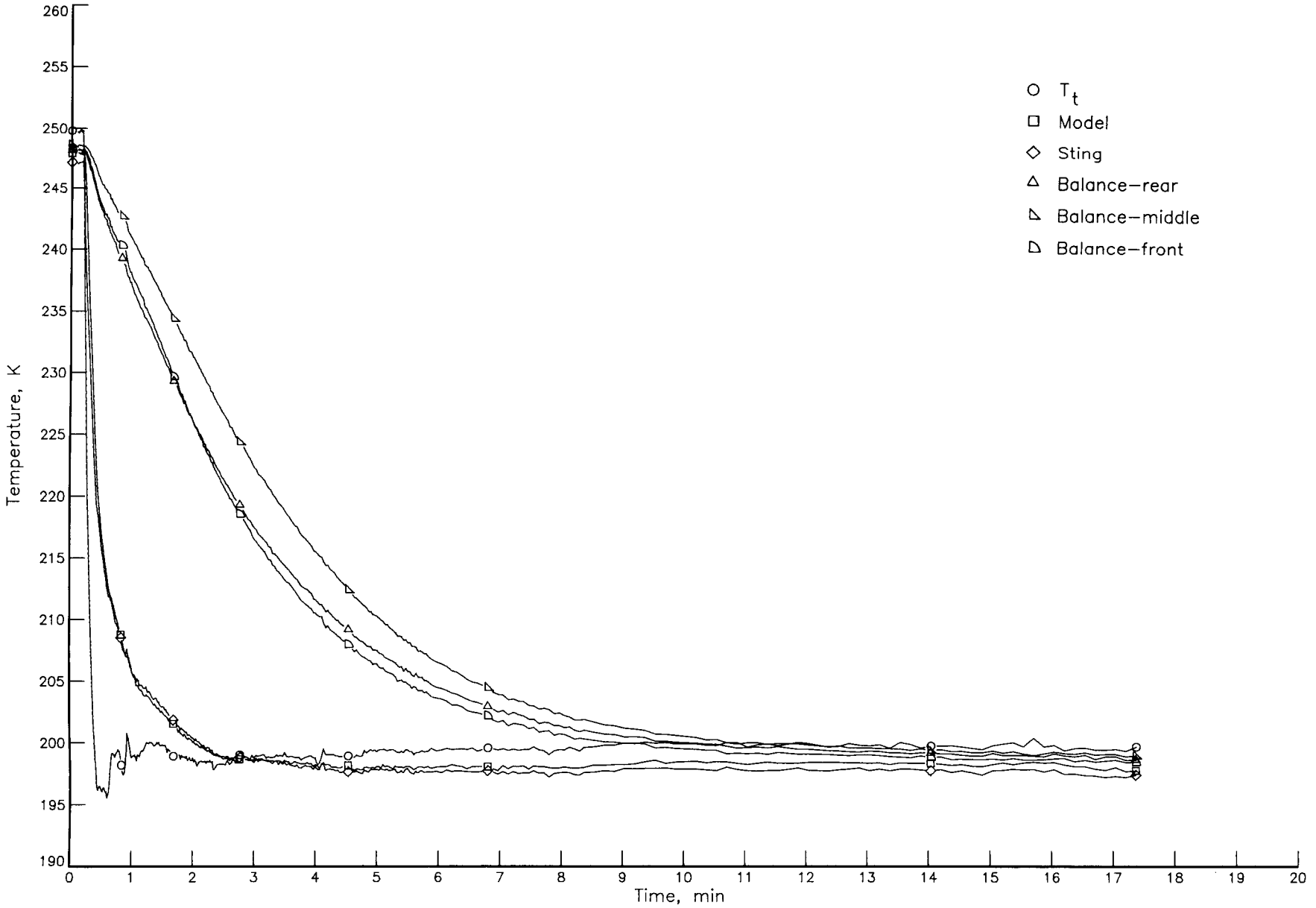

(a) $T_t = 250$ K to 200 K; $p_t = 287$ kPa.

Figure 25. Temperature response with convection shield off at $M = 0.5$. ($\alpha = 0°$ unless otherwise specified.)

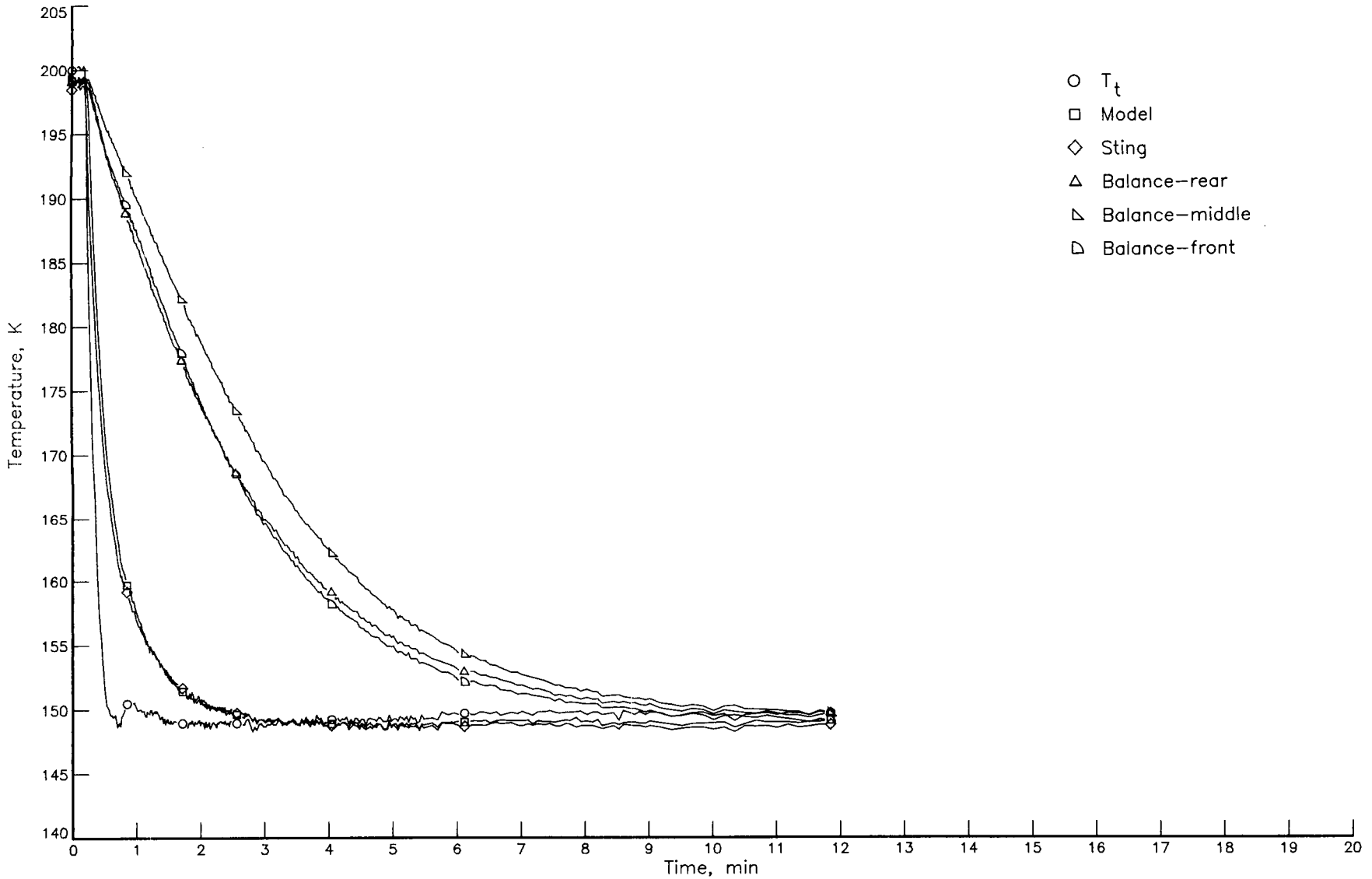

(b) $T_t = 200$ K to 150 K; $p_t = 287$ kPa.

Figure 25. Continued.

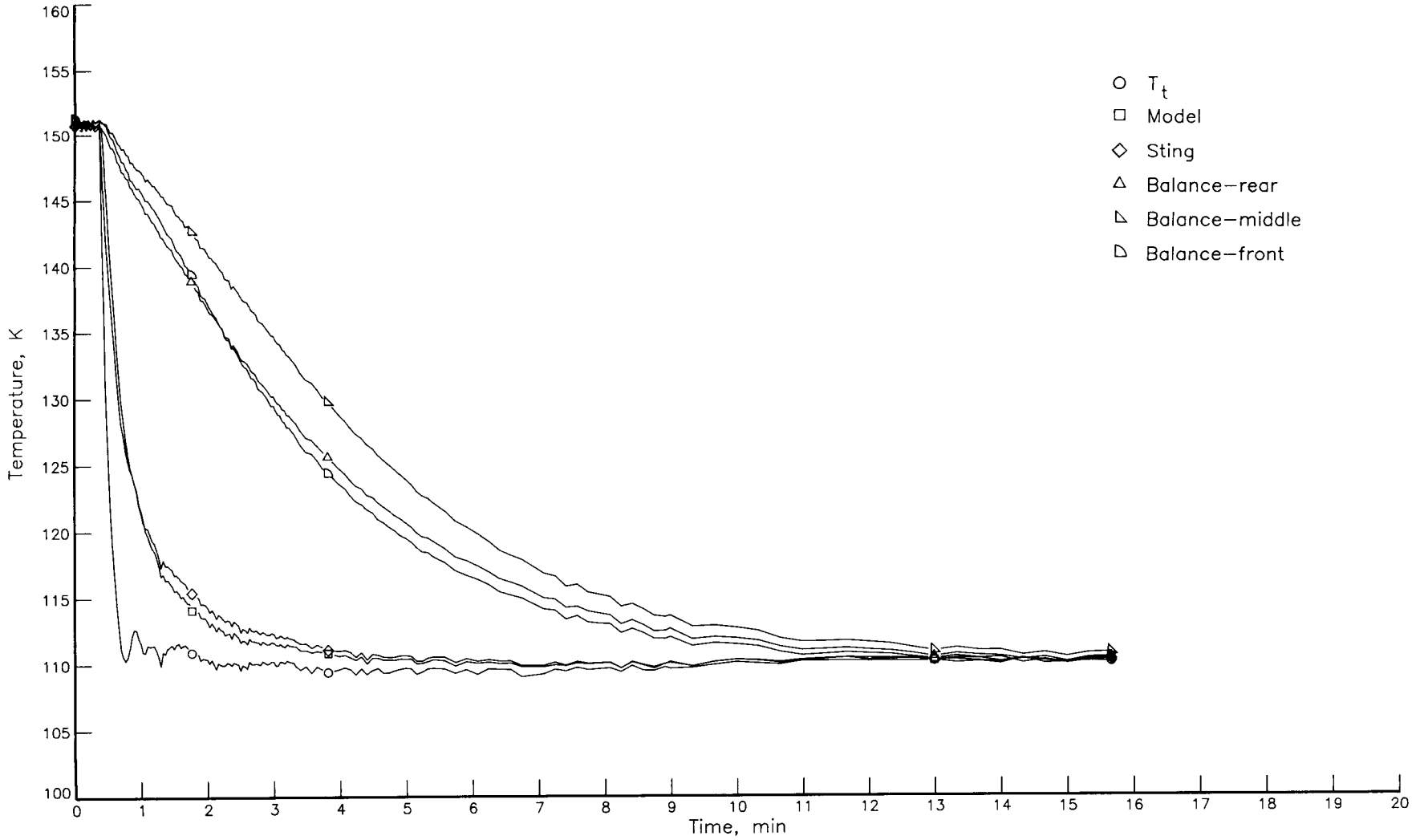

(c) $T_t = 150$ K to 110 K; $p_t = 122$ kPa.

Figure 25. Continued.

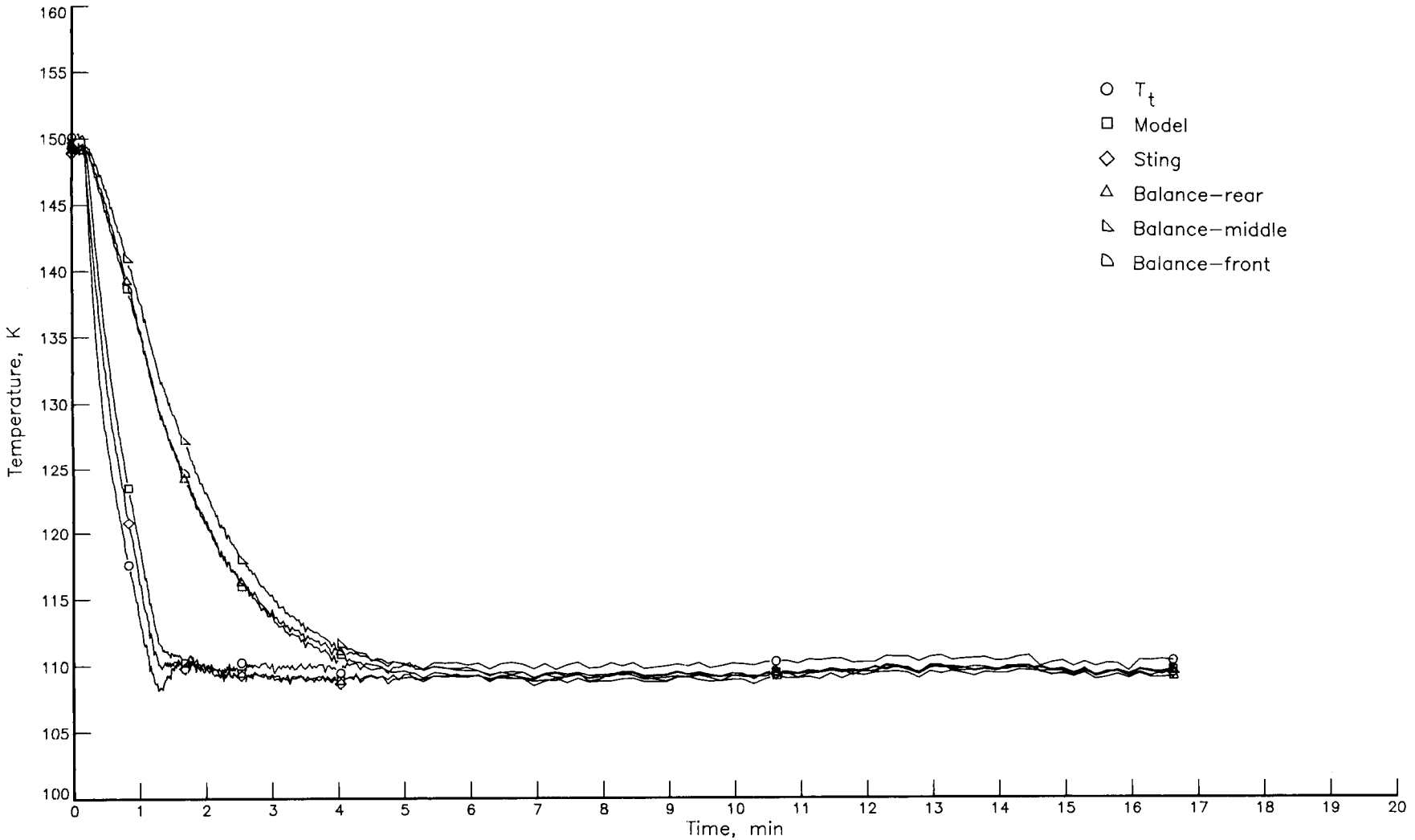

(d) $T_t = 150$ K to 110 K; $p_t = 491$ kPa.

Figure 25. Continued.

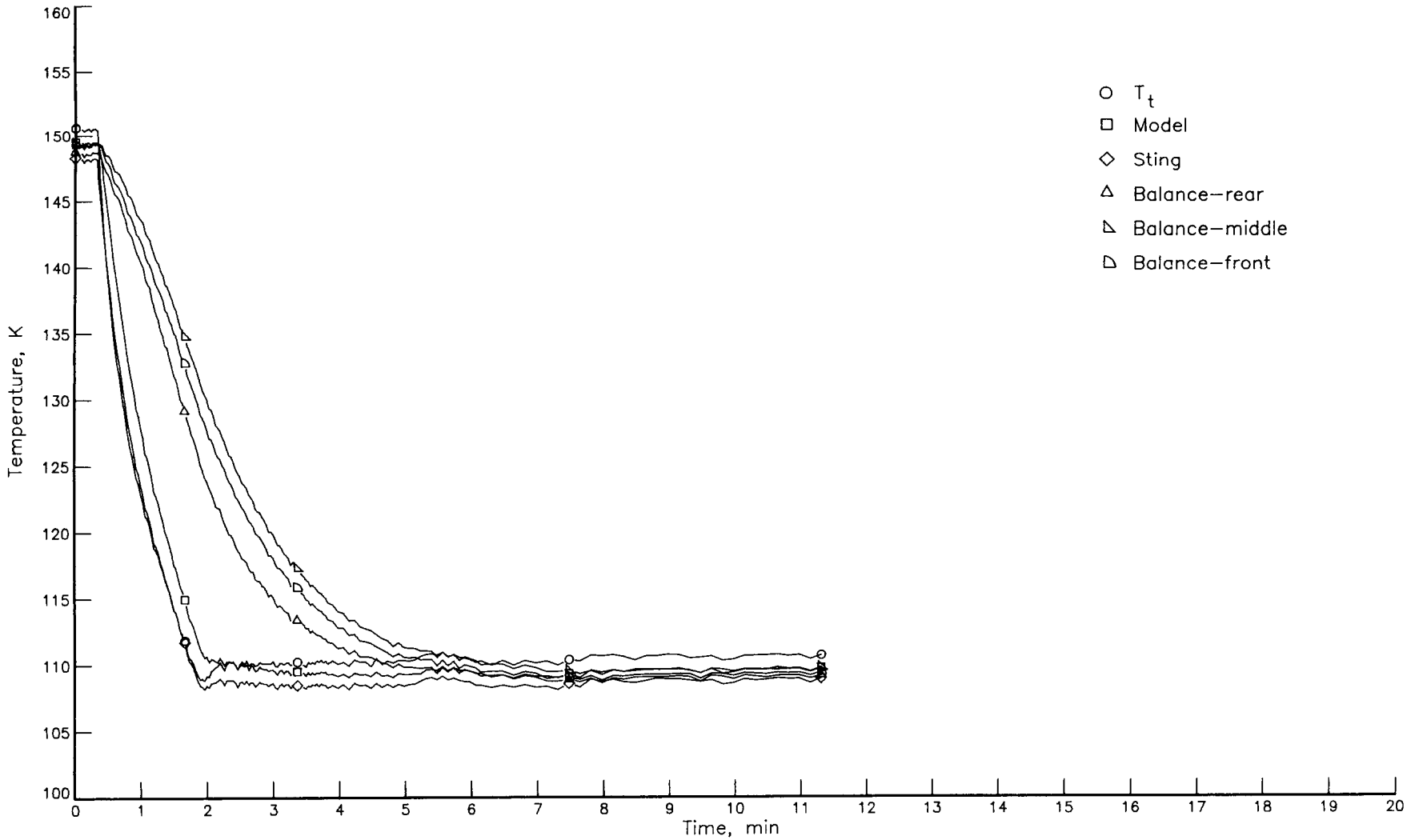

(e) $T_t = 150$ K to 110 K; $p_t = 491$ kPa; $\alpha = 14.8°$.

Figure 25. Continued.

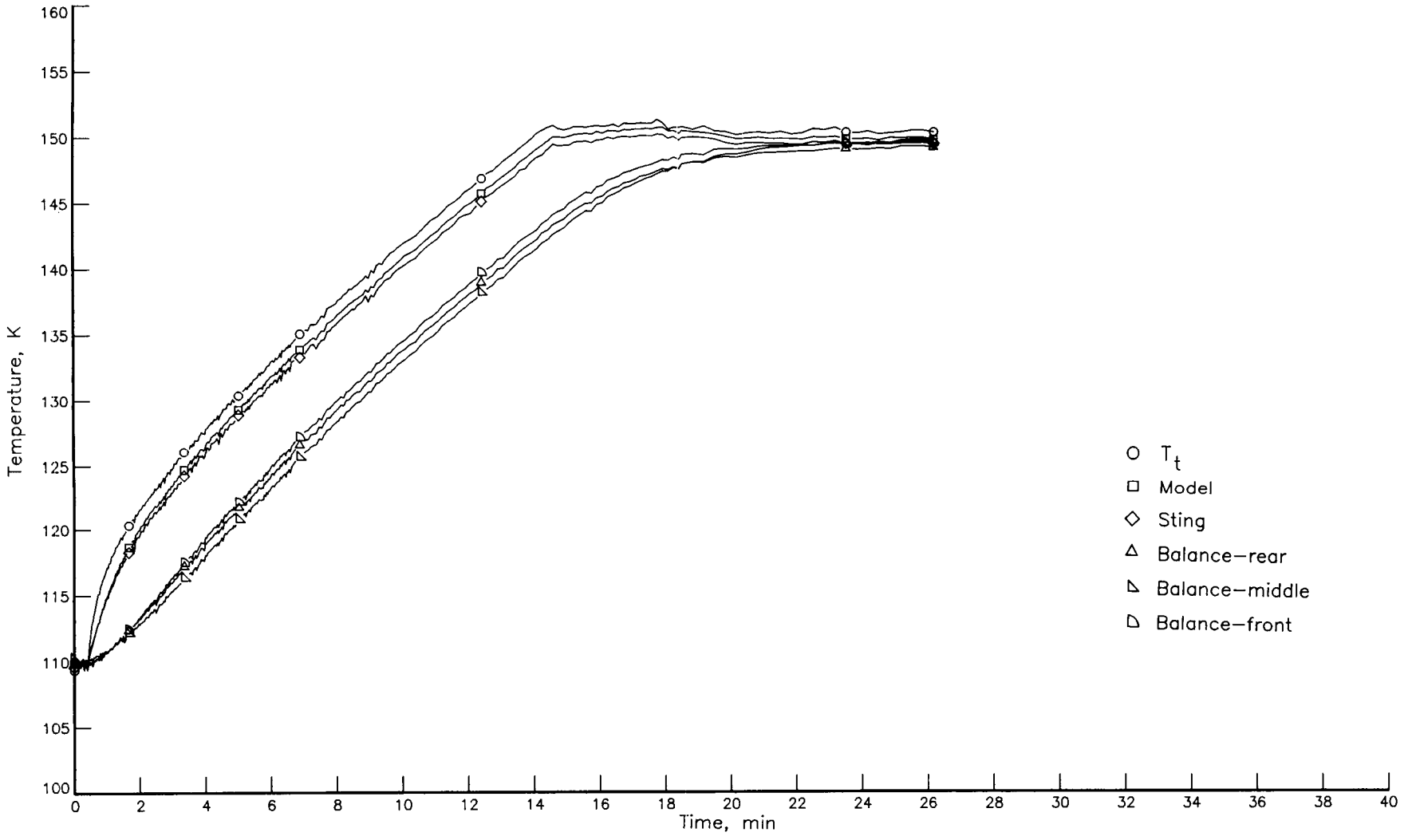

(f) $T_t = 110$ K to 150 K; $p_t = 122$ kPa.

Figure 25. Continued.

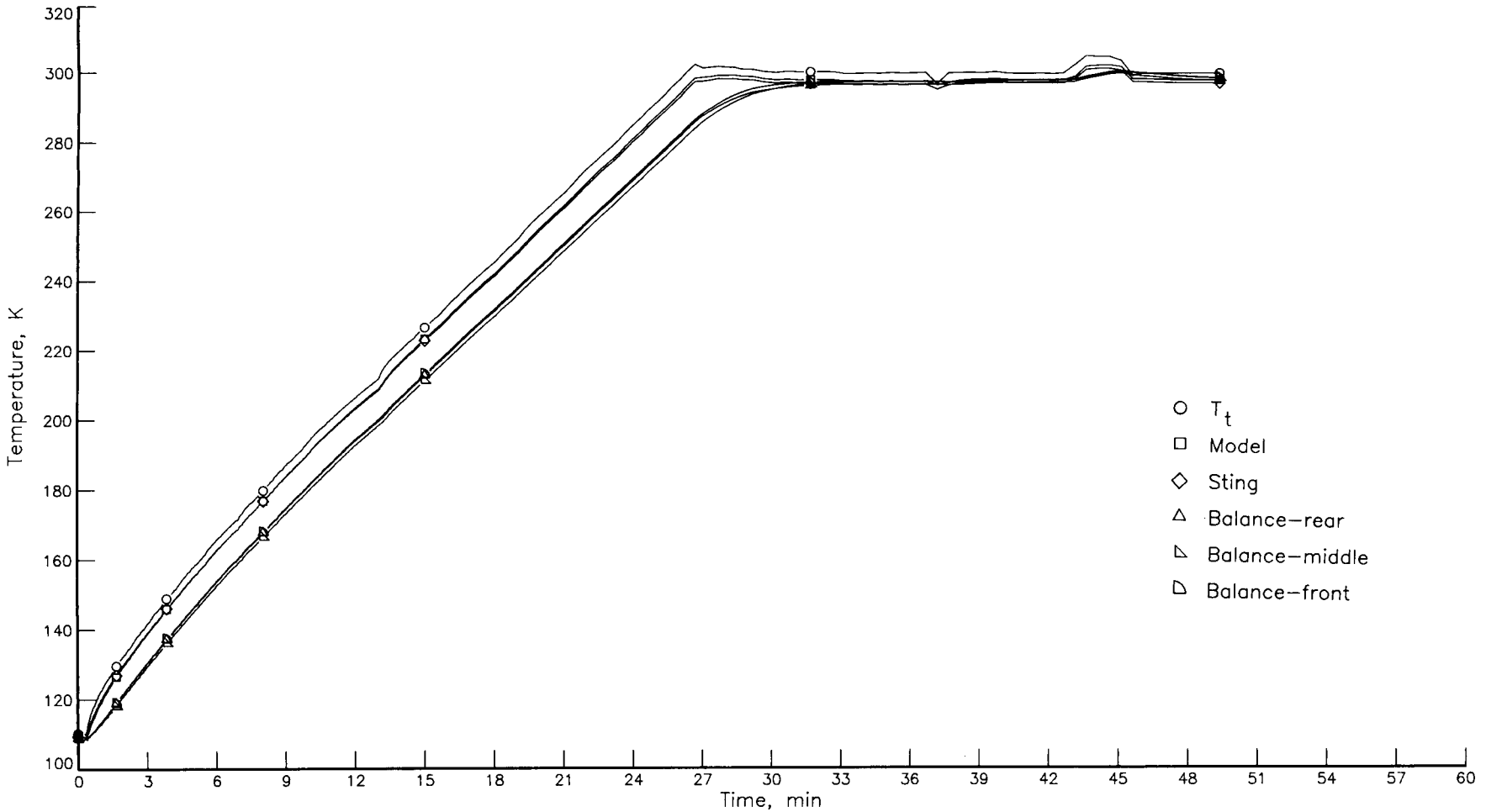

(g) $T_t = 110$ K to 300 K; $p_t = 491$ kPa.

Figure 25. Concluded.

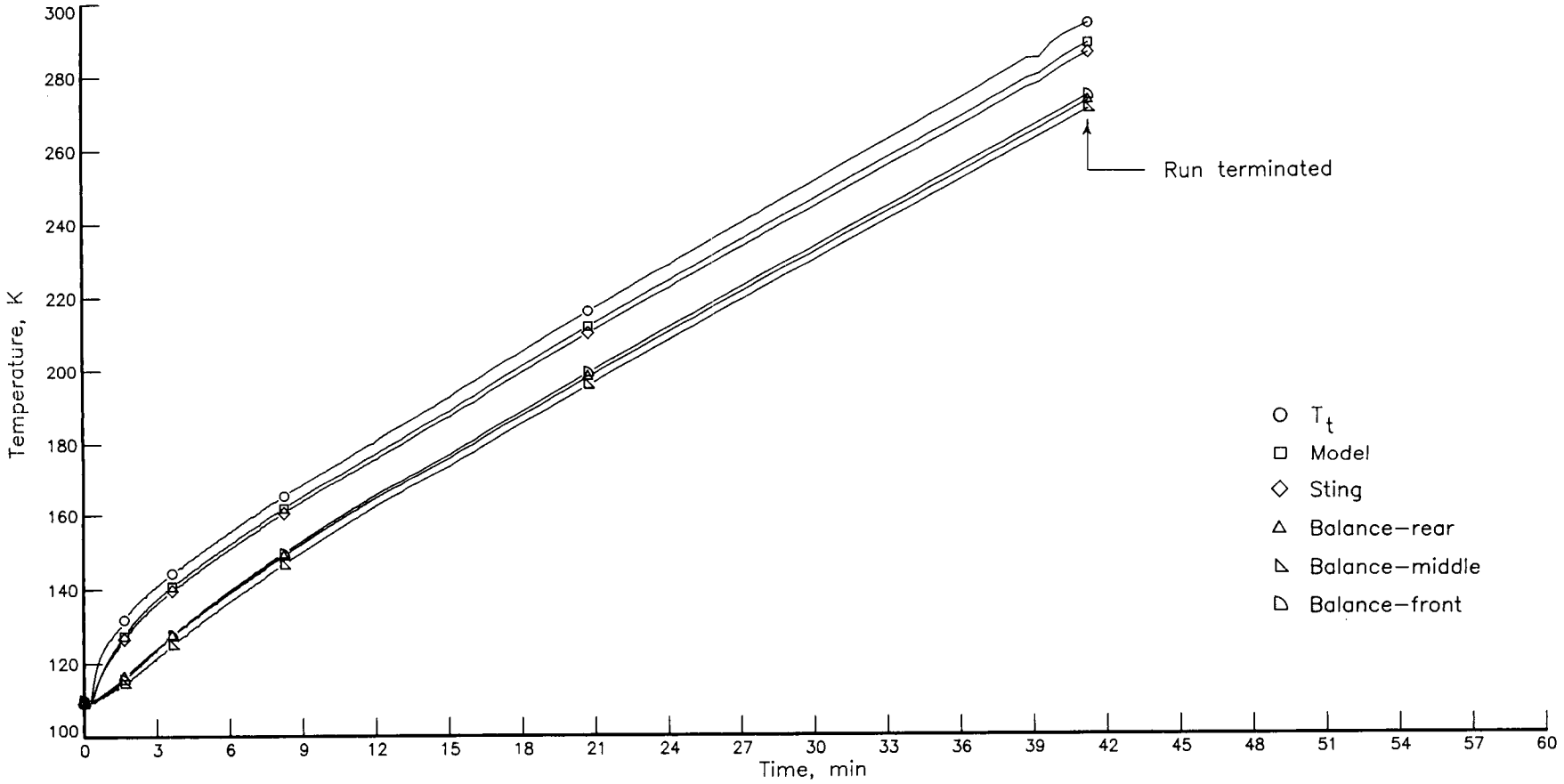

Figure 26. Temperature response with convection shield off at $M = 0.65$. $T_t = 110$ K to 300 K; $p_t = 122$ kPa; $\alpha = 0°$.

NASA
National Aeronautics and Space Administration

Report Documentation Page

1. Report No.	2. Government Accession No.	3. Recipient's Catalog No.
NASA TM-89039		

4. Title and Subtitle	5. Report Date
Aerodynamic Measurements and Thermal Tests of a Strain-Gage Balance in a Cryogenic Wind Tunnel	April 1987
	6. Performing Organization Code
7. Author(s)	8. Performing Organization Report No.
Richmond P. Boyden, Alice T. Ferris, William G. Johnson, Jr., David A. Dress, and Acquilla S. Hill	L-16208
9. Performing Organization Name and Address	10. Work Unit No.
NASA Langley Research Center Hampton, VA 23665-5225	505-61-01-02
	11. Contract or Grant No.
12. Sponsoring Agency Name and Address	13. Type of Report and Period Covered
National Aeronautics and Space Administration Washington, DC 20546-0001	Technical Memorandum
	14. Sponsoring Agency Code

15. Supplementary Notes

16. Abstract

An internal strain-gage balance designed and constructed in Europe for use in cryogenic wind tunnels has been tested in the Langley 0.3-Meter Transonic Cryogenic Tunnel. Part of the evaluation was made at equilibrium balance temperatures and it consisted of comparing the data taken at a tunnel stagnation temperature of 300 K with the data taken at 200 K and 110 K while maintaining either the Reynolds number or the stagnation pressure. A sharp-leading-edge delta-wing model was used to provide the aerodynamic loading for these tests. Results obtained with the balance during the force tests were found to be accurate and repeatable both with and without the use of a convection shield on the balance. An additional part of this investigation involved obtaining data on the transient temperature response of the balance during both normal and rapid changes in the tunnel stagnation temperature. The variation of the temperature with time was measured at three locations on the balance near the physical locations of the strain gages. The use of a convection shield significantly increased the time required for the balance to stabilize at a new temperature during the temperature response tests.

17. Key Words (Suggested by Authors(s))	18. Distribution Statement
Cryogenic force balance Strain-gage balance Cryogenic wind tunnel	Unclassified—Unlimited Subject Category 02, 35

19. Security Classif.(of this report)	20. Security Classif.(of this page)	21. No. of Pages	22. Price
Unclassified	Unclassified	85	A05

For sale by the National Technical Information Service, Springfield, Virginia 22161-2171